



Nonperturbative QCD within the functional renormalization group

Wei-jie Fu

Dalian University of Technology

**12th International Conference on the Exact Renormalization Group
2024 (ERG2024), Les Diablerets, Switzerland, Sep. 23-27, 2024**

Based on:

WF, Xiaofeng Luo, Jan M. Pawłowski, Fabian Rennecke, Shi Yin, arXiv: 2308.15508;

Braun, Chen, WF, Gao, Huang, Ihssen, Pawłowski, Rennecke, Sattler, Tan, Wen, and Yin, arXiv:2310.19853;

Yang-yang Tan, Yong-rui Chen, WF, Wei-Jia Li, arXiv: 2403.03503;

WF, Chuang Huang, Jan M. Pawłowski, Yang-yang Tan, arXiv:2209.13120; arXiv:2401.07638;

WF, Chuang Huang, Jan M. Pawłowski, Yang-yang Tan, Li-jun Zhou, in preparation;

Lei Chang, WF, Chuang Huang, Jan M. Pawłowski, Dao-yu Zhang, in preparation;

WF, Jan M. Pawłowski, Robert D. Pisarski, Fabian Rennecke, Rui Wen, and Shi Yin, in preparation;

Yang-yang Tan, Shi Yin, Yong-rui Chen, Chuang Huang, WF, in preparation.

fQCD collaboration:

Braun, Chen, Fu, Gao, Geissel, Huang, Lu, Ihssen, Pawłowski, Rennecke, Sattler, Schallmo, Stoll, Tan, Töpfel, Turnwald, Wessely, Wen, Wink, Yin, Zheng, Zorbach

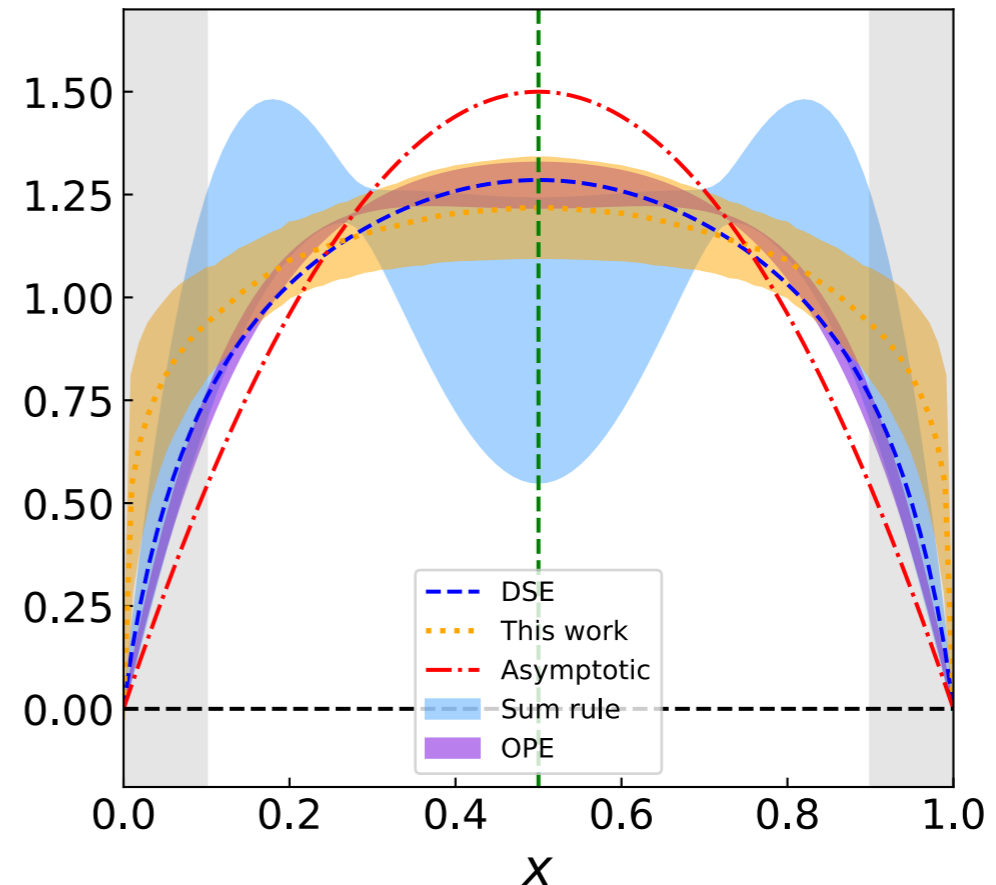
Basic questions in nuclear physics

Mass generation



Image from BNL website

Distribution amplitudes for pion

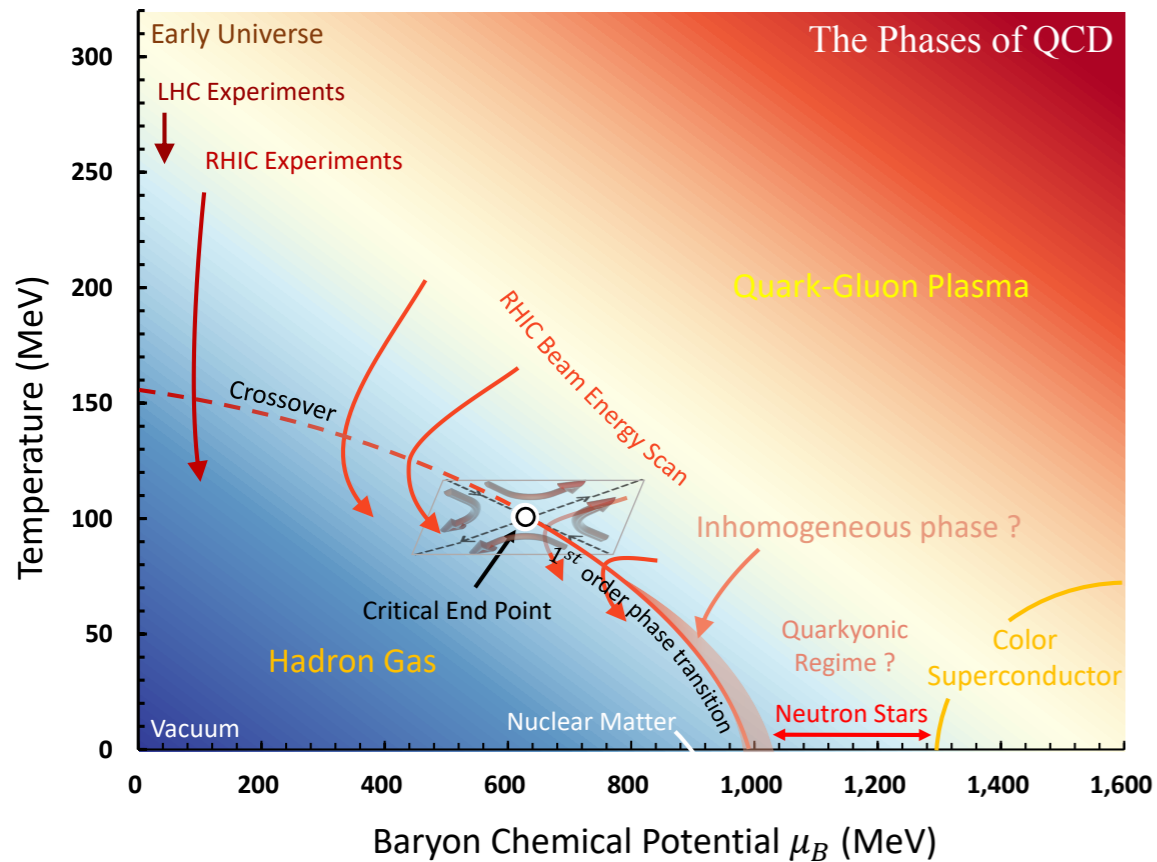


Lattice: J. Hua *et al.* (LPC), *PRL* 129 (2022) 132001;
DSE: C. Roberts *et al.*, *PPNP* 120 (2021) 103883;
Sum rules: P. Ball *et al.*, *JHEP* 08 (2007) 090;
OPE: G. Bali *et al.* (RQCD), *JHEP* 08 (2019) 065; 11 (2020) 37.

- How can we understand mass generation and hadron structure from first-principles QCD?

CEP in QCD phase diagram

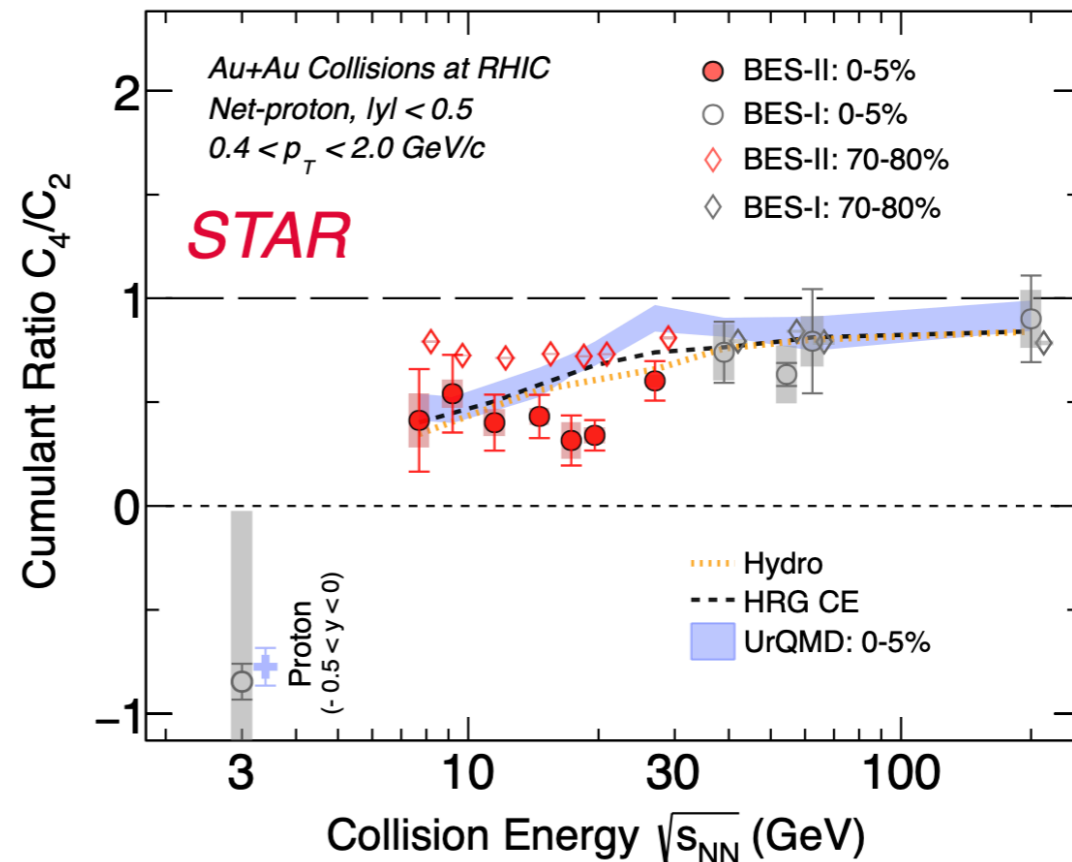
QCD phase diagram



Non-monotonicity:

M. Stephanov, *PRL* 107 (2011) 052301

Fluctuations measured in BES-II

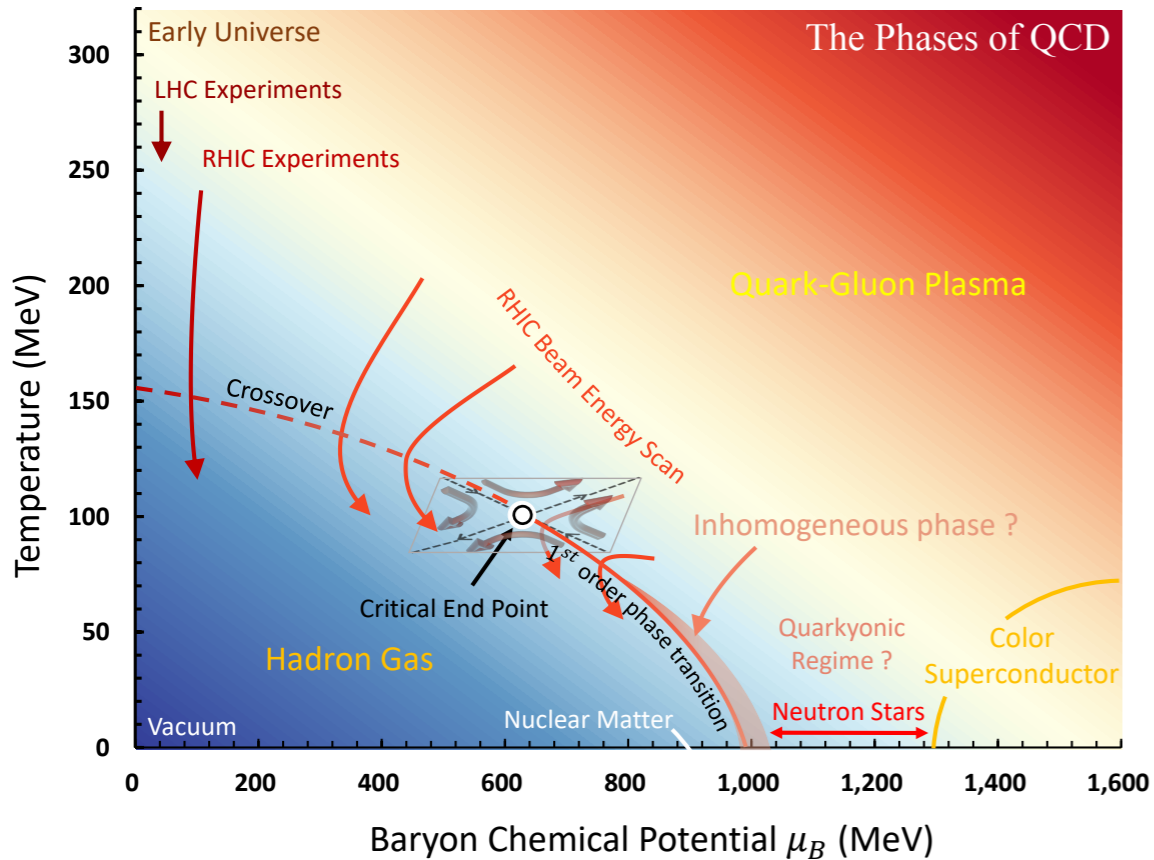


Ashish Pandav for STAR Collaboration in CPOD2024

- Is there a “peak” structure serving as the smoking gun signal for the critical end point in the QCD phase diagram?

CEP in QCD phase diagram

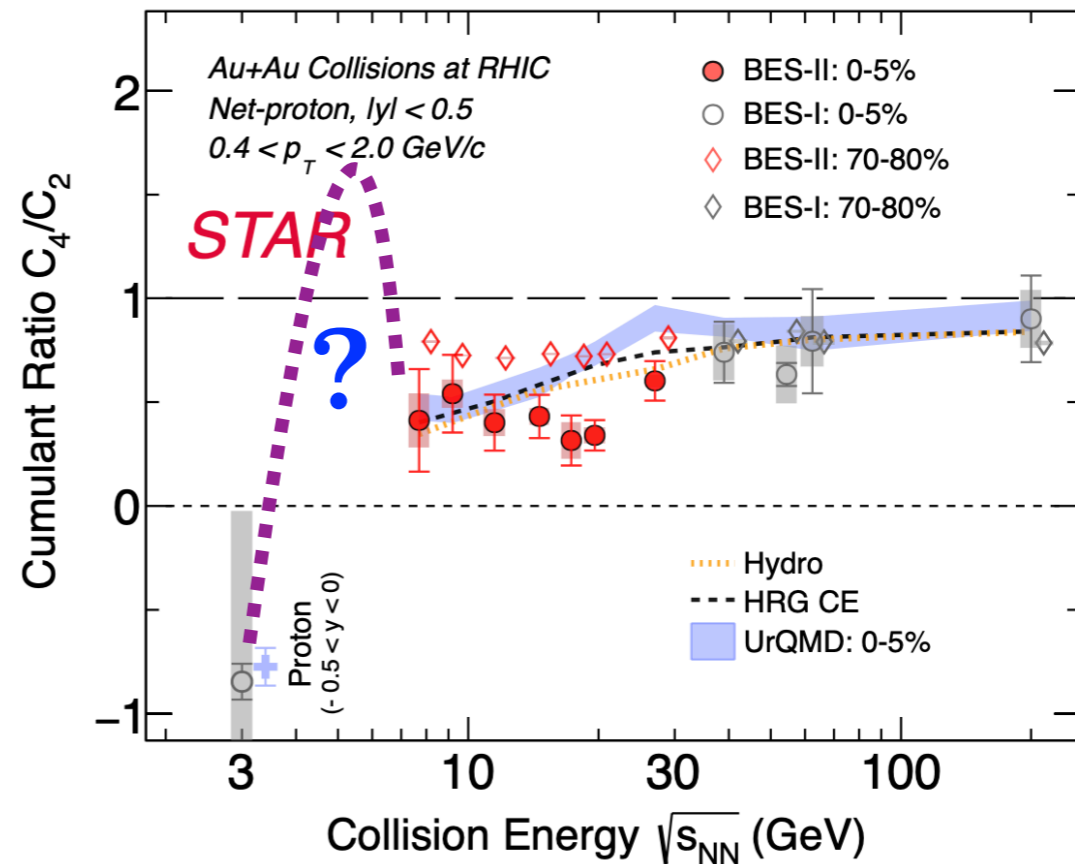
QCD phase diagram



Non-monotonicity:

M. Stephanov, *PRL* 107 (2011) 052301

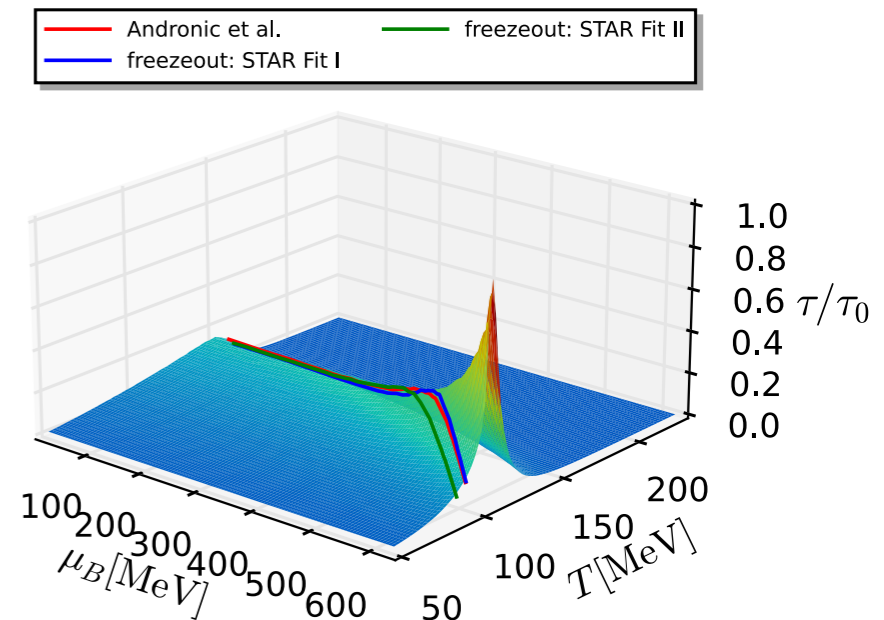
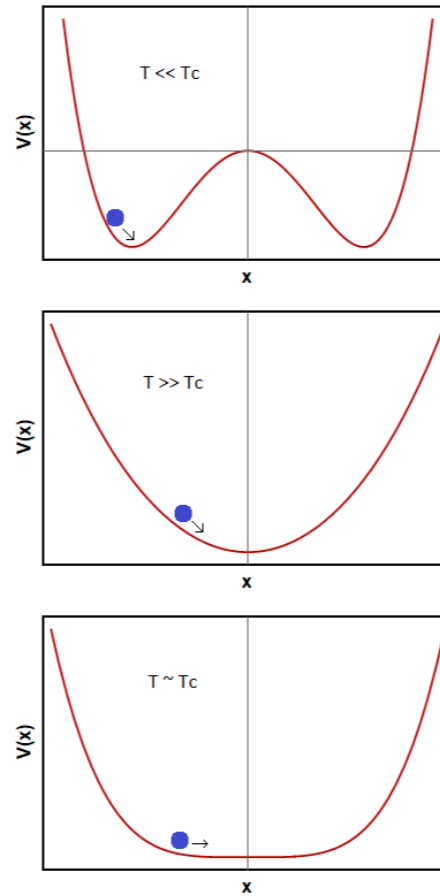
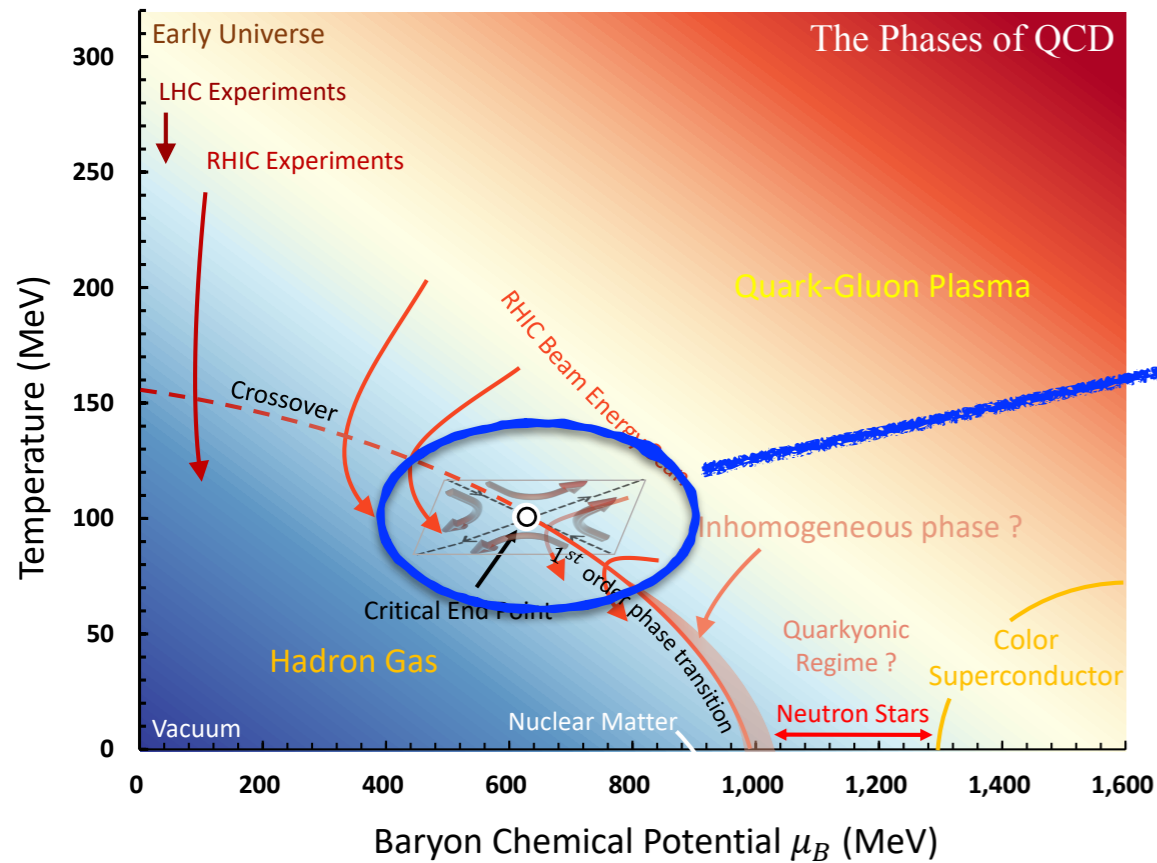
Fluctuations measured in BES-II



Ashish Pandav for STAR Collaboration in CPOD2024

- Is there a “peak” structure serving as the smoking gun signal for the critical end point in the QCD phase diagram?

Critical slowing down near QCD critical point



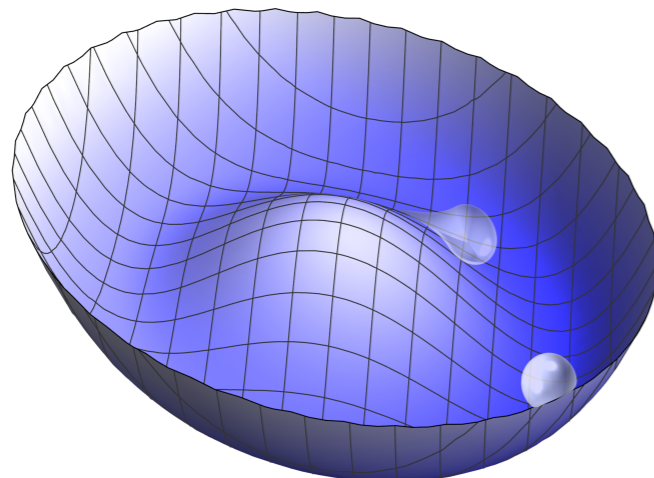
Tan, Yin, Chen, Huang, WF, in preparation

Relaxation time:

$$\tau = \xi^z f(k\xi)$$

z : dynamic critical exponent

Goldstone damping



also cf. talk by Lorenz von Smekal

Call for:

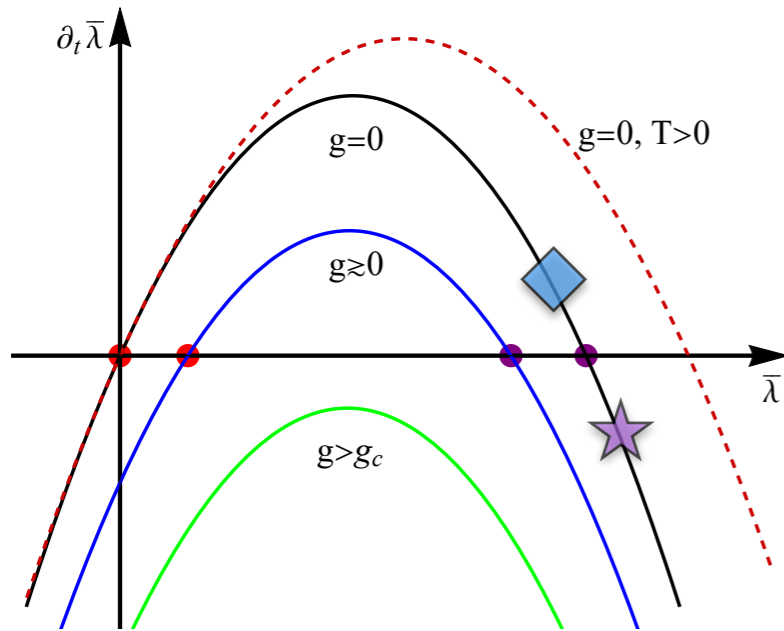
- Real-time description of strongly interacting systems.
- Nonperturbative approach of QCD.

Outline

- * **Introduction**
- * **QCD in vacuum and hadron structure**
- * **QCD at finite temperature and densities**
- * **Real-time dynamics of QCD**
- * **Summary and outlook**

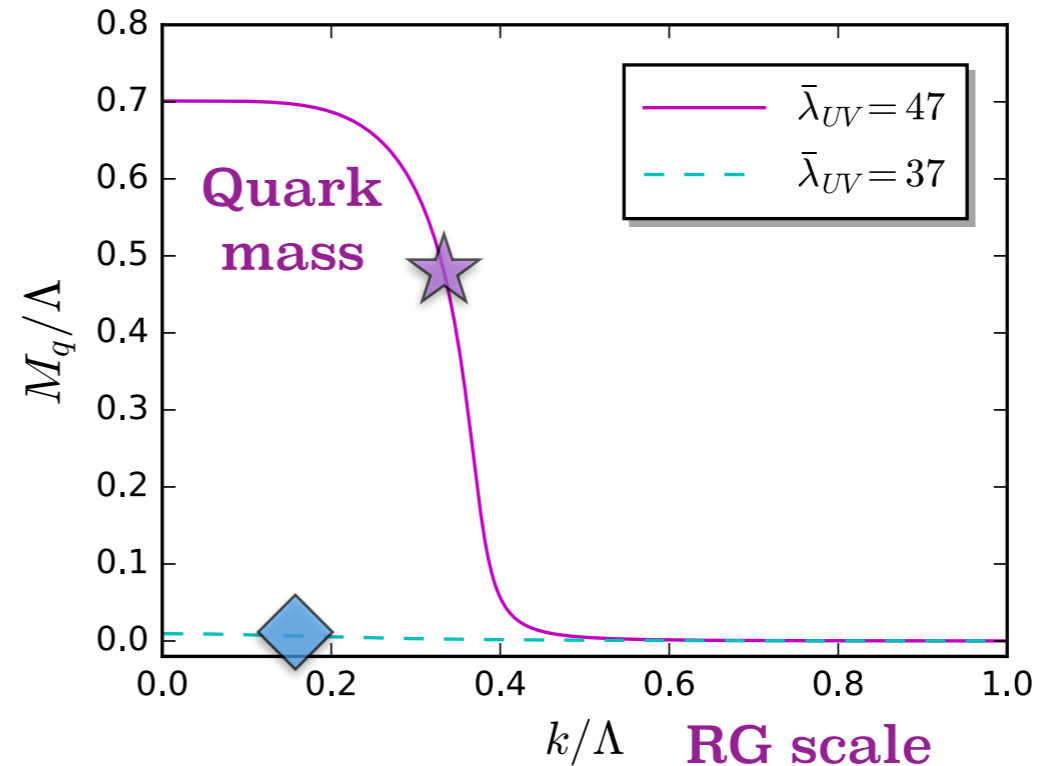
Chiral symmetry breaking and mass generation in RG

- β function of 4-quark coupling:



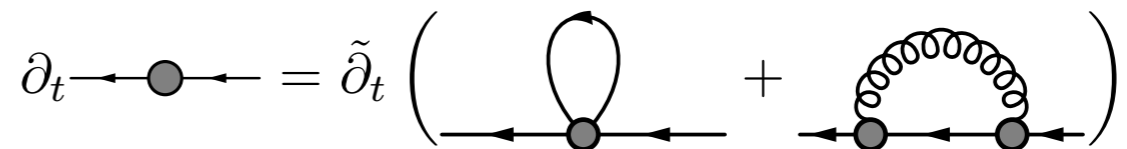
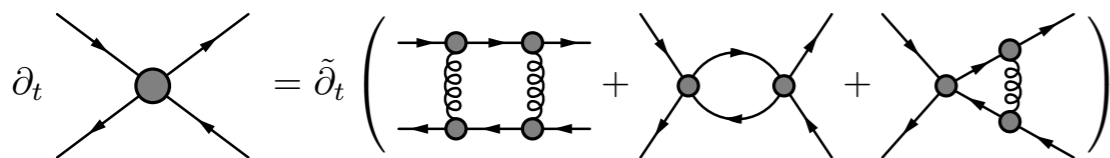
Braun, Gies, *JHEP* 06 (2006) 024.

- Quark mass:



WF, Huang, Pawłowski, Tan, *SciPost Phys.* 14 (2023) 069, arXiv:2209.13120

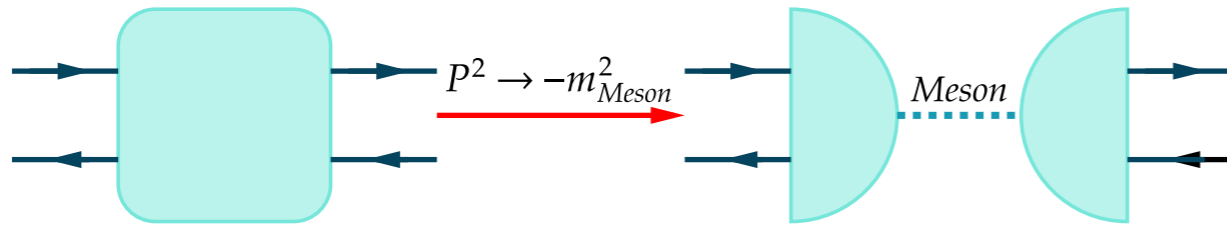
$$\partial_t \bar{\lambda} = (d - 2)\bar{\lambda} - a\bar{\lambda}^2 - b\bar{\lambda}g^2 - cg^4,$$



- Flows of two- and four-quark vertices play the same roles of **gap** and **Bethe-Salpeter** equations.

Bound states in RG

- Bound states encoded in n -point correlation functions:

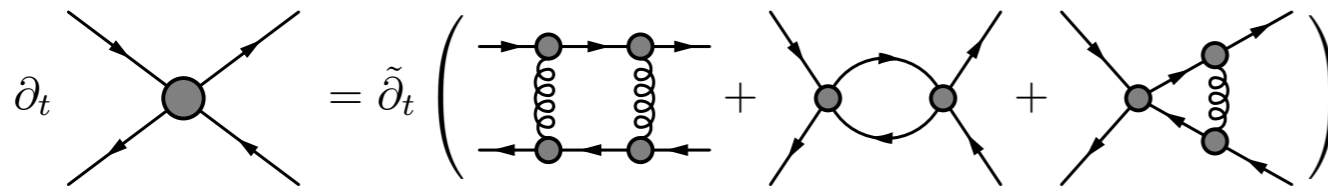


$$\partial_t \lambda_{\pi,k}(P^2) = C_k(P^2) \lambda_{\pi,k}^2(P^2) + A_k(P^2),$$

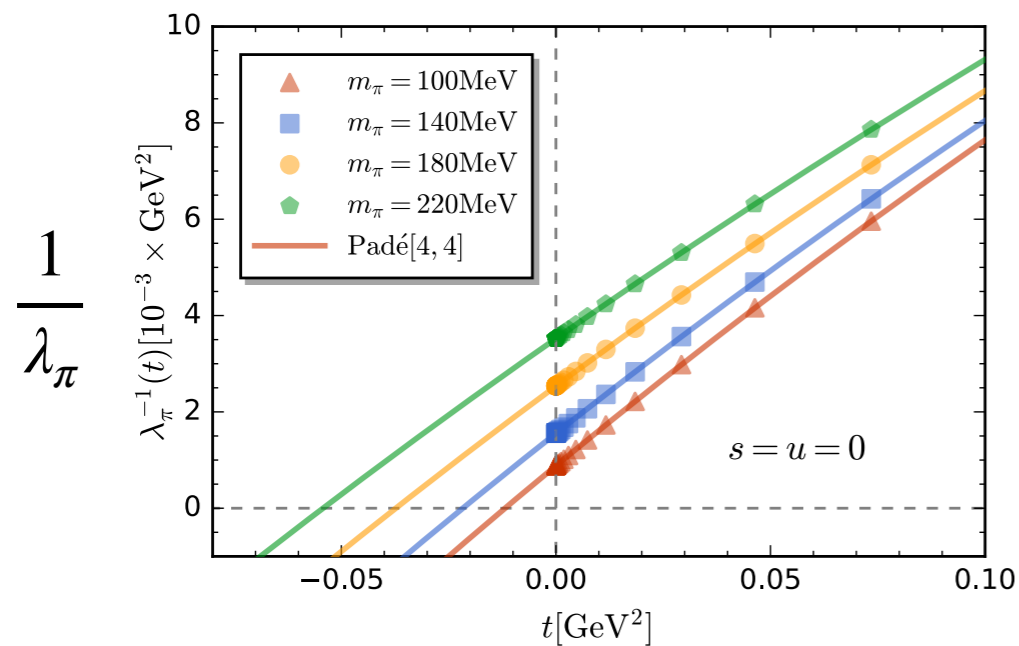


$$\lambda_{\pi,k=0}(P^2) = \frac{\lambda_{\pi,k=\Lambda}}{1 - \lambda_{\pi,k=\Lambda} \int_{\Lambda}^0 C_k(P^2) \frac{dk}{k}},$$

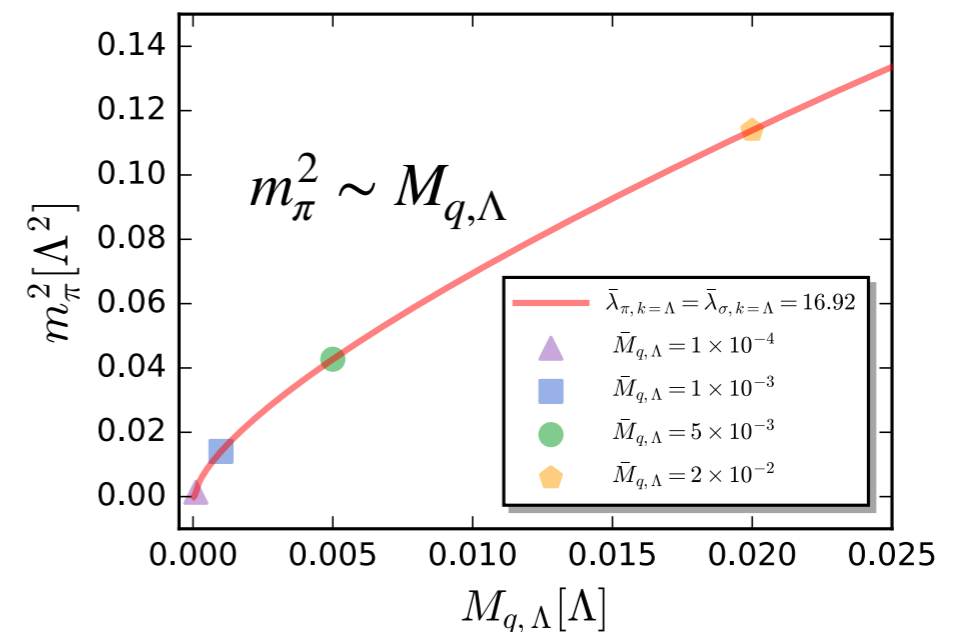
- Flow equation of 4-quark interaction:



Note: playing the same role as the **Bethe-Salpeter equation**.

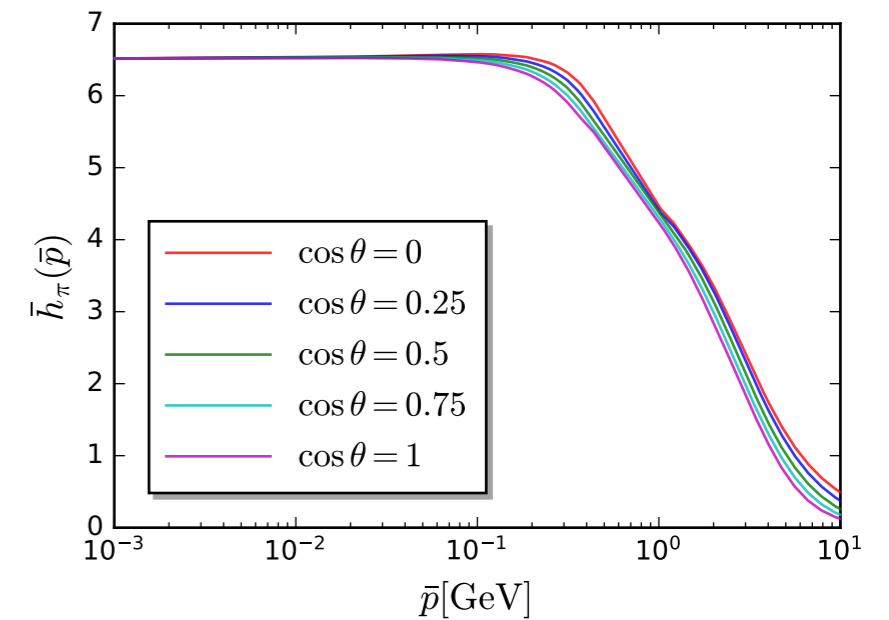
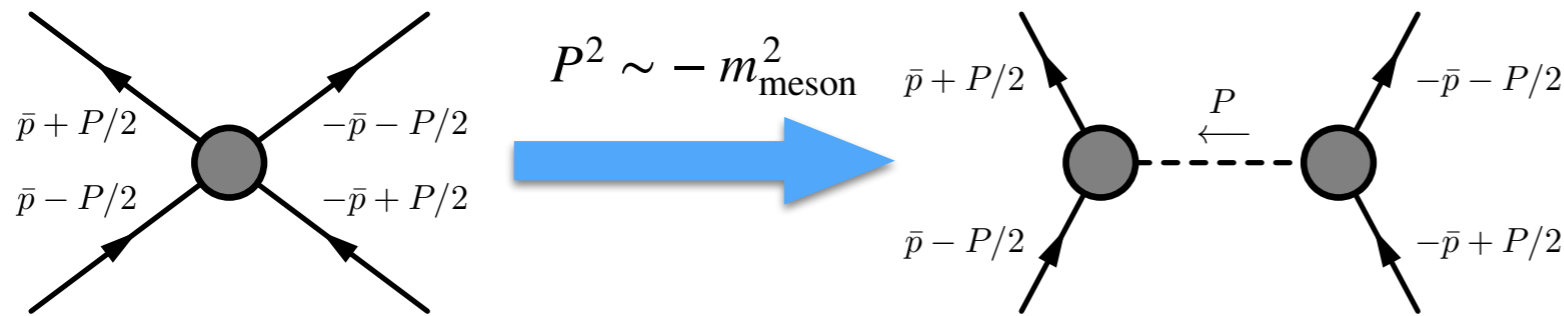


Gell-Mann--Oakes--Renner relation



Bethe-Salpeter amplitude

- Bethe-Salpeter amplitude can be extracted from the 4-quark vertex in the proximity of on-shell momentum of bound states:



The 4-quark vertex near the on-shell momentum

$$\lambda_\pi(P^2, p, \cos \theta) \sim \frac{h_\pi^2(p, \cos \theta)}{P^2 + m_\pi^2}$$

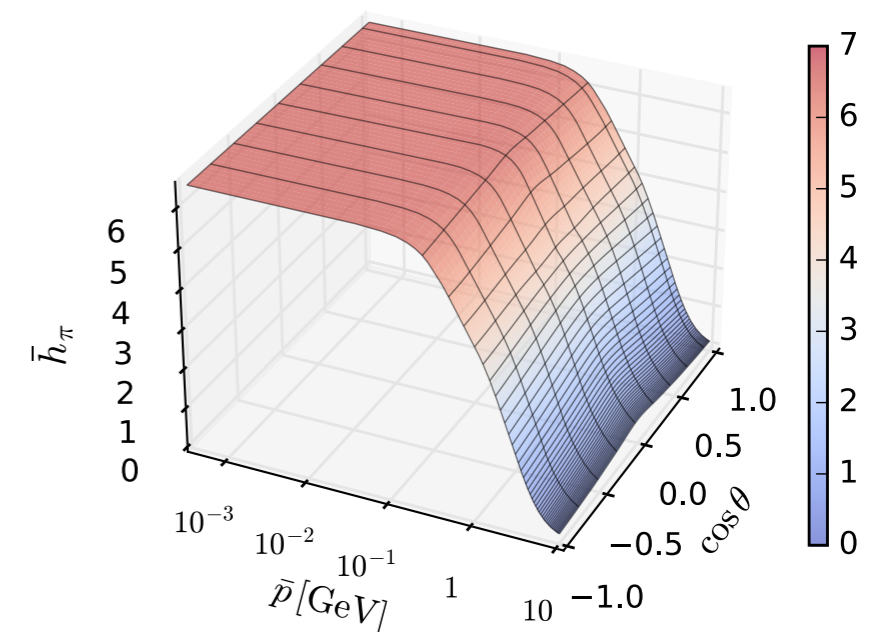
with the BS amplitude

$$h_\pi(p, \cos \theta) = \lim_{P^2 \rightarrow -m_\pi^2} \left[\lambda_\pi(P^2, p, \cos \theta) (P^2 + m_\pi^2) \right]^{1/2}$$

and

$$P_\mu = \sqrt{P^2} (1, 0, 0, 0)$$

$$\bar{p}_\mu = -\bar{p}'_\mu = \sqrt{p^2} (\cos \theta, \sin \theta, 0, 0)$$



QCD within fRG

Glue sector:

$$\partial_t \text{gluon self-energy} = \tilde{\partial}_t \left(\frac{1}{2} \text{gluon loop} + \frac{1}{2} \text{ghost loop} - \text{ghost loop} - \text{ghost loop} \right)$$

$$\partial_t \text{ghost self-energy} = \tilde{\partial}_t \left(\text{ghost loop} \right)$$

$$\partial_t \text{3-gluon vertex} = \tilde{\partial}_t \left(\text{triangle} - \text{triangle} - \text{triangle} + \frac{1}{2} \text{gluon loop} \right)$$

$$\partial_t \text{ghost-gluon vertex} = \tilde{\partial}_t \left(\text{triangle} + \text{triangle} \right)$$

Matter sector:

$$\partial_t \text{quark self-energy} = \tilde{\partial}_t \left(\text{triangle} + \text{triangle} - \text{ghost loop} \right)$$

$$\partial_t \text{ghost self-energy} = \tilde{\partial}_t \left(\text{ghost loop} - \text{ghost loop} \right)$$

$$\partial_t \text{quark-gluon vertex} = \tilde{\partial}_t \left(\text{triangle} - \text{ghost loop} + \text{triangle} \right)$$

QCD with dynamical hadronization

Introducing a RG scale dependent composite field:

$$\hat{\phi}_k(\hat{\phi}), \text{ with } \hat{\phi} = (\hat{A}, \hat{c}, \hat{\bar{c}}, \hat{q}, \hat{\bar{q}}),$$

$$\langle \partial_t \hat{\phi}_k \rangle = \dot{A}_k \bar{q} \tau q + \dot{B}_k \phi + \dot{C}_k \hat{e}_\sigma,$$

Gies, Wetterich, *PRD* 65 (2002) 065001; 69 (2004) 025001;
Pawlowski, *AP* 322 (2007) 2831;
Flörchinger, Wetterich, *PLB* 680 (2009) 371

Wetterich equation is modified as

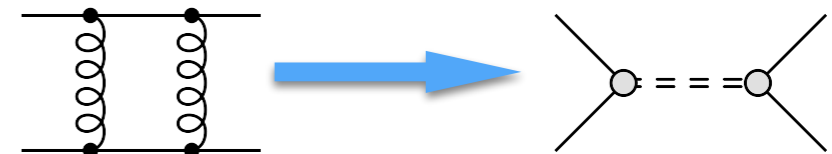
$$\partial_t \Gamma_k[\Phi] = \frac{1}{2} \text{STr}(G_k[\Phi] \partial_t R_k) + \text{Tr} \left(G_{\phi\Phi_a}[\Phi] \frac{\delta \langle \partial_t \hat{\phi}_k \rangle}{\delta \Phi_a} R_\phi \right) - \int \langle \partial_t \hat{\phi}_{k,i} \rangle \left(\frac{\delta \Gamma_k[\Phi]}{\delta \phi_i} + c_\sigma \delta_{i\sigma} \right),$$

Mitter, Pawlowski, Strodthoff, *PRD* 91 (2015) 054035, arXiv:1411.7978;
Braun, Fister, Pawlowski, Rennecke, *PRD* 94 (2016) 034016, arXiv:1412.1045;
Rennecke, *PRD* 92 (2015) 076012, arXiv:1504.03585;
Cyrol, Mitter, Pawlowski, Strodthoff, *PRD* 97 (2018) 054006, arXiv:1706.06326;
WF, Pawlowski, Rennecke, *PRD* 101 (2020) 054032

Flow equation:

$$\partial_t \Gamma_k[\Phi] = \frac{1}{2} \text{Tr}(\text{ghost loop}) - \text{Tr}(\text{dotted ghost loop}) - \text{Tr}(\text{quark loop}) + \frac{1}{2} \text{Tr}(\text{gluon loop})$$

four-quark interaction encoded in Yukawa coupling:

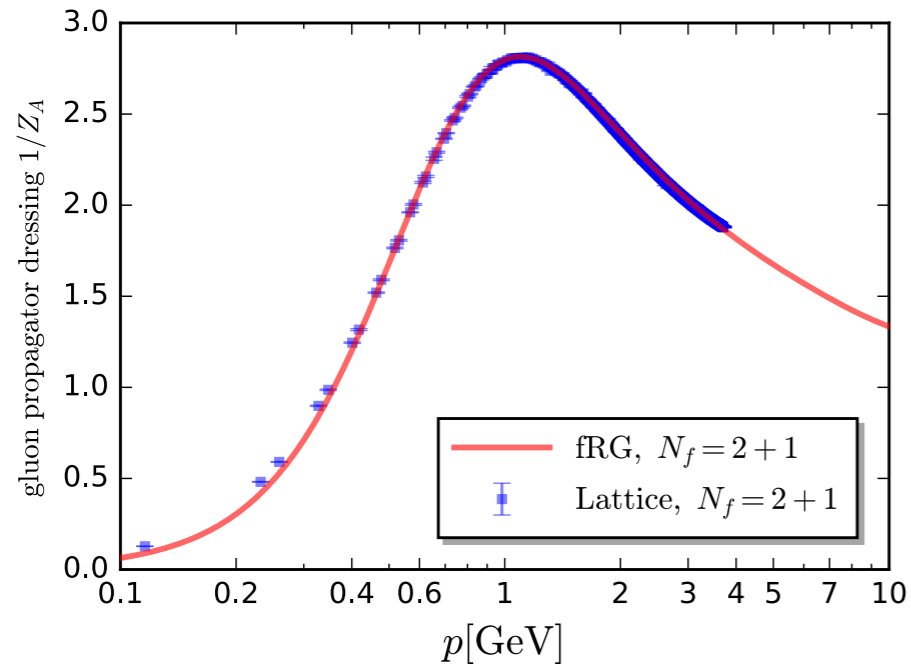


See also recent work:
Ihssen, Pawlowski, Sattler, Wink, arXiv:2408.08413

also cf. talks by Franz R. Sattler and Friederike Ihssen

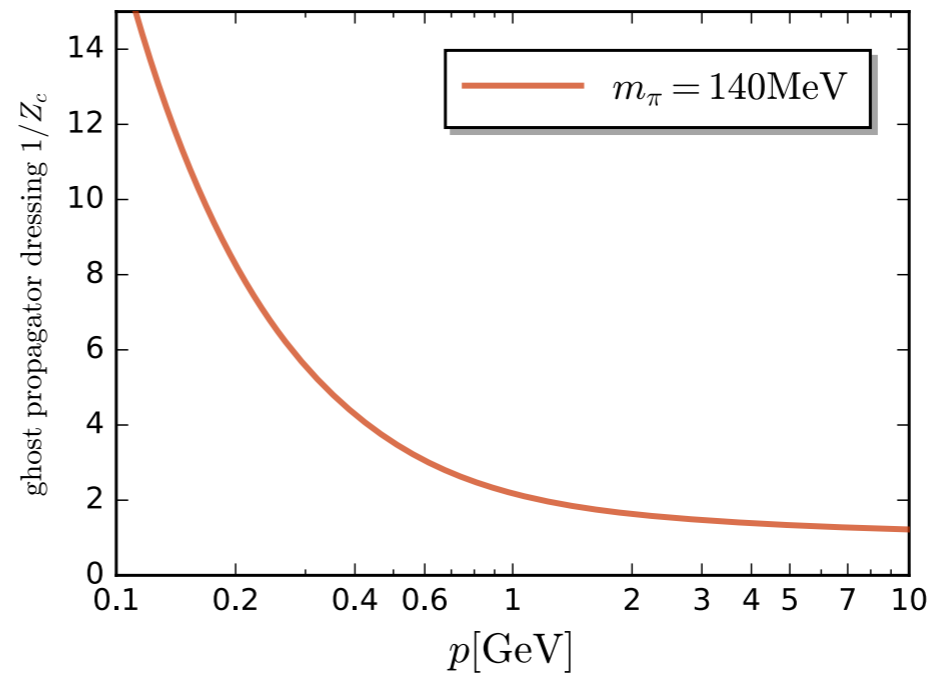
QCD within fRG in vacuum

Gluon dressing:



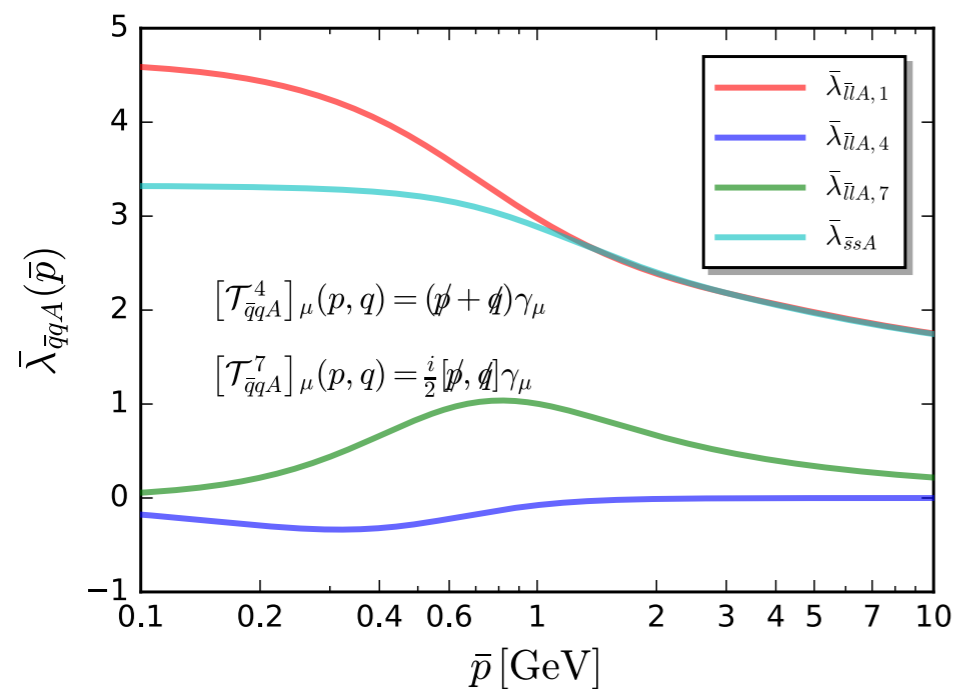
Lattice: Boucaud *et al.*, *PRD* 98 (2018) 114515

Ghost dressing:

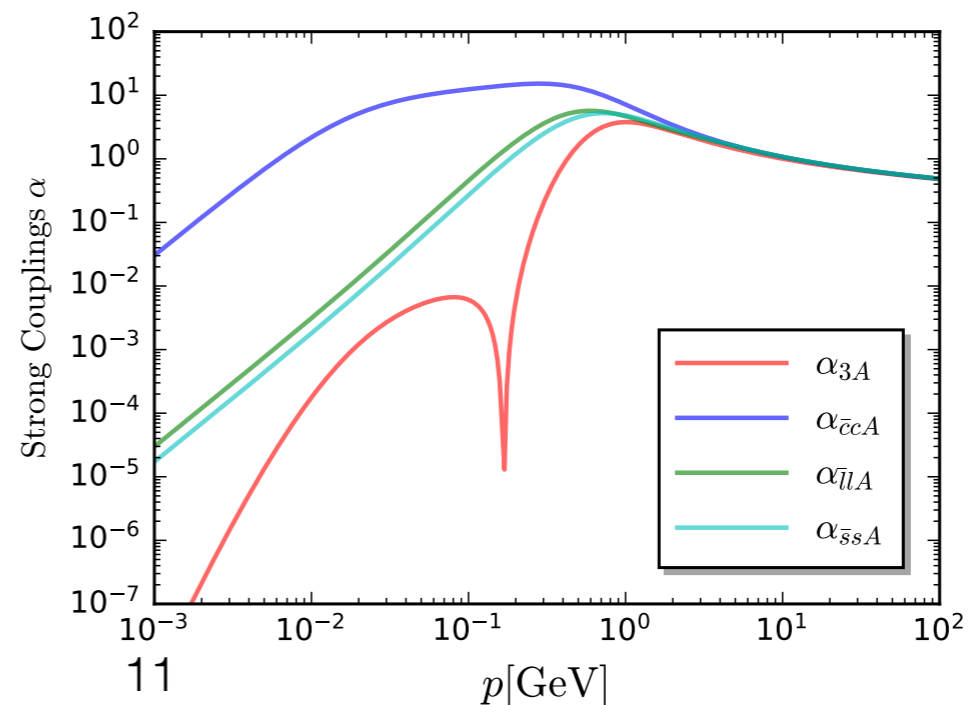


fRG: WF, Huang, Pawłowski, Tan, Zhou, in preparation

Quark-gluon vertex:

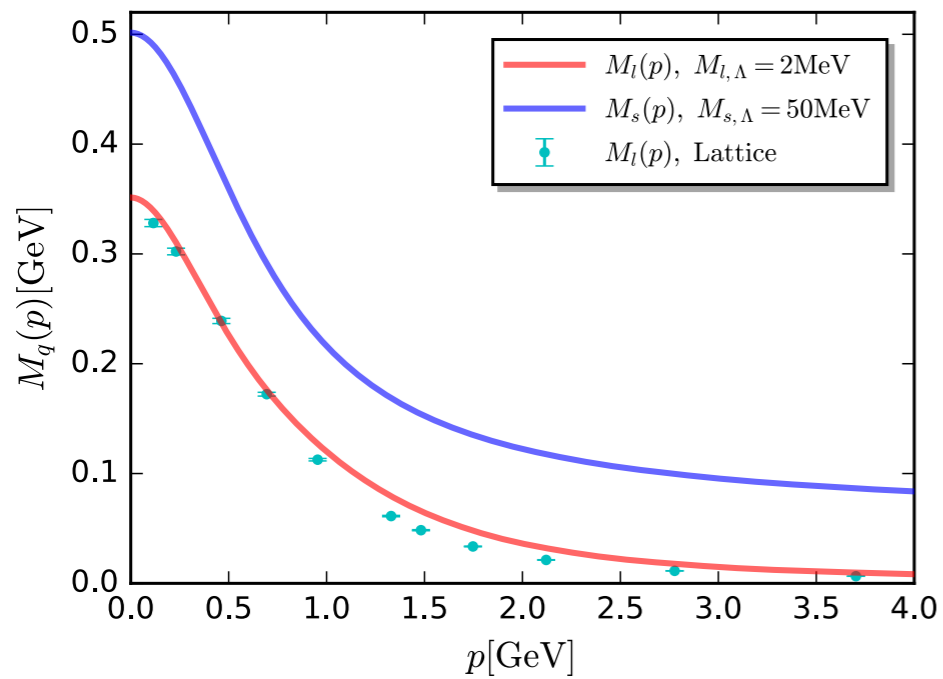


Strong couplings:

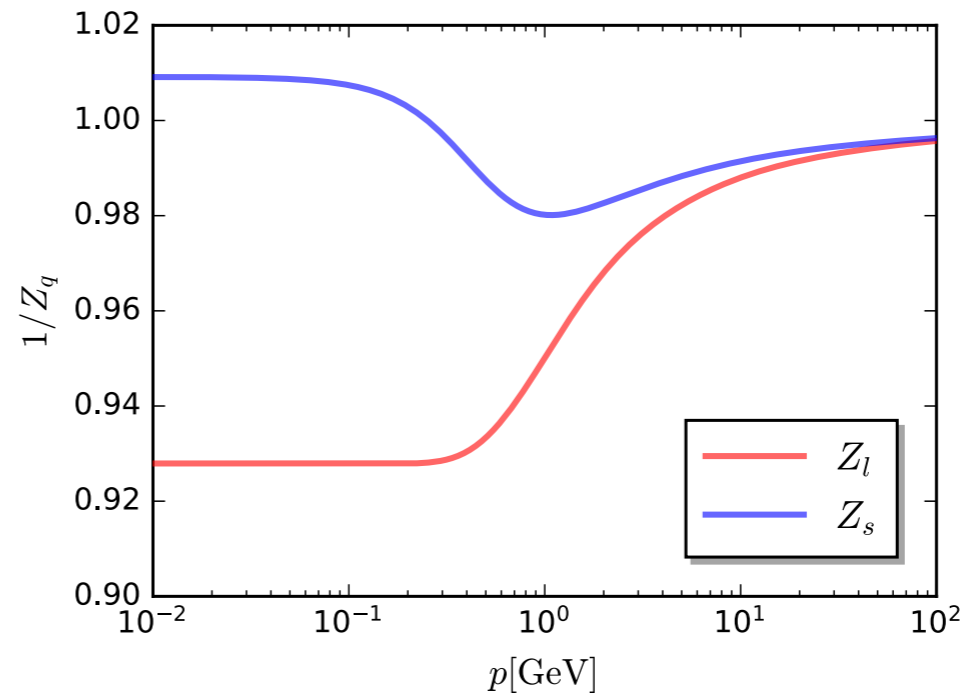


QCD within fRG in vacuum

Quark mass:

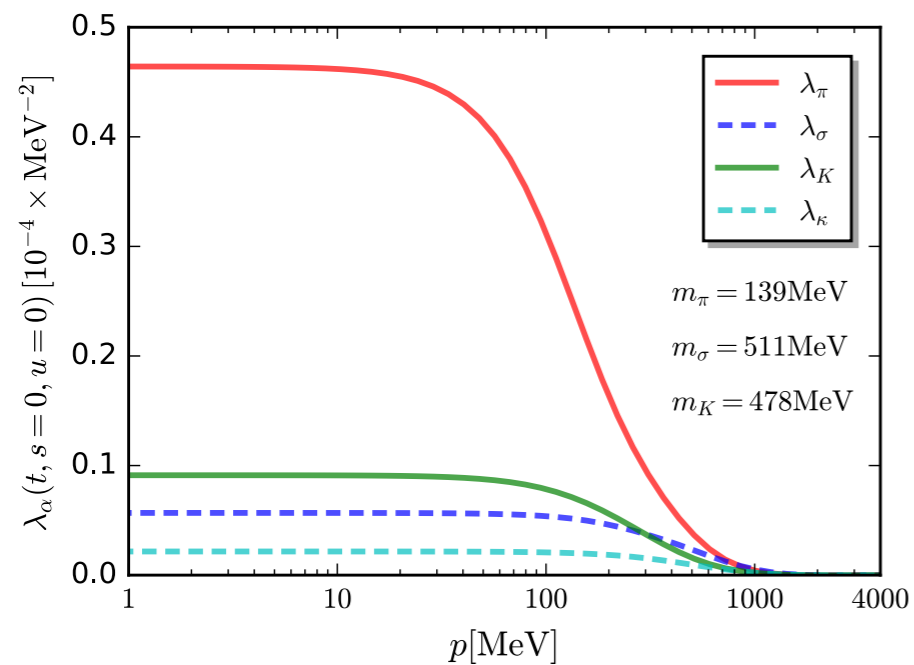


Quark wave function:

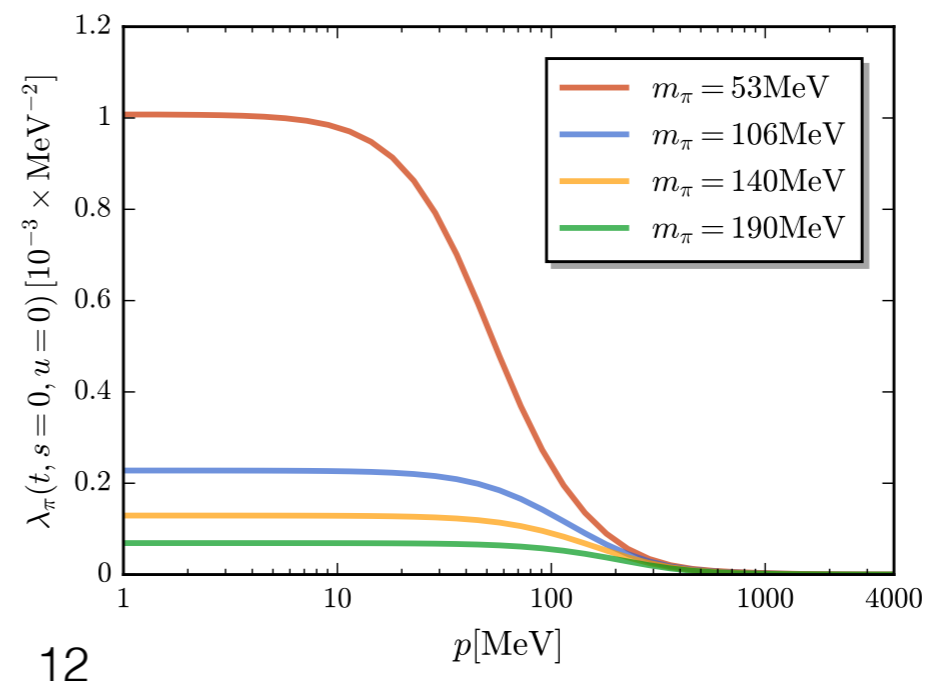


Lattice: Chang *et al.*, *PRD* 104 (2021) 094509

Four-quark vertex:



Four-quark vertex (pion channel):



fRG: WF, Huang,
Pawlowski, Tan,
Zhou, in preparation

Quasi-PDA of pion

- **Bethe-Salpeter amplitude** (unamputated):

$$\chi_\pi(k; P) = G_q(k_+) \Gamma(k; P) G_q(k_-)$$

with

$$\Gamma(k; P) = i\gamma_5 h_\pi(k; P)$$

and $P = (iE_\pi, P_z, 0, 0)$, $E_\pi = \sqrt{P_z^2 + m_\pi^2}$ and $k_\pm = k \pm P/2$

- **Quasi parton distribution amplitude** (qPDA) reads

$$\phi_\pi(x, P_z) = \frac{1}{f_\pi} \text{Tr}_{\text{CD}} \left[\int \frac{d^4 k}{(2\pi)^4} \delta(\tilde{n} \cdot k_+ - x \tilde{n} \cdot P) \gamma_5 \gamma \cdot \tilde{n} \chi_\pi(k; P) \right]$$

with $\tilde{n} = (0, 1, 0, 0)$. Integrating k_3 firstly by using the delta function, one is led to

$$\begin{aligned} \phi_\pi(x, P_z) = & \frac{1}{f_\pi} \frac{4N_c}{(2\pi)^4} \int d^2 k_\perp dk_0 h_\pi(k; P) P_z [x M_q(k_-^2) + (1-x) M_q(k_+^2)] \\ & \times \frac{1}{Z_q(k_+^2) Z_q(k_-^2)} \frac{1}{k_+^2 + M_q^2(k_+^2)} \frac{1}{k_-^2 + M_q^2(k_-^2)} \end{aligned}$$

$$\begin{aligned} k_\mu &= \left(k_0, (x - 1/2)P_z, k_\perp \right), \\ k_{+\mu} &= \left(k_0 + iE_\pi/2, xP_z, k_\perp \right), \\ k_{-\mu} &= \left(k_0 - iE_\pi/2, (x - 1)P_z, k_\perp \right) \end{aligned}$$

Quasi-PDA and PDA

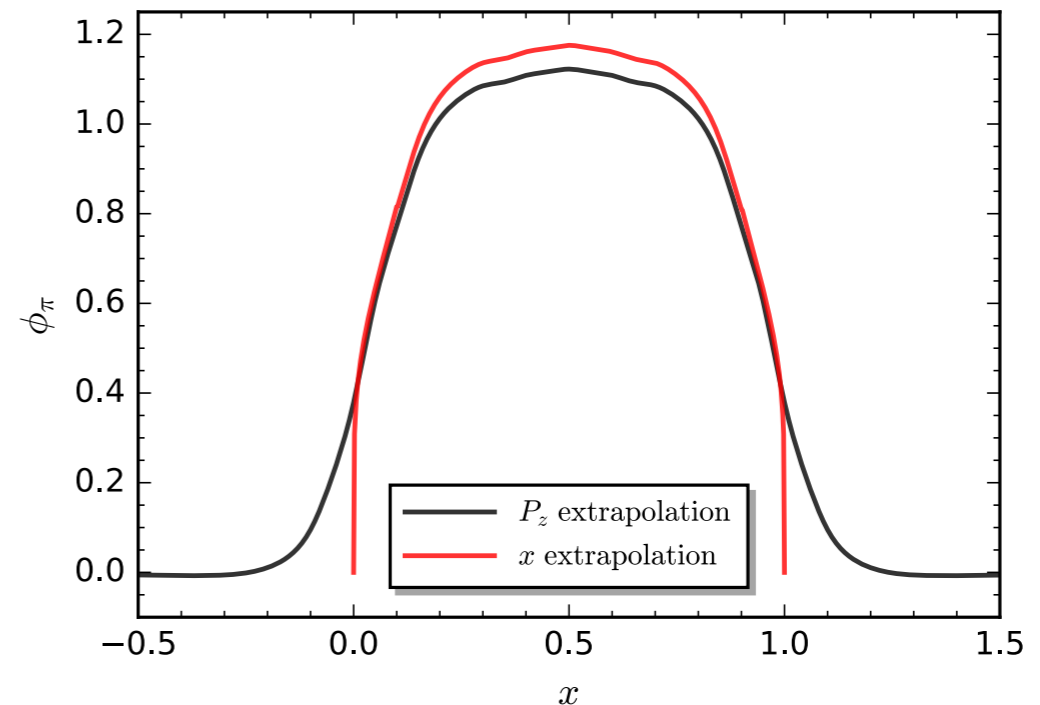
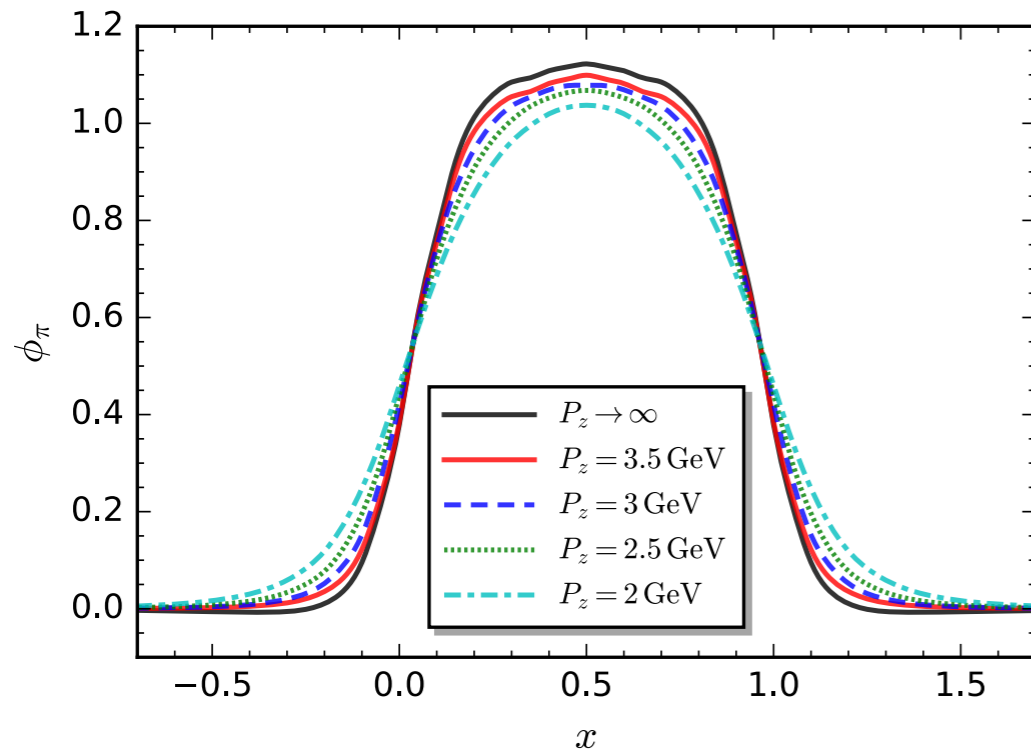
- Quasi-PDA at finite P_z can be used to extrapolate the PDA with $P_z \rightarrow \infty$ based on LaMET Ji, *PRL* 110 (2013) 262002

$$\phi_\pi(x, P_z) = \phi_\pi(x, P_z \rightarrow \infty) + \frac{c_2(x)}{P_z^2} + \mathcal{O}\left(\frac{1}{P_z^4}\right)$$

- But, in the endpoint region, say $0 < x < 0.1$ and $0.9 < x < 1$, LaMET cannot be reliably used, we adopt a phenomenological extrapolation $x^a(1-x)^a$ J. Hua *et al.* (LPC), *PRL* 129 (2022) 132001

Quasi-PDA:

fRG: Chang, WF, Huang, Pawlowski, Zhang, in preparation

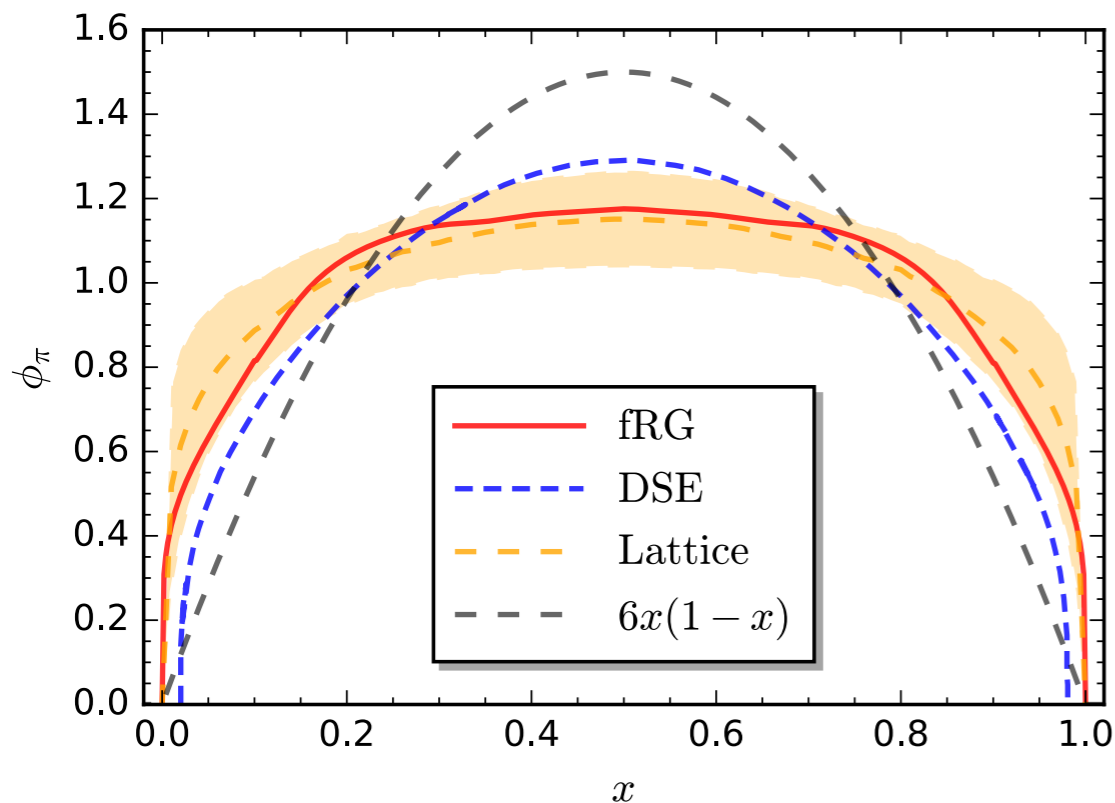


PDA and its moments

- Moments of pion PDA

$$\langle \xi^n \rangle \equiv \int_0^1 dx (2x - 1)^n \phi_\pi(x)$$

Pion PDA:



fRG: Chang, WF, Huang, Pawlowski, Zhang, in preparation

Moments:

Method	ξ_π^2	ξ_π^4	ξ_π^6
fRG (This Work)	0.271	0.142	0.092
Lattice LaMET (LPC)	0.300(41)	-	-
DSE	0.251	0.128	-
Lattice OPE (RQCD)	$0.234_{-6}^{+6}(4)(4)(2)$	-	-
Lattice OPE (RBC and UKQCD)	0.28(1)(2)	-	-
Sum Rule	0.271(13)	0.138(10)	0.087(6)

Lattice LaMET: J. Hua *et al.* (LPC), *PRL* 129 (2022) 132001.

DSE: C. Roberts *et al.*, *PPNP* 120 (2021) 103883; Chang *et al.*, *PRL* 110 (2013) 132001.

Lattice OPE: G. Bali *et al.* (RQCD), *JHEP* 08 (2019) 065; 11 (2020) 37.

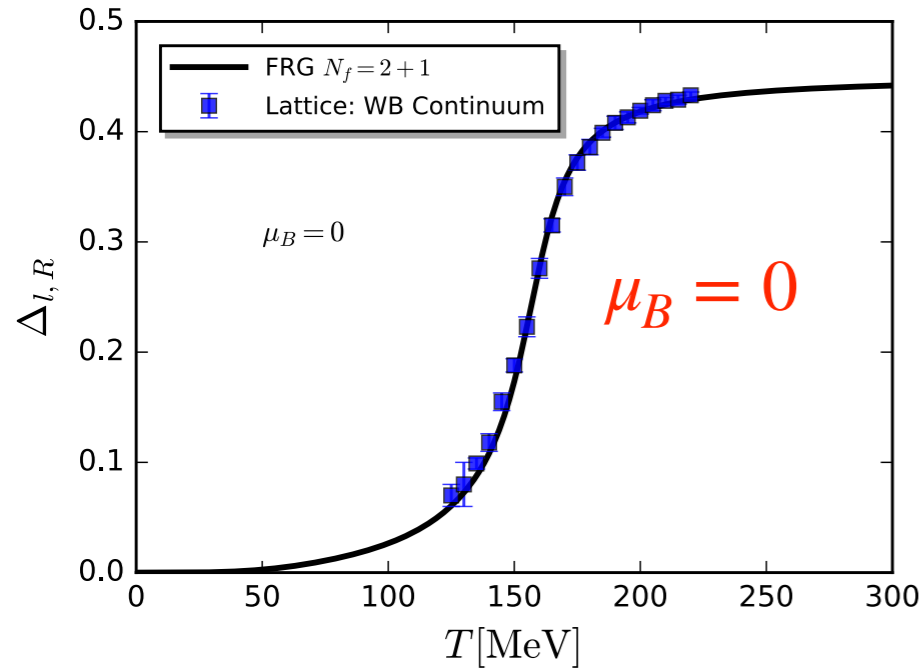
Lattice OPE: R. Arthur *et al.* (RBC and UKQCD), *PRD* 83 (2011) 074505.

Sum rules: P. Ball *et al.*, *JHEP* 08 (2007) 090; T. Zhong *et al.*, *PRD* 104 (2021) 016021

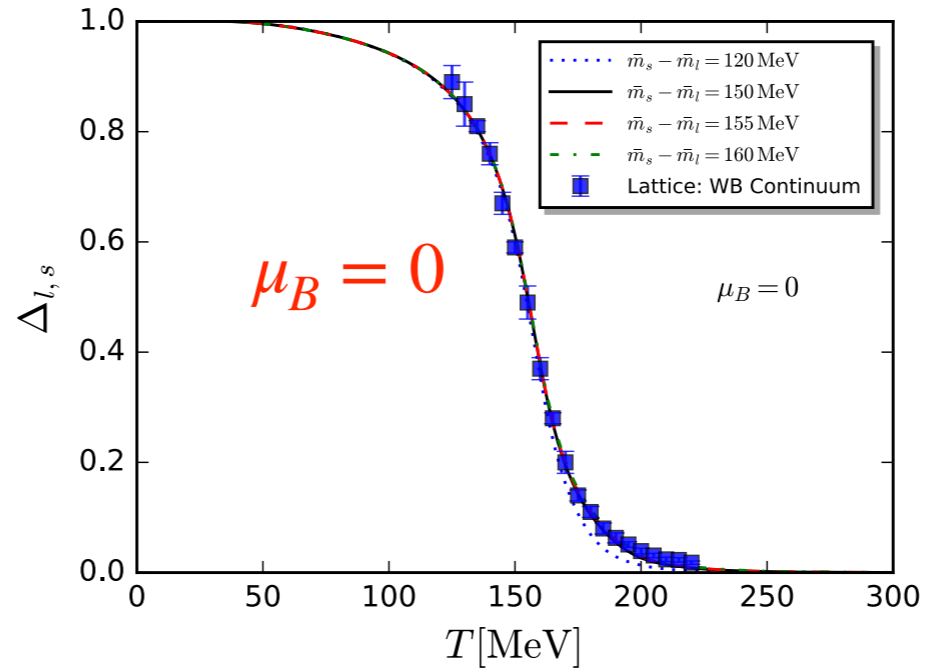
Asymptotic: $6x(1-x)$

QCD phase transitions

Renormalized light quark condensate:

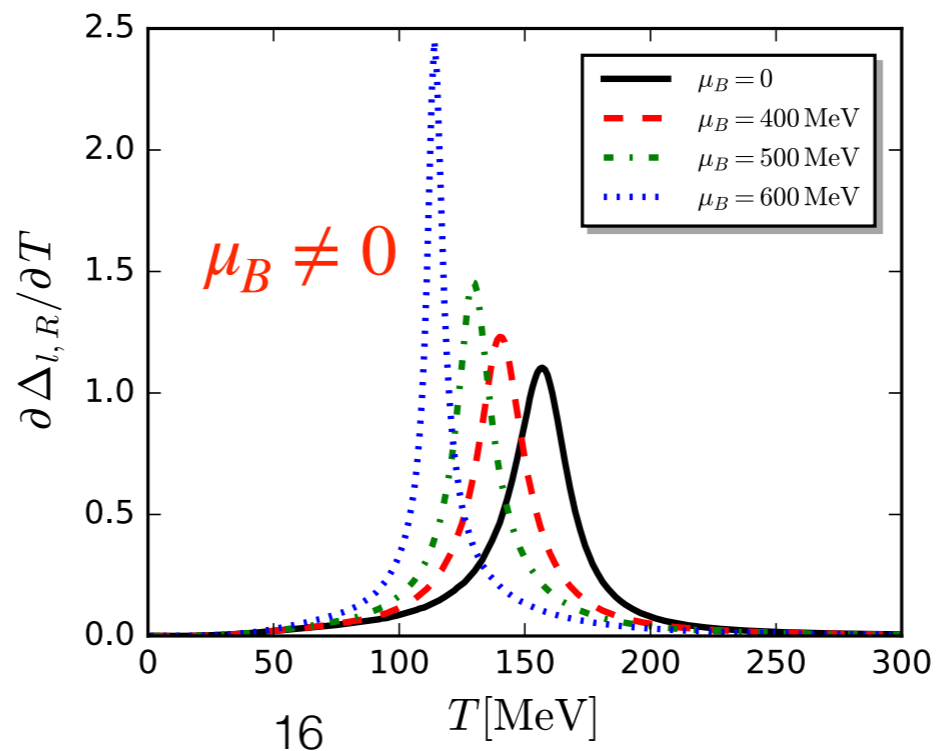
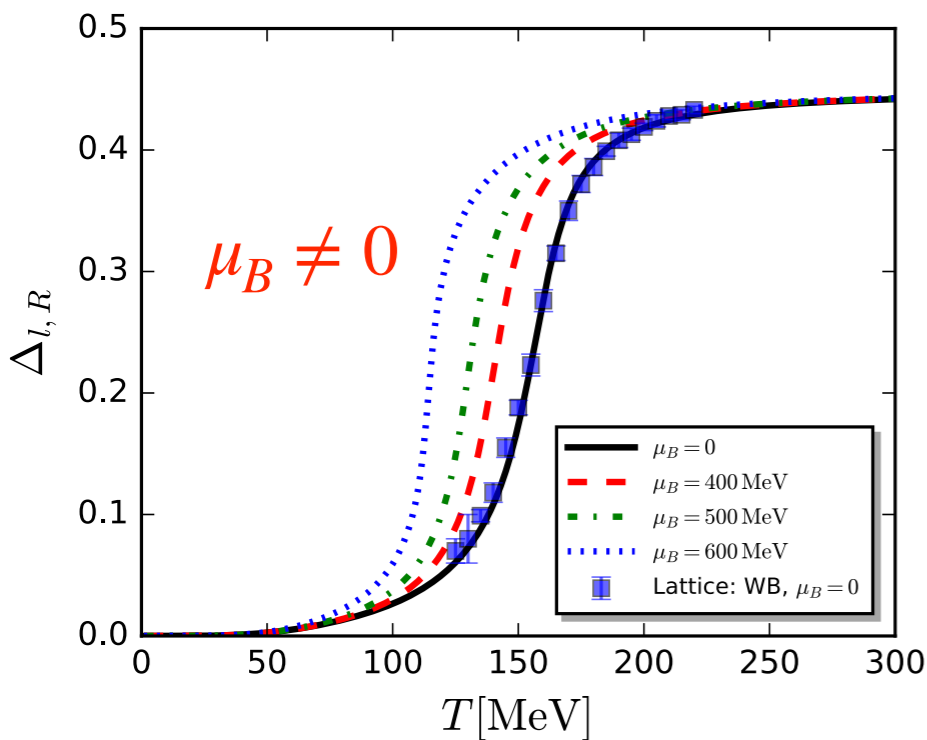


Reduced condensate:



fRG: WF, Pawłowski, Rennecke, *PRD* 101 (2020) 054032

Lattice: Borsanyi *et al.* (WB), *JHEP* 09 (2010) 073



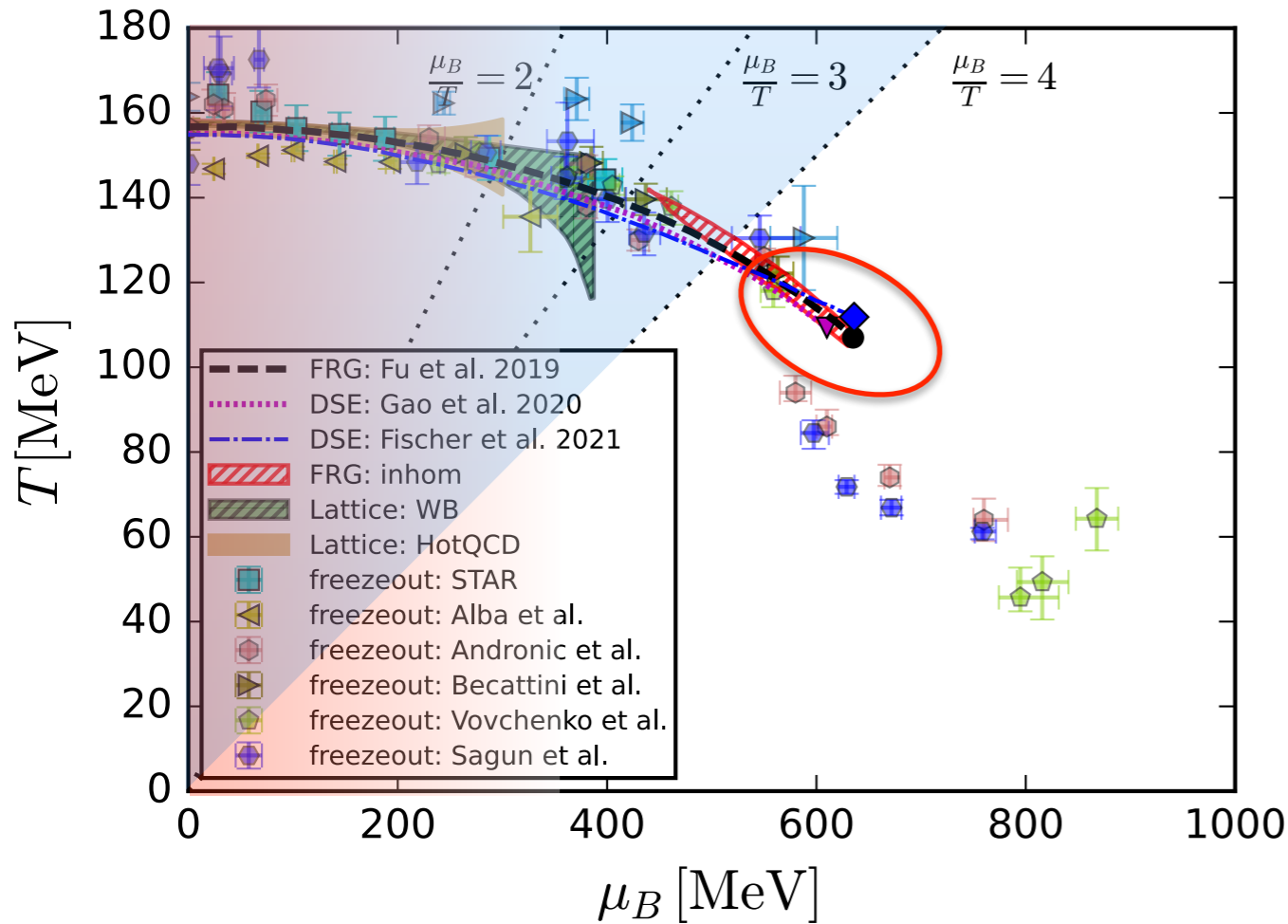
Quark condensate:

$$\Delta_{q_i} \simeq -m_{q_i}^0 T \sum_{n \in \mathbb{Z}} \int \frac{d^3 q}{(2\pi)^3} \text{tr} G_{q_i \bar{q}_i}(q),$$

Reduced condensate:

$$\Delta_{l,s}(T, \mu_q) = \frac{\Delta_l(T, \mu_q) - \left(\frac{m_l^0}{m_s^0}\right)^2 \Delta_s(T, \mu_q)}{\Delta_l(0,0) - \left(\frac{m_l^0}{m_s^0}\right)^2 \Delta_s(0,0)}$$

CEP from first-principles functional QCD



Passing through strict benchmark tests in comparison to lattice QCD at vanishing and small μ_B .

Regime of quantitative reliability of functional QCD with $\mu_B/T \lesssim 4$.

also cf. talks by Rui Wen

Estimates of the location of CEP from first-principles functional QCD:

fRG:

$$\bullet (T, \mu_B)_{\text{CEP}} = (107, 635)\text{MeV}$$

fRG: WF, Pawłowski, Rennecke, *PRD* 101 (2020), 054032

DSE:

$$\blacktriangledown (T, \mu_B)_{\text{CEP}} = (109, 610)\text{MeV}$$

DSE (fRG): Gao, Pawłowski, *PLB* 820 (2021) 136584

$$\blacklozenge (T, \mu_B)_{\text{CEP}} = (112, 636)\text{MeV}$$

DSE: Gunkel, Fischer, *PRD* 104 (2021) 5, 054022

- No CEP observed in $\mu_B/T \lesssim 2 \sim 3$ from lattice QCD. Karsch, *PoS CORFU2018* (2019)163
- Recent studies of QCD phase structure from both fRG and DSE have shown convergent estimate for the location of CEP: $600 \text{ MeV} \lesssim \mu_{B\text{CEP}} \lesssim 650 \text{ MeV}$.

CEP from other approaches

Recent estimates of the location of CEP:

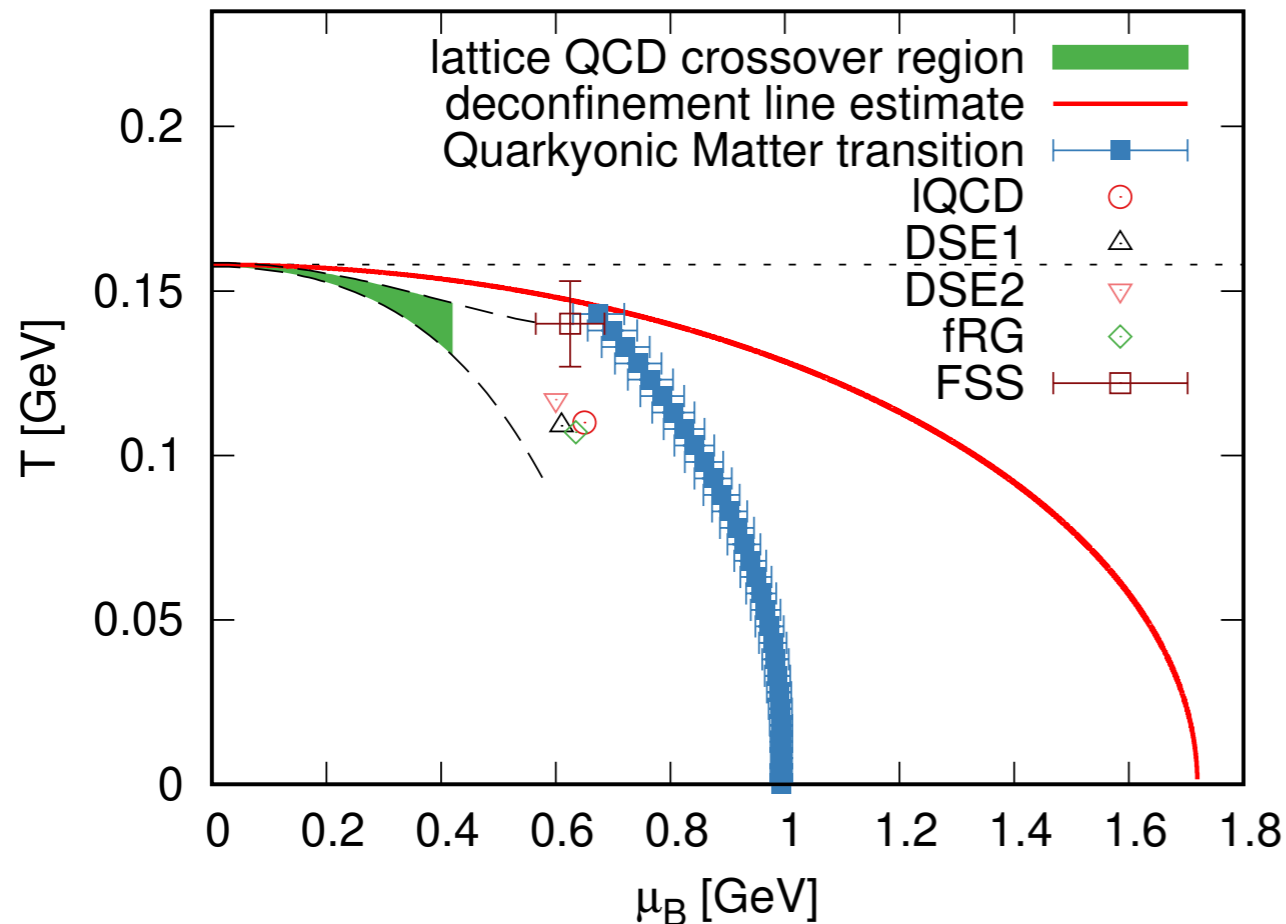


Figure from:
Bluhm, Fujimoto, McLerran, Nahrgang, arXiv:2409.12088

- fRG:
WF, Pawłowski, Rennecke, *PRD* 101 (2020), 054032, arXiv:1909.02991.
- DSE1:
Gao, Pawłowski, *PLB* 820 (2021) 136584, arXiv:2010.13705.
- DSE2:
Gunkel, Fischer, *PRD* 104 (2021) 054022, arXiv:2106.08356.
- Lattice extrapolation (Yang-Lee edge singularities):
David A. Clarke *et al.*, arXiv:2405.10196.
- Finite-size-scaling analysis:
A. Sorensen, P. Sorensen, arXiv:2405.10278.

- Estimates of the location of CEP in the QCD phase diagram have arrived at convergence from different approaches.

CEP from other approaches

Recent estimates of the location of CEP:

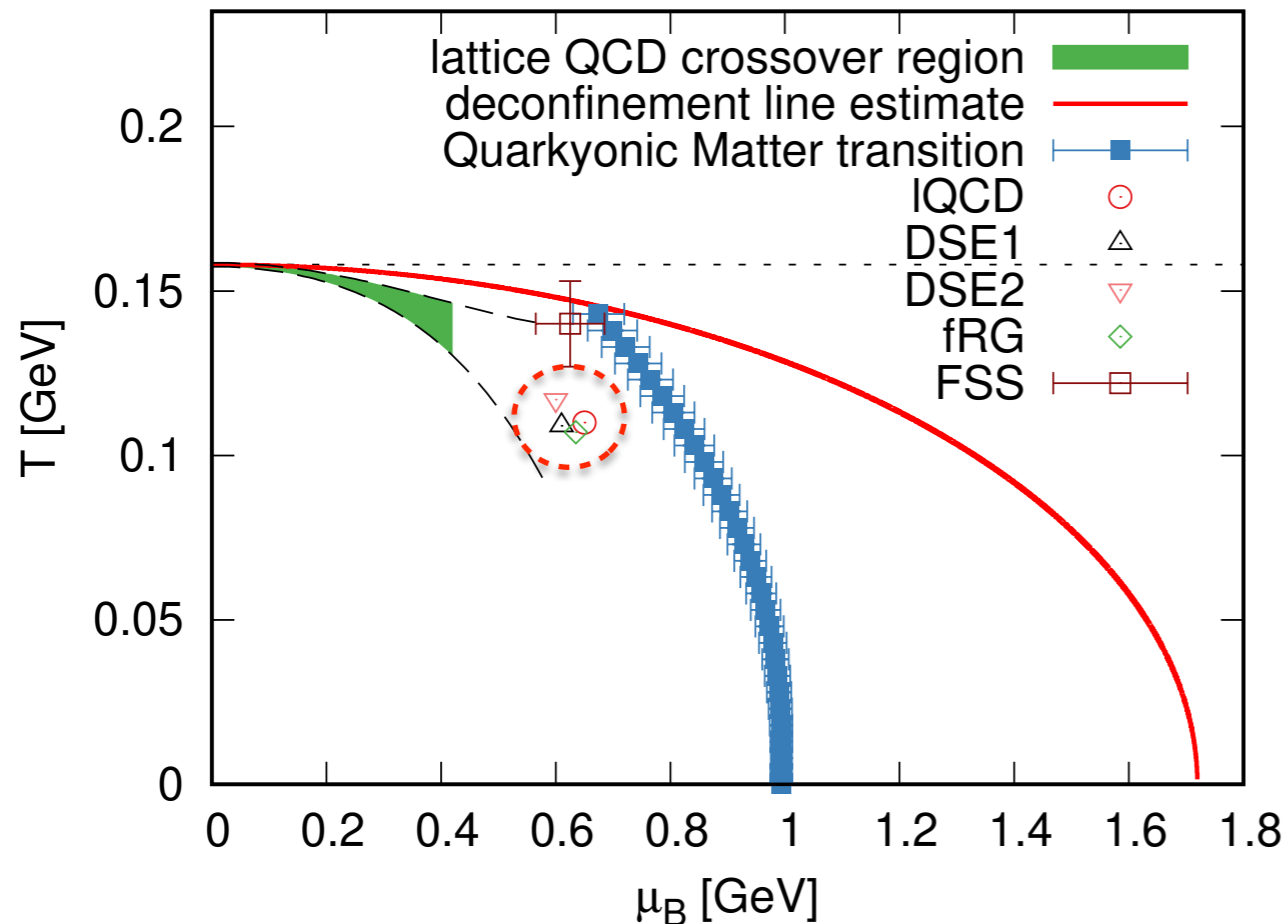


Figure from:
Blum, Fujimoto, McLerran, Nahrgang, arXiv:2409.12088

fRG:

WF, Pawłowski, Rennecke, *PRD* 101 (2020), 054032, arXiv:1909.02991.

DSE1:

Gao, Pawłowski, *PLB* 820 (2021) 136584, arXiv:2010.13705.

DSE2:

Gunkel, Fischer, *PRD* 104 (2021) 054022, arXiv:2106.08356.

Lattice extrapolation (Yang-Lee edge singularities):

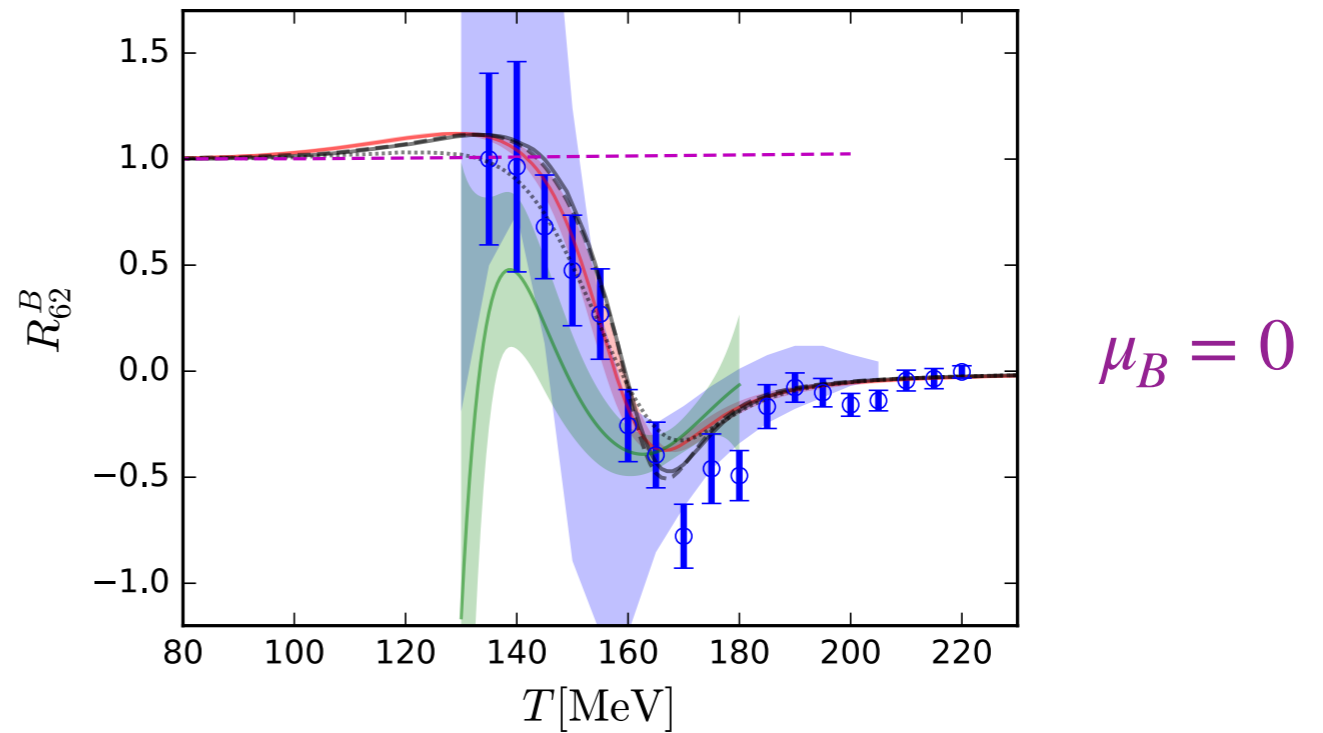
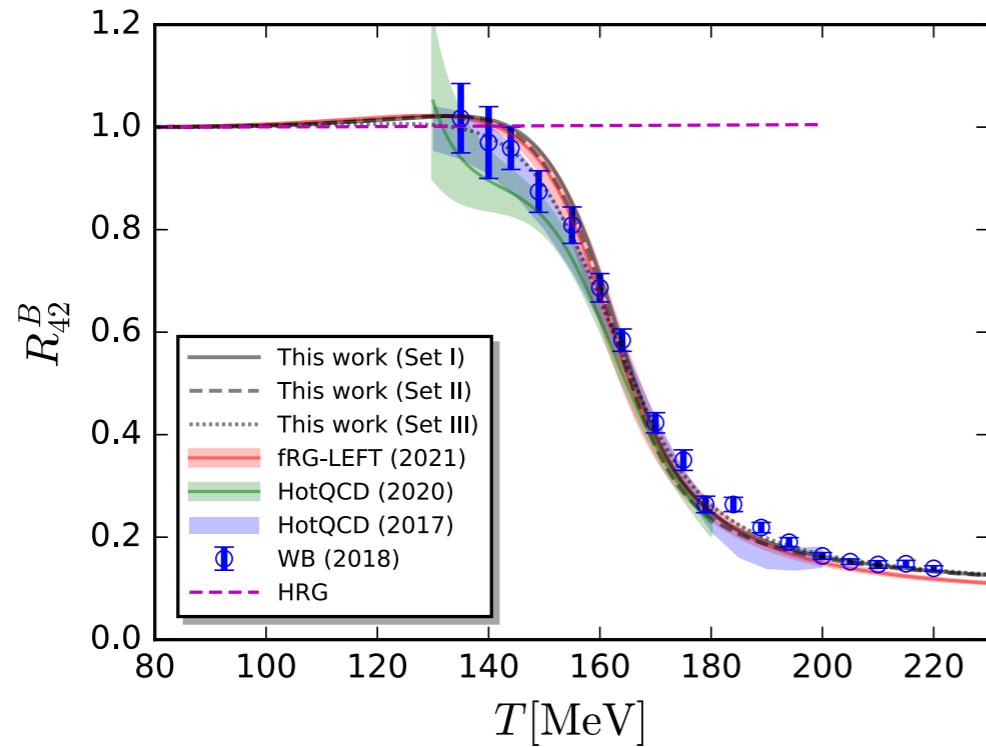
David A. Clarke *et al.*, arXiv:2405.10196.

Finite-size-scaling analysis:

A. Sorensen, P. Sorensen, arXiv:2405.10278.

- Estimates of the location of CEP in the QCD phase diagram have arrived at convergence from different approaches.

Baryon number fluctuations



fRG: WF, Luo, Pawłowski, Rennecke, Yin, arXiv: 2308.15508;
WF, Luo, Pawłowski, Rennecke, Wen, Yin, *PRD* 104 (2021) 094047

HotQCD: A. Bazavov *et al.*, arXiv: *PRD* 95 (2017), 054504; *PRD* 101 (2020), 074502

WB: S. Borsanyi *et al.*, arXiv: *JHEP* 10 (2018) 205

baryon number fluctuations

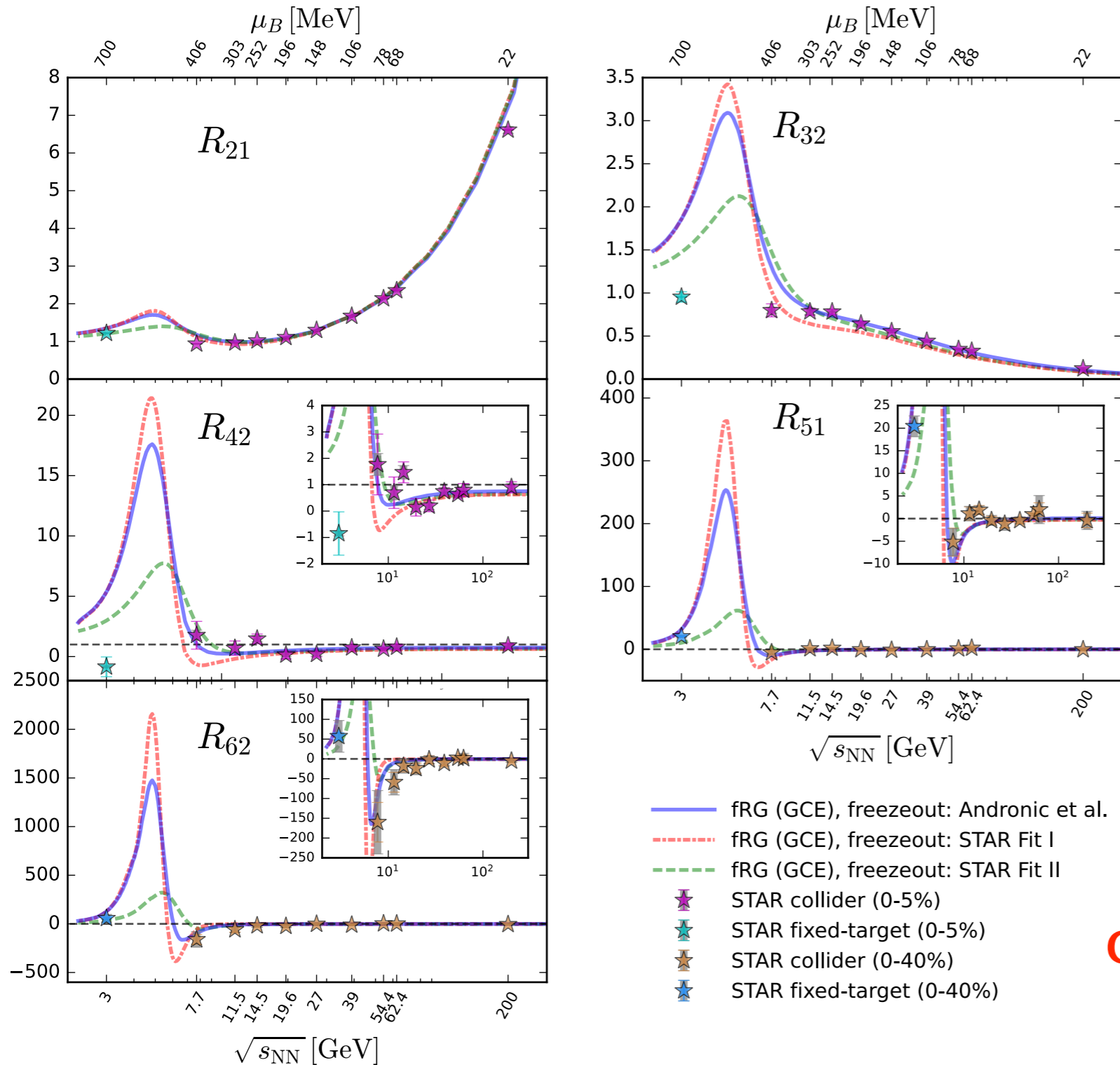
$$\chi_n^B = \frac{\partial^n}{\partial(\mu_B/T)^n} \frac{p}{T^4} \quad R_{nm}^B = \frac{\chi_n^B}{\chi_m^B}$$

relation to the cumulants

$$\frac{M}{VT^3} = \chi_1^B, \quad \frac{\sigma^2}{VT^3} = \chi_2^B, \quad S = \frac{\chi_3^B}{\chi_2^B \sigma}, \quad \kappa = \frac{\chi_4^B}{\chi_2^B \sigma^2},$$

- In comparison to lattice results and our former results, the improved results of baryon number fluctuations at vanishing chemical potential in the QCD-assisted LEFT are **convergent** and **consistent**.

Grand canonical fluctuations at the freeze-out



STAR: Adam *et al.* (STAR), *PRL* 126 (2021) 092301;
 Abdallah *et al.* (STAR), *PRL* 128 (2022) 202303;
 Aboona *et al.* (STAR), *PRL* 130 (2023) 082301

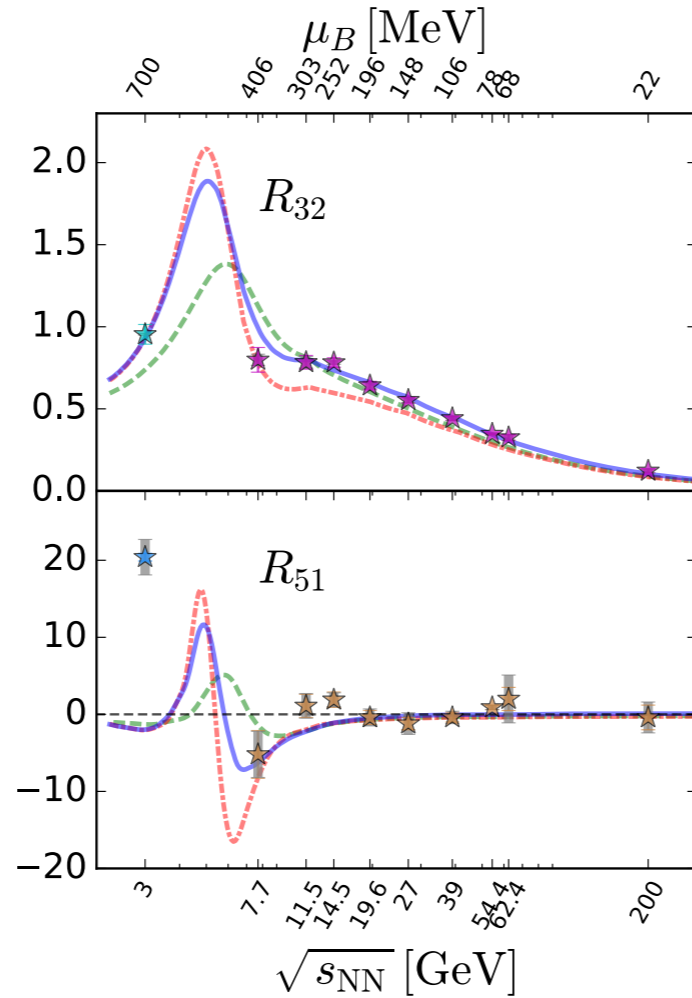
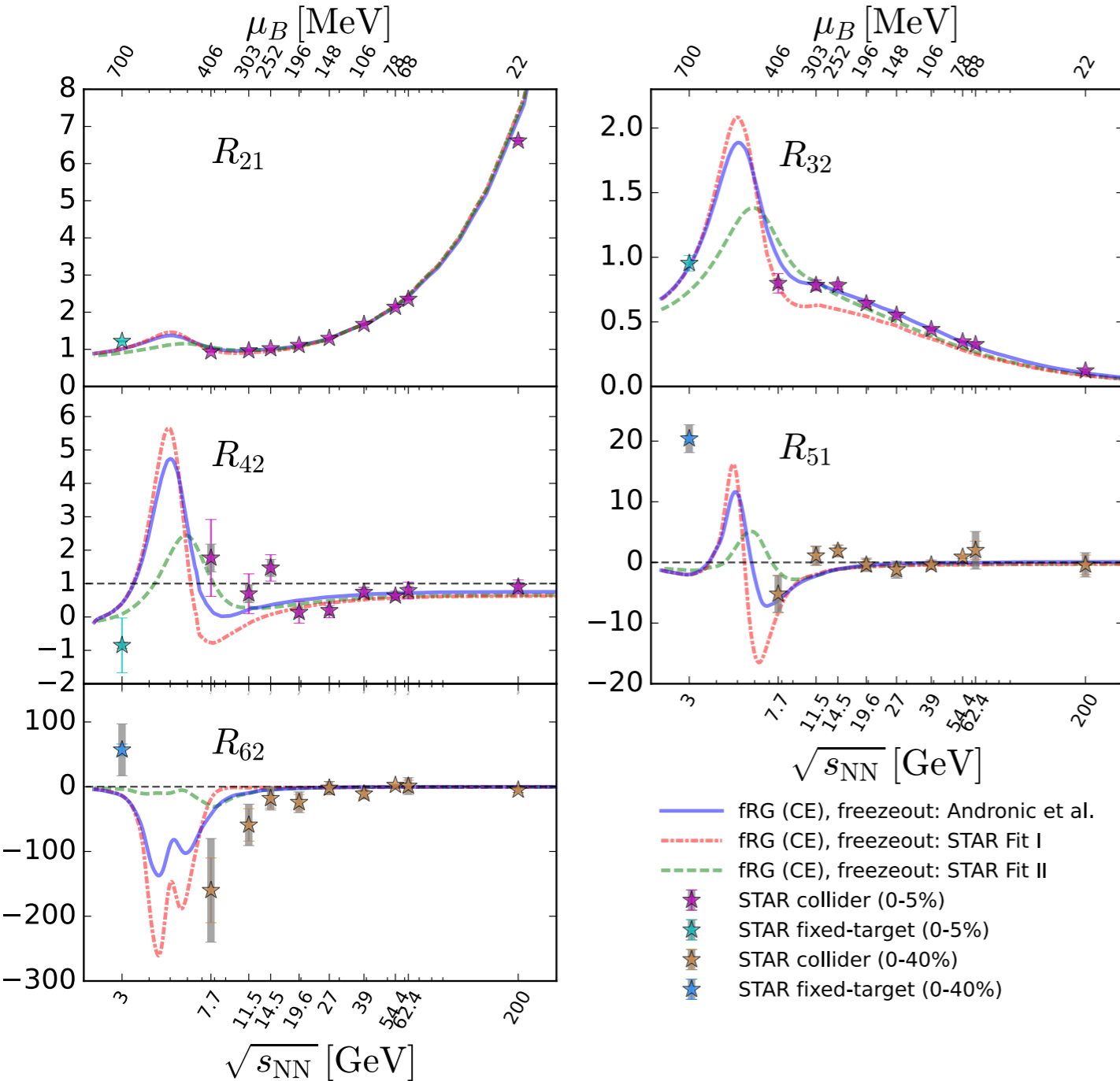
fRG: WF, Luo, Pawlowski, Rennecke, Yin, arXiv:
 2308.15508

- Results in fRG are obtained in the QCD-assisted LEFT with a CEP at $(T_{\text{CEP}}, \mu_{B_{\text{CEP}}}) = (98, 643)$ MeV.
- Peak structure is found in 3 GeV $\lesssim \sqrt{s_{\text{NN}}} \lesssim 7.7$ GeV.
- Agreement between the theory and experiment is worsening with $\sqrt{s_{\text{NN}}} \gtrsim 11.5$ GeV.
- Effects of global baryon number conservation in the regime of low collision energy should be taken into account.

Caveat:

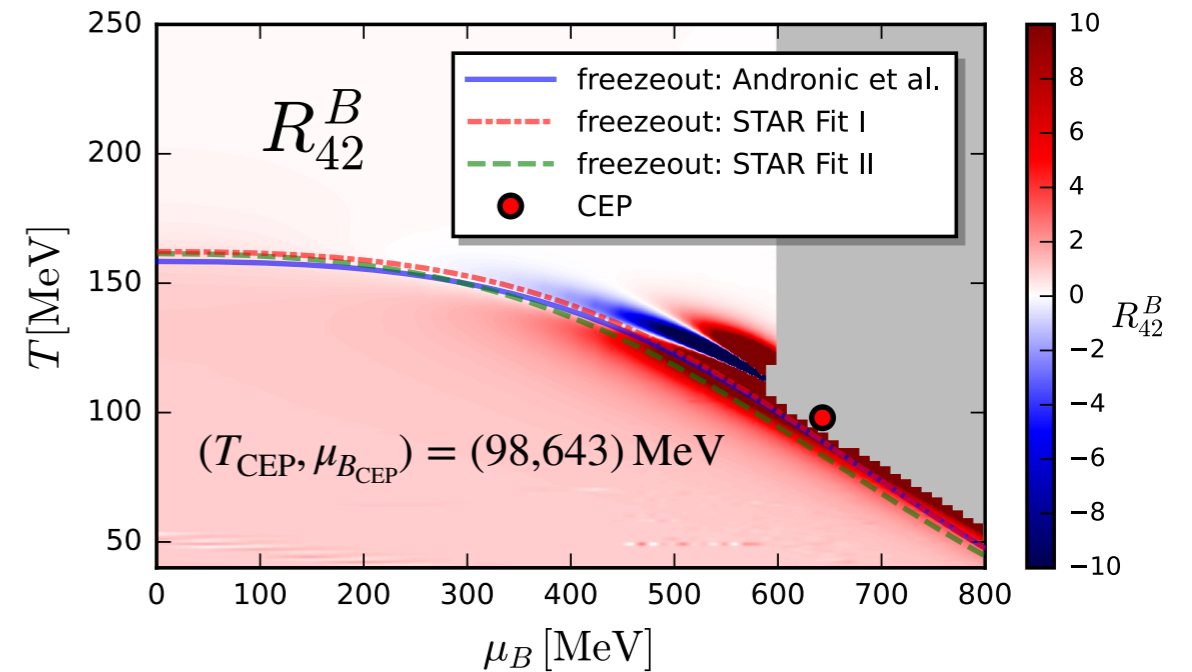
Fluctuations of baryon number in theory are compared with those of proton number in experiments.

Canonical fluctuations at the freeze-out



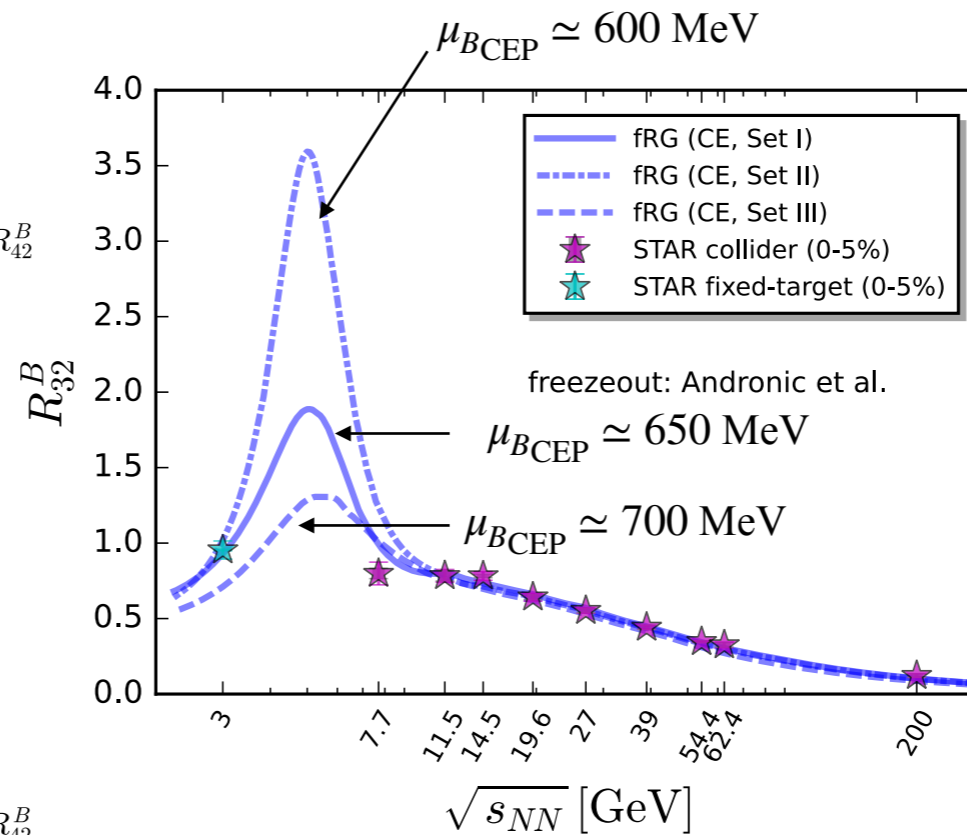
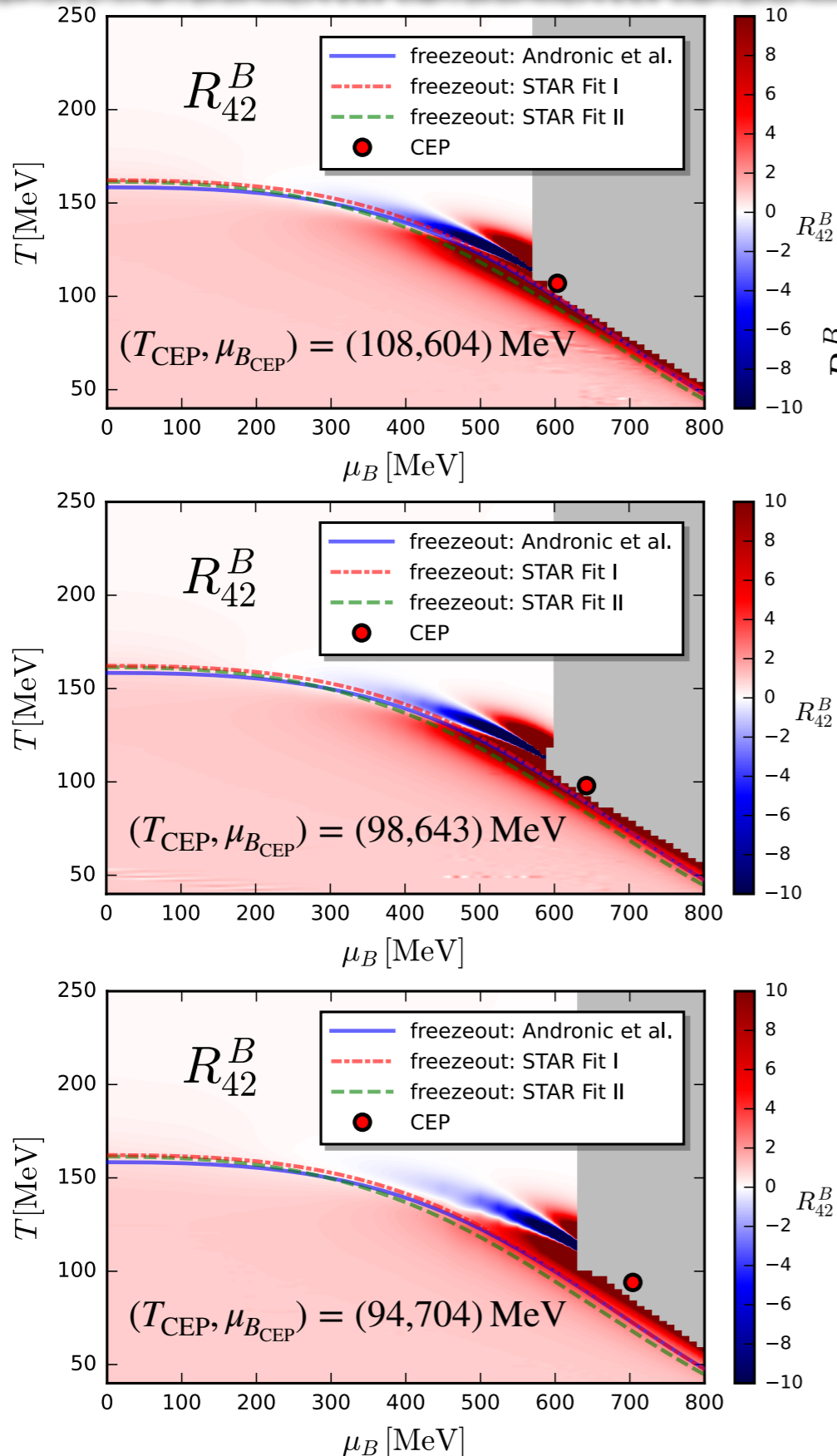
STAR: Adam *et al.* (STAR), *PRL* 126 (2021) 092301;
 Abdallah *et al.* (STAR), *PRL* 128 (2022) 202303;
 Aboona *et al.* (STAR), *PRL* 130 (2023) 082301

fRG: WF, Luo, Pawłowski, Rennecke, Yin, arXiv:
 2308.15508



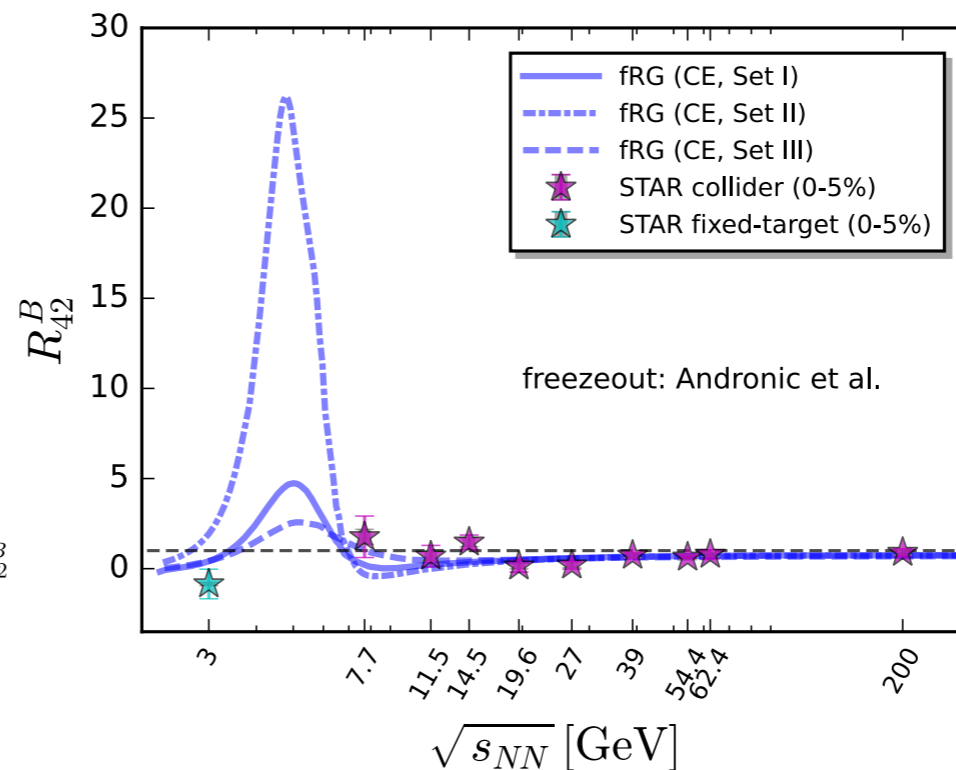
- Peak structure is found in 3 GeV $\lesssim \sqrt{s_{NN}} \lesssim 7.7 \text{ GeV}$.
- Position of peak in R_{42} is $\mu_{B_{\text{peak}}} = 536, 541$ and 486 MeV for the three freeze-out curves, significantly smaller than $\mu_{B_{\text{CEP}}} = 643 \text{ MeV}$.

Dependence on the location of the CEP



STAR: Adam *et al.* (STAR), *PRL* 126 (2021) 092301

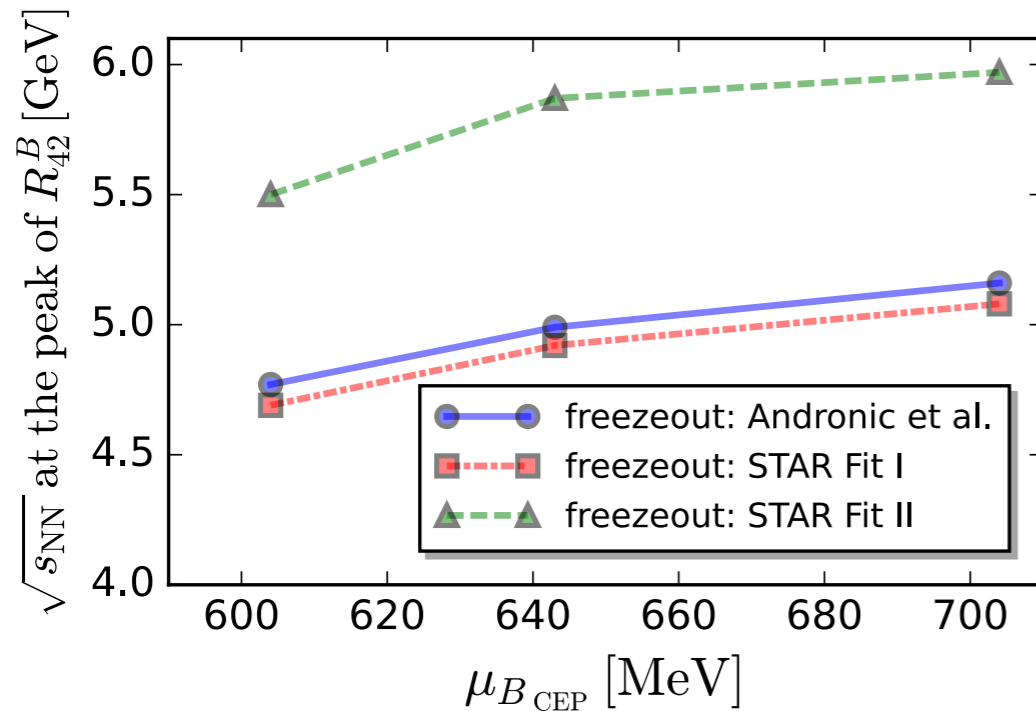
fRG: WF, Luo, Pawlowski, Rennecke, Yin, arXiv: 2308.15508



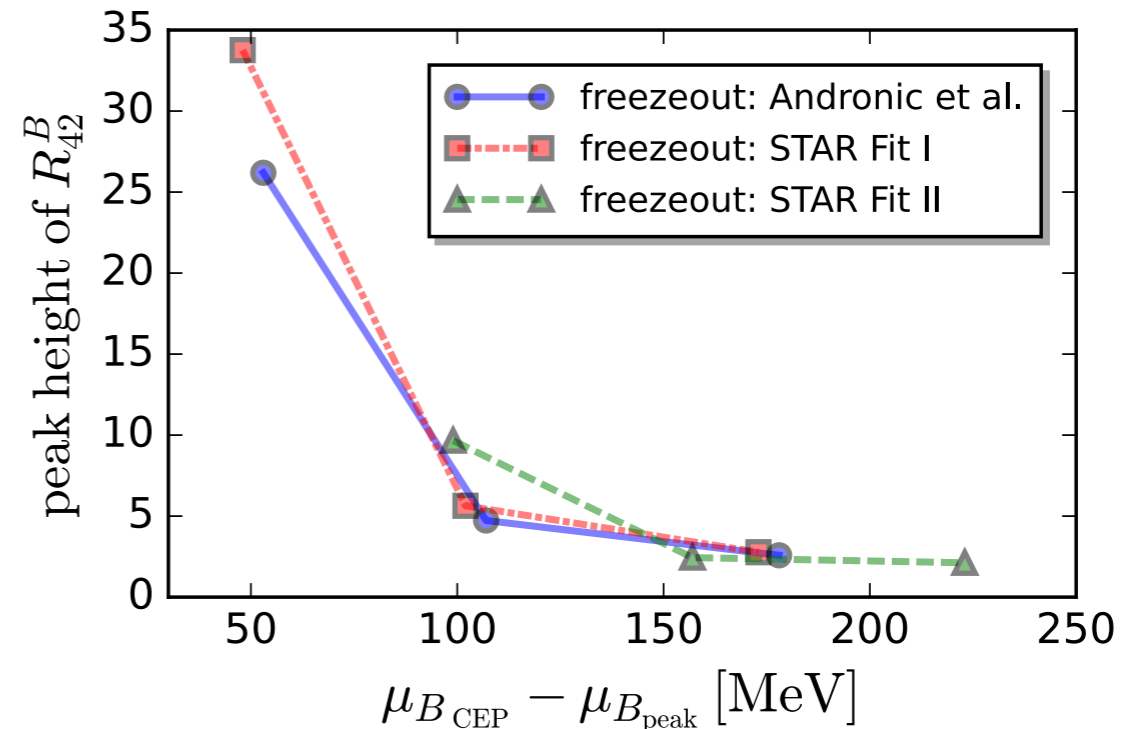
- **Position** of the peak is **insensitive** to the location of CEP.
- **Height** of peak **decreases** as CEP moves towards larger μ_B .

Ripples of the QCD critical point

Position of peak:



Height of peak:

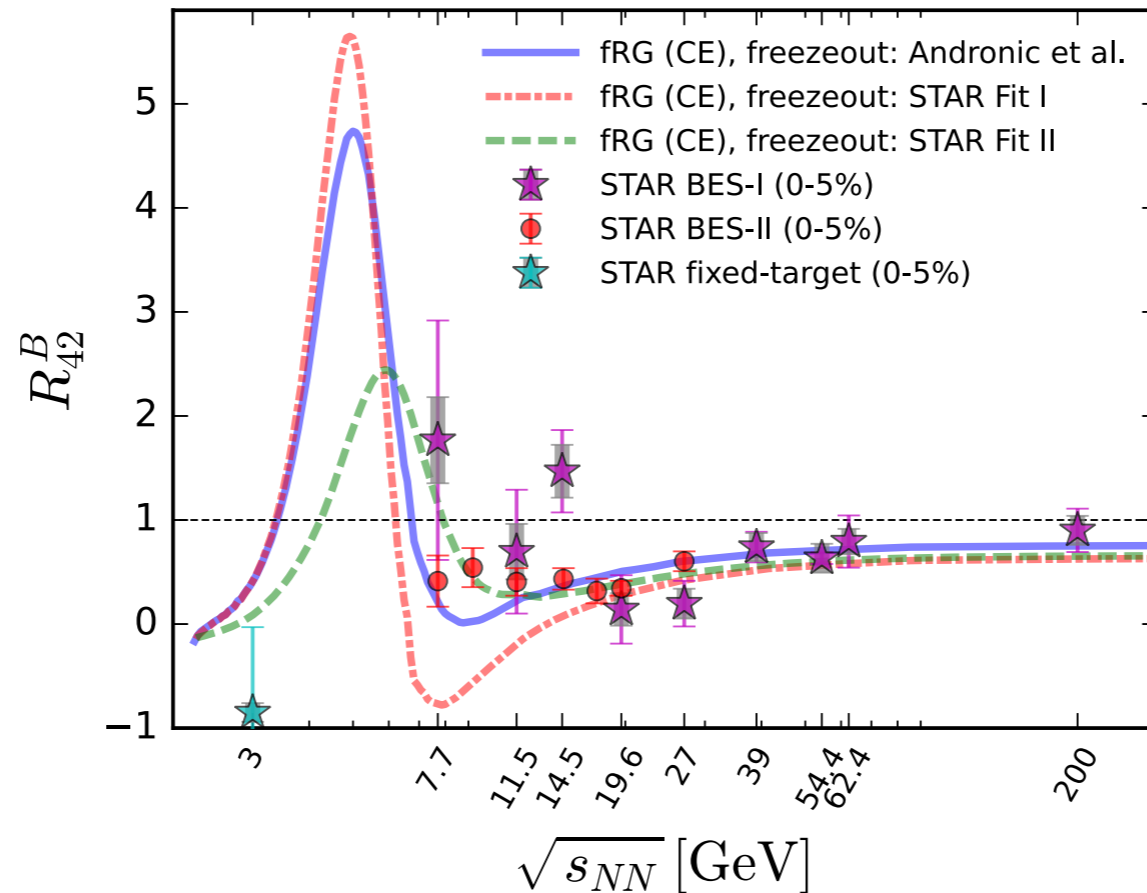


fRG: WF, Luo, Pawłowski, Rennecke, Yin, arXiv: 2308.15508

- Note that the ripples of CEP are far away from the critical region characterized by the universal scaling properties, e.g., the critical slowing down.
- But, the information of CEP, such as its location and properties, etc., is still encoded in the ripples.

Comparison to BES-II

Net baryon (proton) number Kurtosis:



- In comparison to BES-I, BES-II results are **better** consistent with the theoretical prediction.
- Experimental results in the energy regime of fixed-target experiments, i.e. $3 \text{ GeV} \lesssim \sqrt{s_{NN}} \lesssim 7.7 \text{ GeV}$, are now very important!! It will finally tell us whether there is a CEP.

Magnetic equation of state

- The magnetic equation of state (EoS) is obtained via the chiral condensate:

$$\Delta_q = m_q \frac{\partial \Omega(T; m_q(T))}{\partial m_q} = m_q \frac{T}{V} \int_x \langle \bar{q}(x) q(x) \rangle$$

- The chiral properties of the magnetic EoS are encoded in the magnetic susceptibility:

$$\chi_M = -\frac{\partial \bar{\Delta}_l}{\partial m_l}, \quad \text{with} \quad \bar{\Delta}_l = \frac{\Delta_l}{m_l}$$

- In the critical region, the magnetic EoS can be expressed as a universal scaling function $f_G(z)$ through

$$\bar{\Delta}_l = m_l^{1/\delta} f_G(z)$$

with

$$z = t m_l^{-1/\beta\delta}, \quad \text{and} \quad t = (T - T_c)/T_c$$

z is the scaling variable and t is the reduced temperature.

- The pseudo-critical temperature T_{pc} , which is defined through the peak location of χ_M , is readily obtained from the scaling function as

$$T_{pc}(m_\pi) \approx T_c + c m_\pi^p, \quad \text{with} \quad p = 2/(\beta\delta)$$

Critical exponent in fRG for 3d-O(4):

$$\beta = 0.405, \quad \delta = 4.784, \quad \theta_H = 0.272,$$

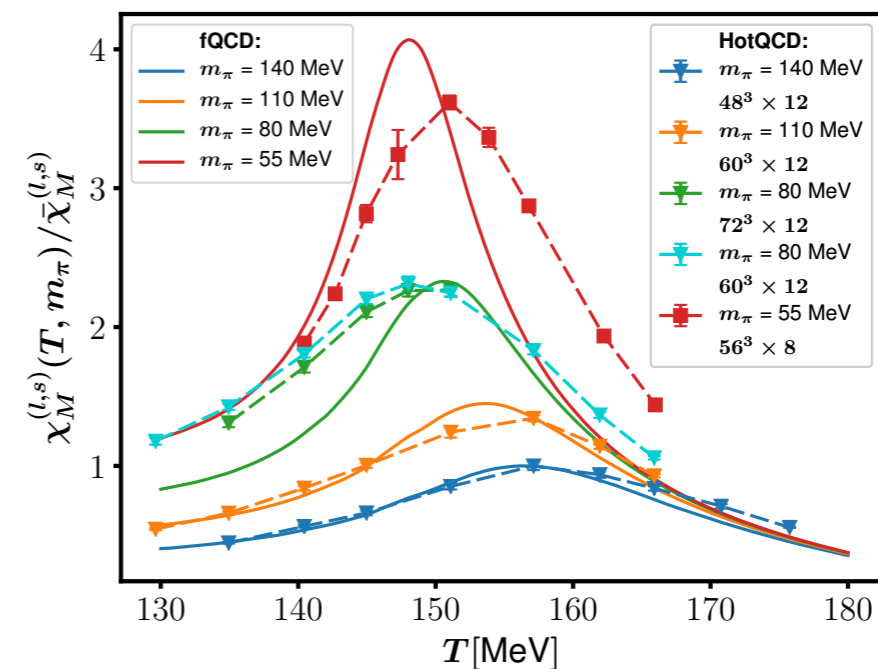
obtained from the fixed-point equation for the Wilson-Fisher fixed point, which leads us

$$p_{\text{fRG}} = 1.03$$

Critical exponent in mean field:

$$\beta_{\text{MF}} = 1/2, \quad \delta_{\text{MF}} = 3,$$

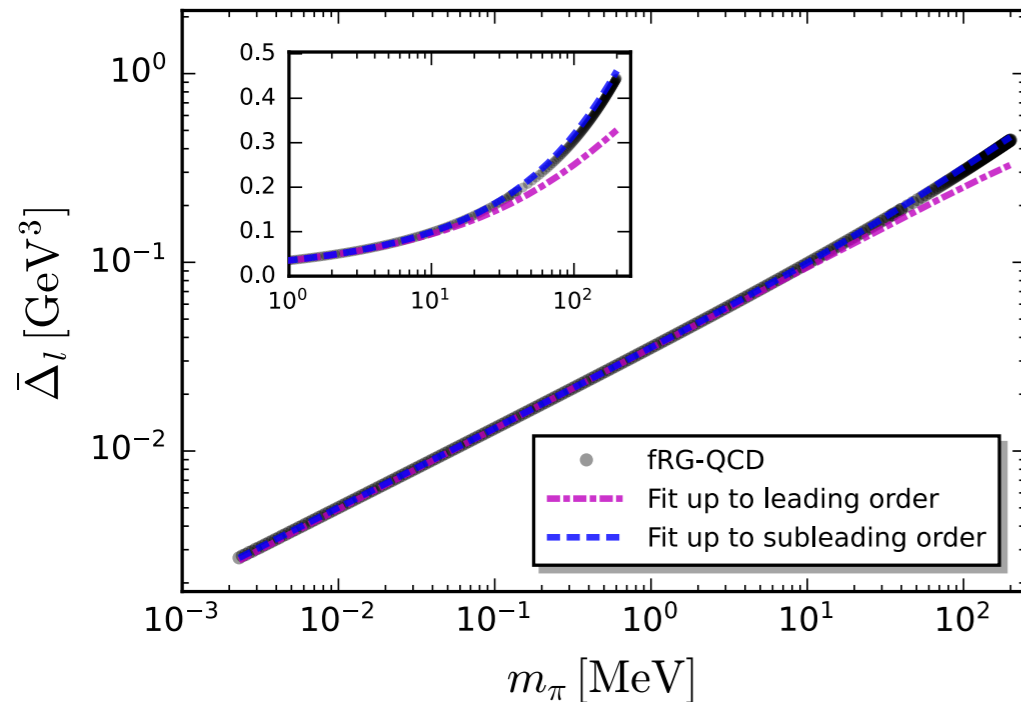
thus, one has $p_{\text{MF}} = 4/3$



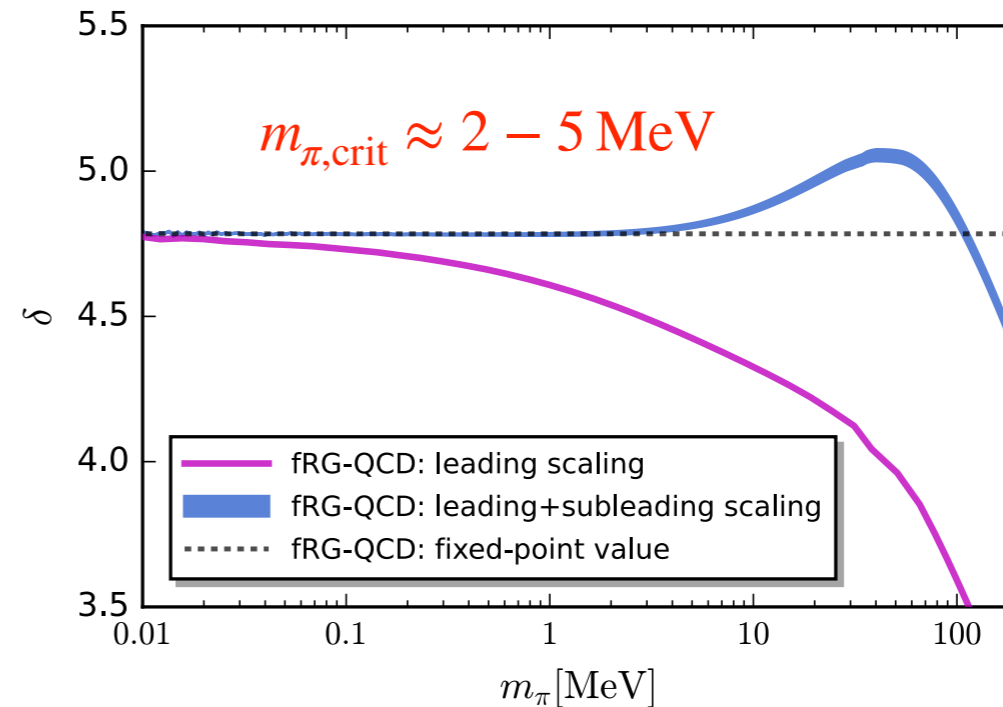
Braun, WF, Pawłowski, Rennecke, Rosenblüh, Yin, *PRD* 102 (2020), 056010.

Critical region in QCD

Scaling in the external field:

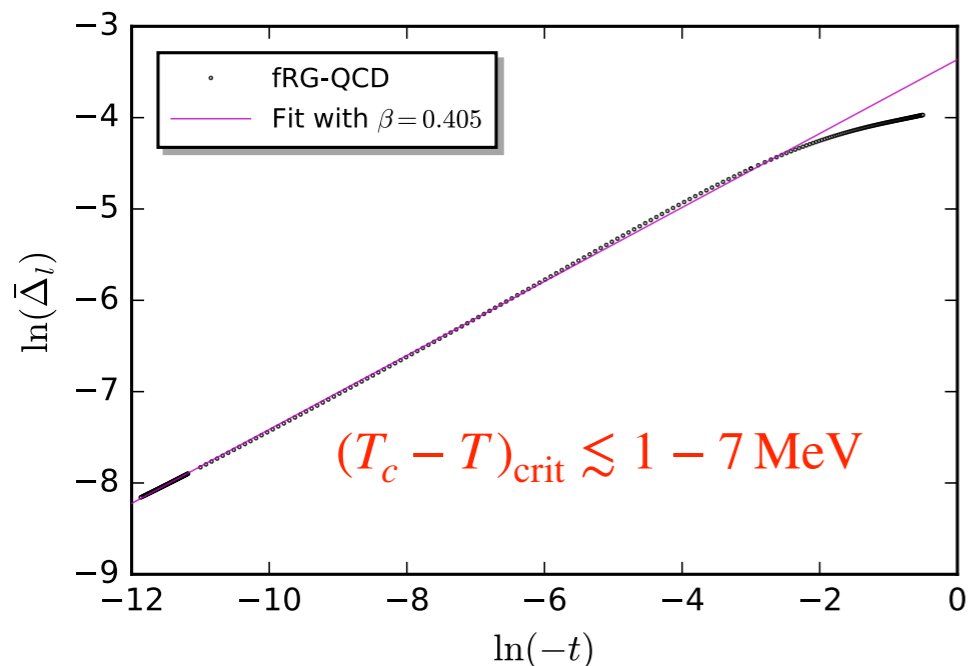


Critical exponent δ :



$$\bar{\Delta}_l^{(\text{crit})}(m_\pi) = B_c m_\pi^{2/\delta} [1 + a_m m_\pi^{2\theta_H}]$$

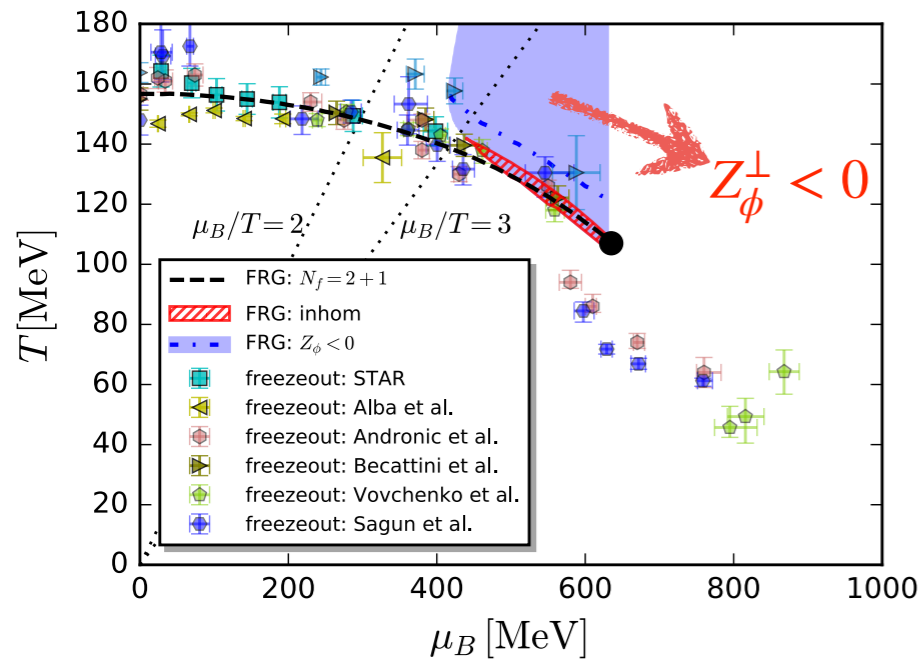
Scaling in the temperature:



- QCD at physical light quark mass is far away from the critical region.
- The scaling behavior is observed for the first time in the calculations of first-principles QCD.

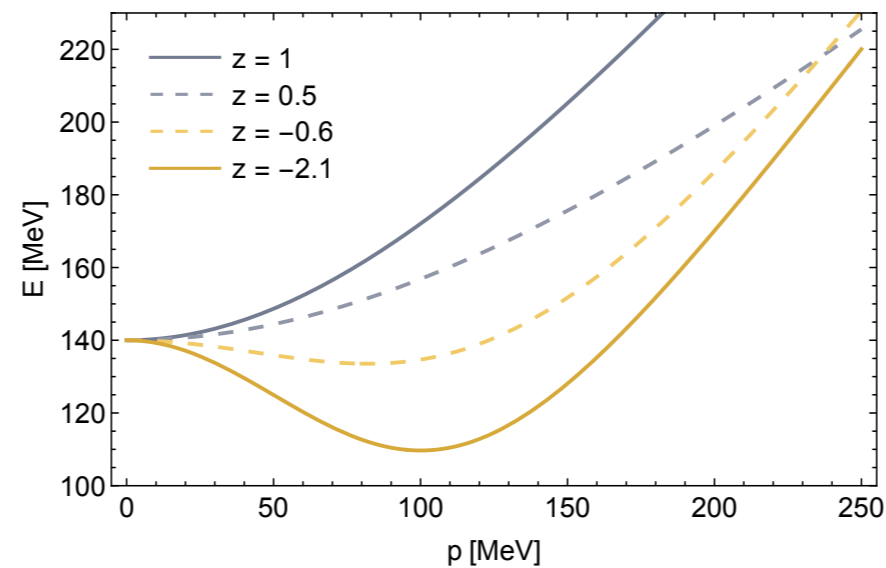
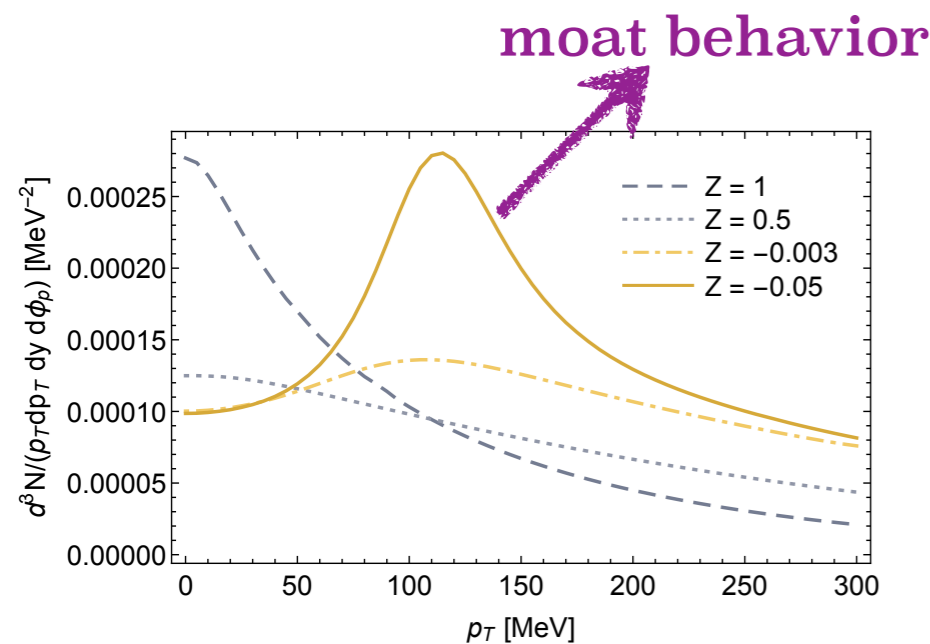
Braun, Chen, WF, Gao, Huang, Ihssen,
 Pawłowski, Rennecke, Sattler, Tan, Wen, and
 Yin, arXiv:2310.19853.

Moat regime in QCD phase diagram



WF, Pawłowski, Rennecke, *PRD* 101 (2020) 054032

- Transverse momentum spectrum of one particle:



Mesonic two-point correlation function:

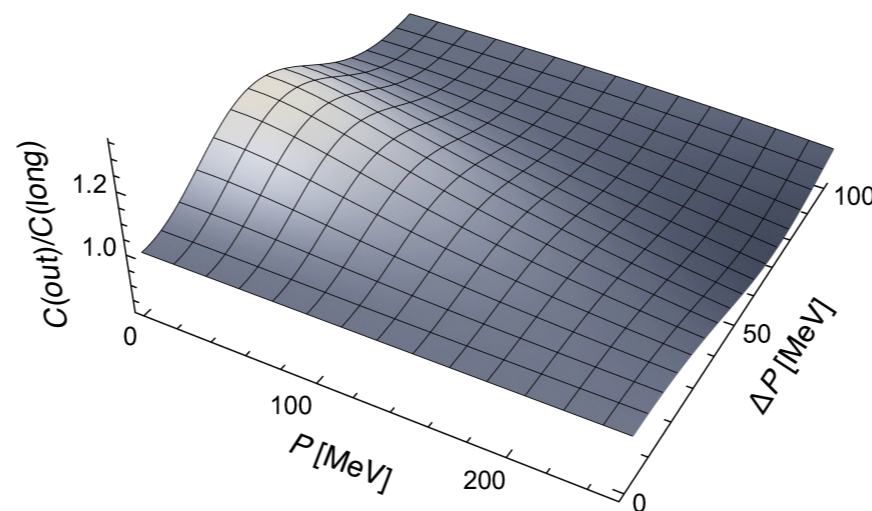
$$\Gamma_{\phi\phi}^{(2)}(p) = [Z_\phi^\parallel(p_0, \mathbf{p}) p_0^2 + Z_\phi^\perp(p_0, \mathbf{p}) \mathbf{p}^2] + m_\phi^2$$

with

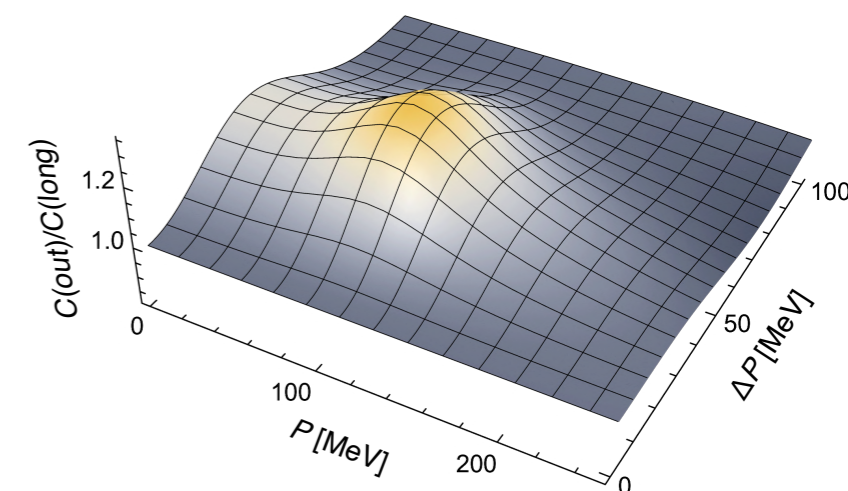
$$\Gamma_{\phi\phi,k}^{(2)} = \left. \frac{\delta^2 \Gamma_k[\Phi]}{\delta\phi\delta\phi} \right|_{\Phi=\Phi_{\text{EoM}}}$$

Pisarski, Rennecke, *PRL* 127 (2021) 152302;
 Rennecke, Pisarski, *PoS CPOD2021* (2022);
 Rennecke, Pisarski, Rischke, *PRD* 107 (2023) 116011

- Two-particle correlation:



normal phase

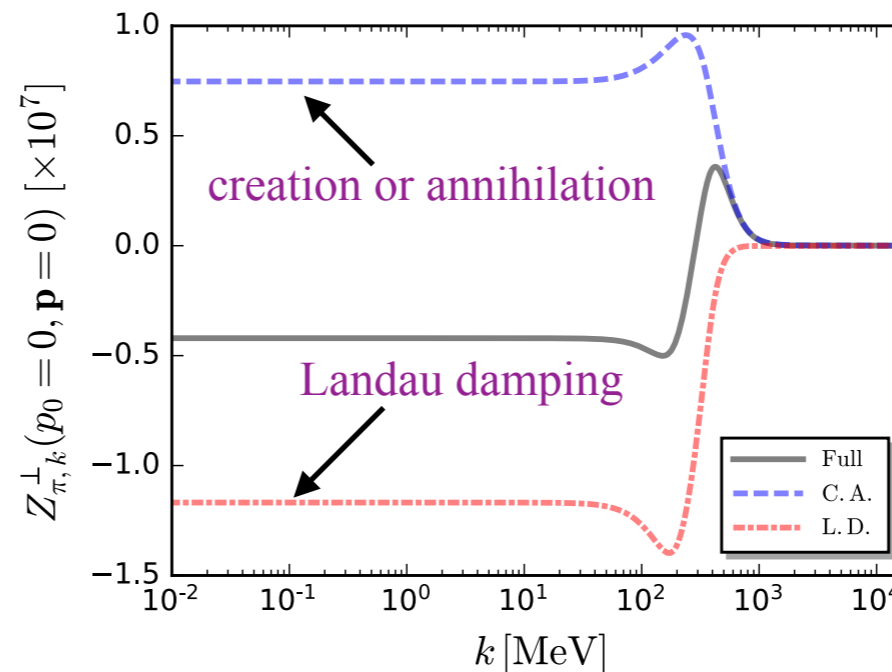
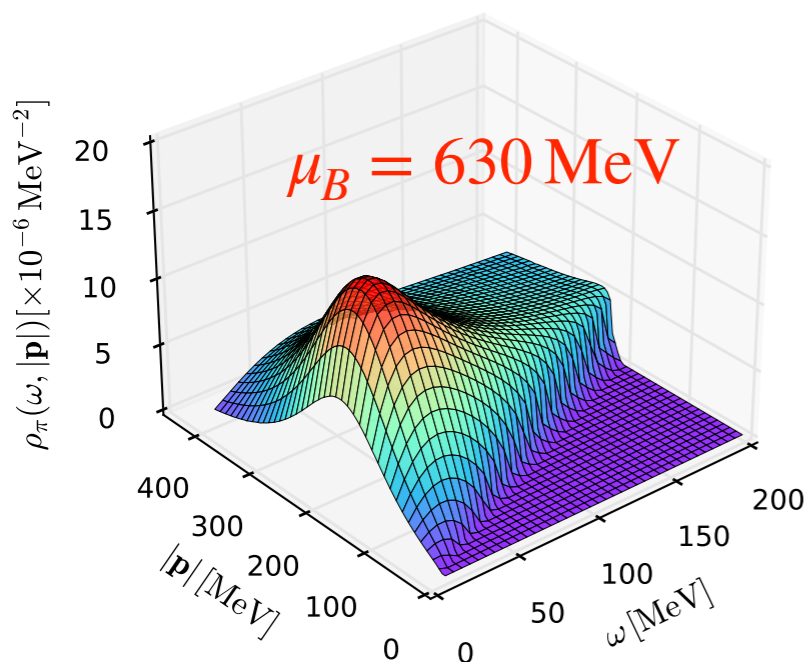
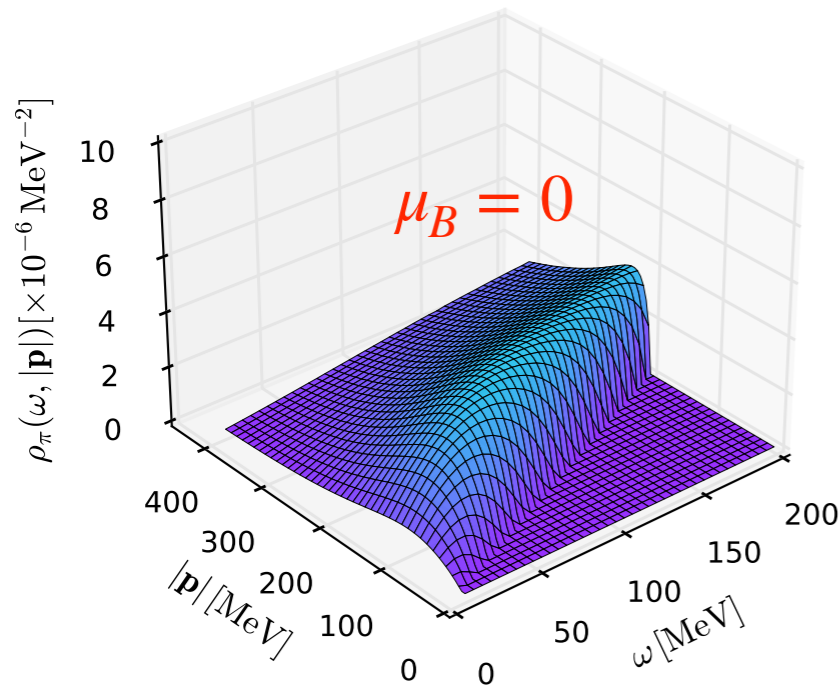


moat regime

Spectral functions in moat regime

Flow equation for mesonic two-point functions:

$$\partial_t \text{---} \bullet \text{---} = \tilde{\partial}_t \left(\text{---} \bullet \text{---} + \frac{1}{2} \text{---} \bullet \text{---} + \frac{1}{2} \text{---} \bullet \text{---} \right)$$



WF, Pawłowski, Pisarski, Rennecke, Wen, Yin, in preparation.

- Moat regime is found to be resulted from **Landau damping** of quarks in thermal bath in the regime of large baryon chemical potential.

Relaxation dynamics of the critical mode

- Langevin dynamics of the critical mode:

$$Z_\phi^{(t)} \partial_t \sigma - Z_\phi^{(i)} \partial_i^2 \sigma + U'(\sigma) = \xi$$

with the correlation of the Gaussian white noise

$$\langle \xi(t, \mathbf{x}) \xi(t', \mathbf{x}') \rangle = 2 Z_\phi^{(t)} T \delta(t - t') \delta(\mathbf{x} - \mathbf{x}')$$

- Inputs from first-principles functional QCD: [WF, Pawłowski, Rennecke, PRD 101 \(2020\) 054032](#)

Effective potential:

$$U'(\sigma) = \left. \frac{\delta \Gamma[\Phi]}{\delta \sigma} \right|_{\substack{\sigma(x) = \sigma \\ \tilde{\Phi} = \tilde{\Phi}_{\text{EoM}}}}$$

Spatial wave function:

$$Z_\phi^{(i)} = \left. \frac{\partial \Gamma_{\sigma\sigma}^{(2)}(p_0, \mathbf{p})}{\partial \mathbf{p}^2} \right|_{\substack{p_0 = 0 \\ \mathbf{p} = 0}}$$

Temporal wave function:

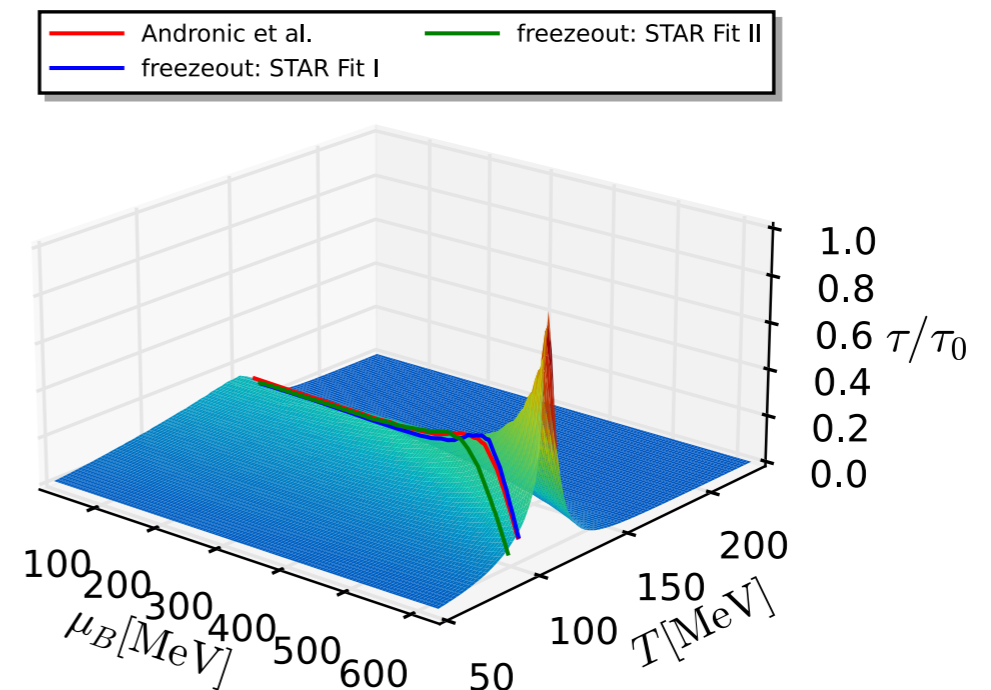
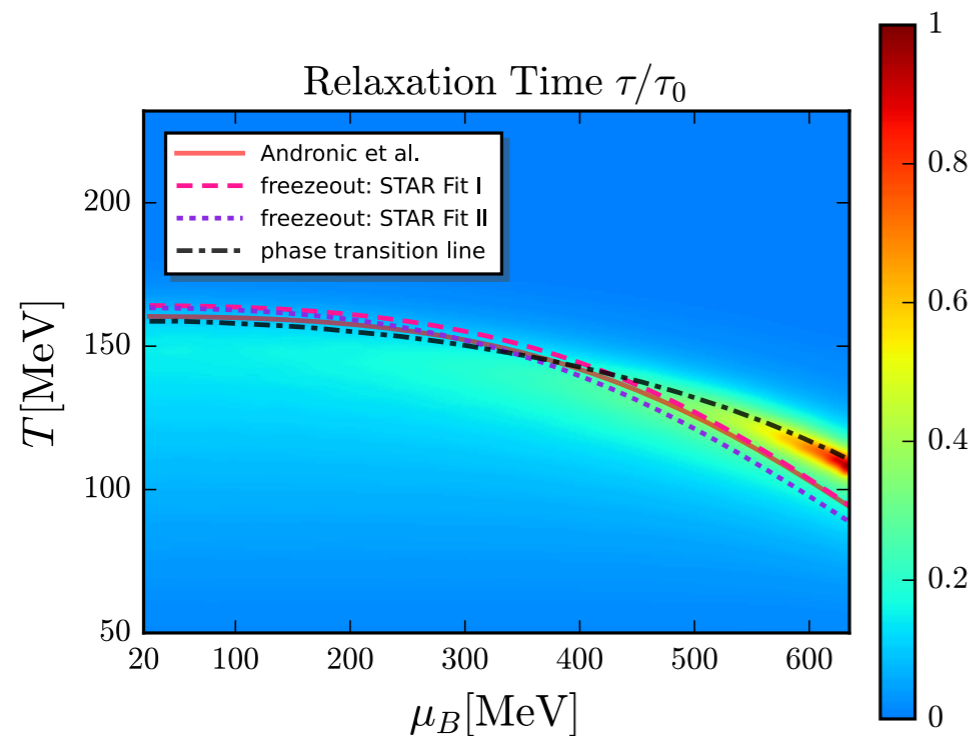
$$Z_\phi^{(t)} = \lim_{|\mathbf{p}| \rightarrow 0} \lim_{\omega \rightarrow 0} \frac{\partial}{\partial \omega} \text{Im} \Gamma_{\sigma\sigma, \text{R}}^{(2)}(\omega, \mathbf{p})$$

with

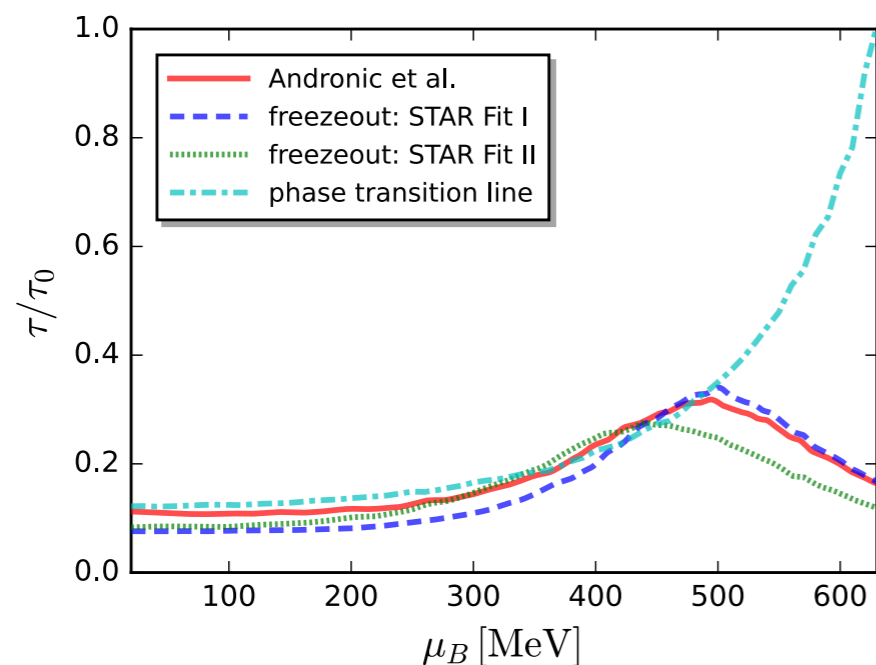
$$\Gamma_{\sigma\sigma, \text{R}}^{(2)}(\omega, \mathbf{p}) = \lim_{\epsilon \rightarrow 0^+} \Gamma_{\sigma\sigma}^{(2)}(p_0 = -i(\omega + i\epsilon), \mathbf{p})$$

Relaxation time in QCD phase diagram

Relaxation time:



Relaxation time at the freezeout :



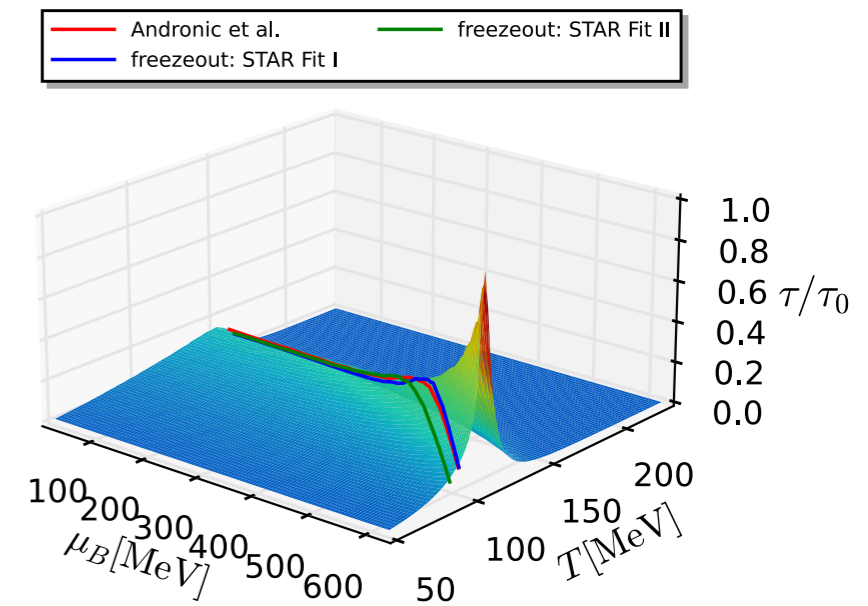
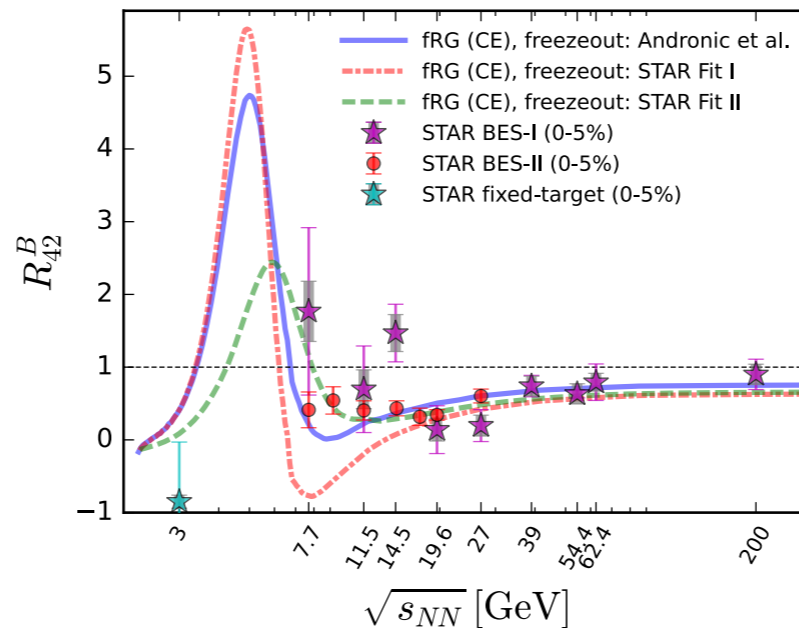
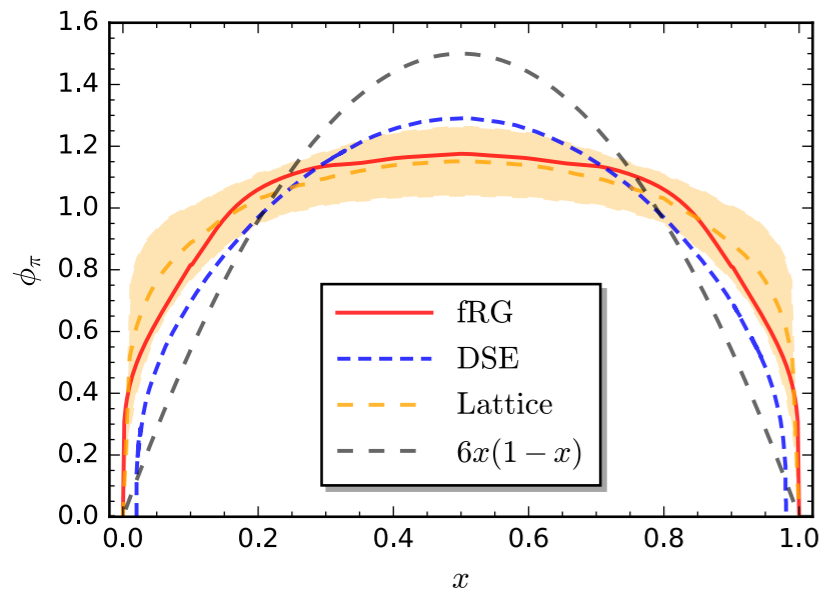
Tan, Yin, Chen, Huang, WF, in preparation

See also:

M. Bluhm *et al.*, *NPA* 982 (2019) 871

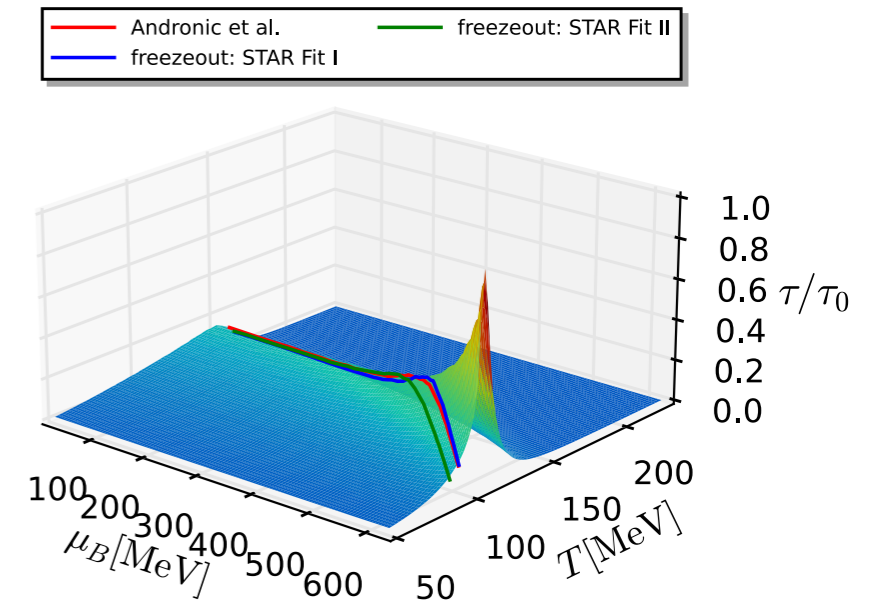
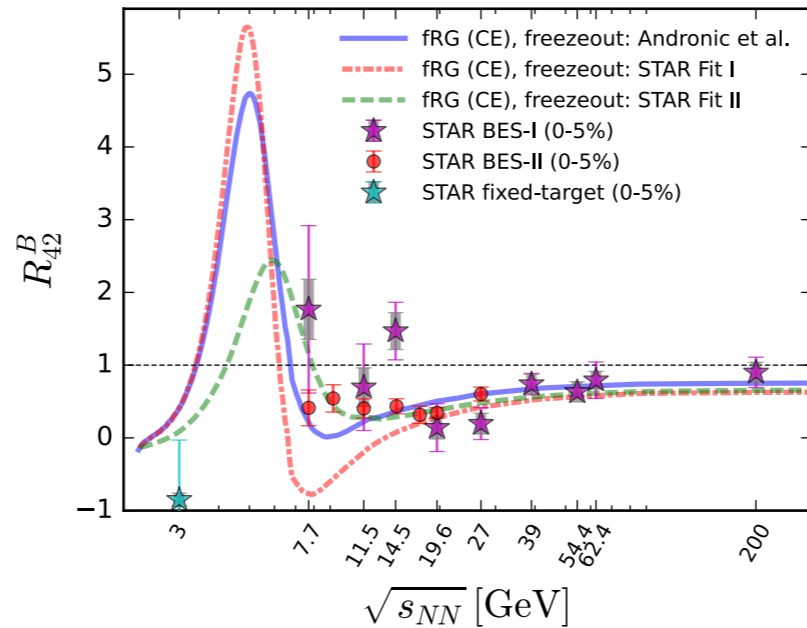
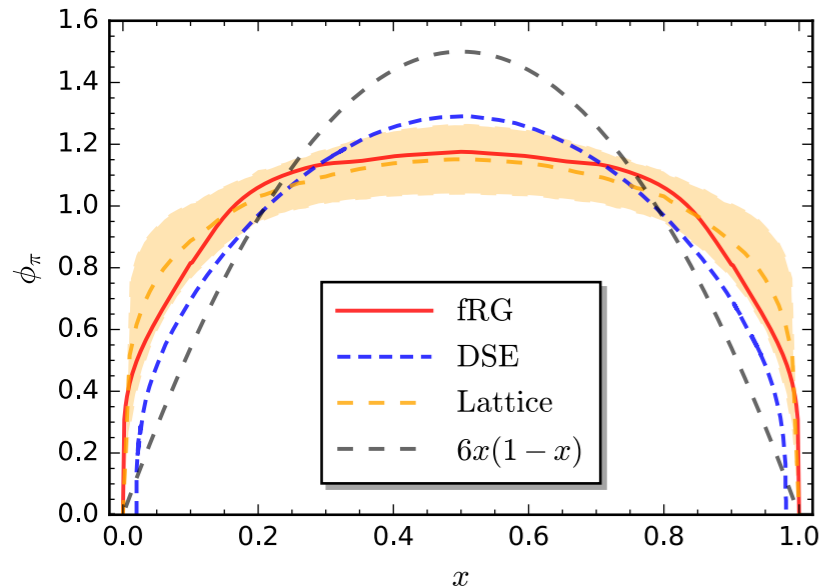
- Relaxation time drops quickly once the system is away from the critical regime.

Summary and outlook



- ★ Functional renormalization group provides us with a powerful approach to study nonperturbative problems, e.g., hadron structure, QCD phase diagram, real-time dynamics, from first-principles QCD.
- ★ There are also challenges and problems to be solved: larger P_z , error controls at large baryon densities, better analytic continuations, etc.

Summary and outlook



- ★ Functional renormalization group provides us with a powerful approach to study nonperturbative problems, e.g., hadron structure, QCD phase diagram, real-time dynamics, from first-principles QCD.
- ★ There are also challenges and problems to be solved: larger P_z , error controls at large baryon densities, better analytic continuations, etc.

Thank you very much for your attentions!

Backup

Four-quark vertices

- 4-quark effective action:

$$\Gamma_{4q,k} = - \int \frac{d^4 p_1}{(2\pi)^4} \dots \frac{d^4 p_4}{(2\pi)^4} (2\pi)^4 \delta(p_1 + p_2 + p_3 + p_4) \\ \times \sum_{\alpha} \lambda_{\alpha}(\mathbf{p}) \mathcal{T}_{ijlm}^{(\alpha)}(\mathbf{p}) \bar{q}_i(p_1) q_j(p_2) \bar{q}_l(p_3) q_m(p_4),$$

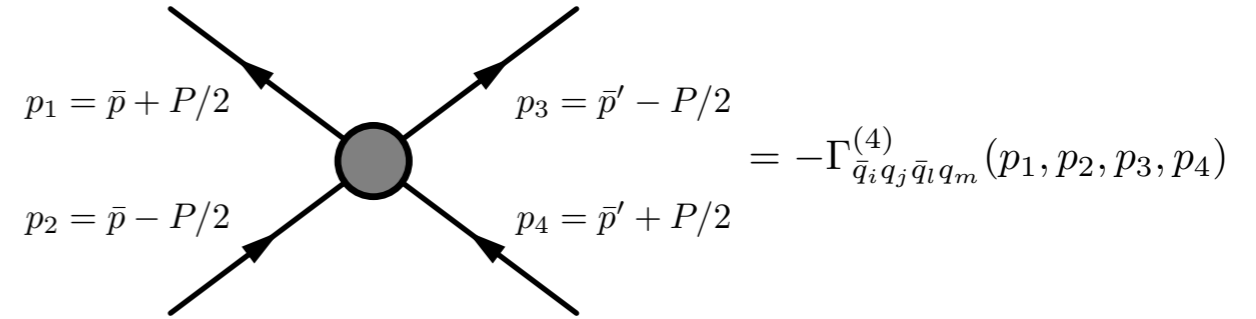
With $\mathbf{p} = (p_1, p_2, p_3, p_4)$, $\mathcal{T}^{(\alpha)}(\mathbf{p})$ is comprised of 512 tensors. [Eichmann, PRD 84 \(2011\) 014014](#)

A basis of the lowest momentum-independent order includes ten elements

$$\alpha \in \left\{ \sigma, \pi, a, \eta, (V \pm A), (V - A)^{\text{adj}}, \right. \\ \left. (S \pm P)_{-}^{\text{adj}}, (S + P)_{+}^{\text{adj}} \right\},$$

- 4-quark vertex:

$$\Gamma_{\bar{q}_i q_j \bar{q}_l q_m}^{(4)}(\mathbf{p}) = \frac{\delta^4 \Gamma_k[q, \bar{q}]}{\delta \bar{q}_i(p_1) \delta q_j(p_2) \delta \bar{q}_l(p_3) \delta q_m(p_4)} \\ = -4 (2\pi)^4 \delta(p_1 + p_2 + p_3 + p_4) \\ \times \sum_{\alpha} \left[\lambda_{\alpha}^{+}(\mathbf{p}) \mathcal{T}_{ijlm}^{(\alpha^{-})} + \lambda_{\alpha}^{-}(\mathbf{p}) \mathcal{T}_{ijlm}^{(\alpha^{+})} \right]$$



where we have used 4-quark dressings and tensor structures with definite symmetries, viz.,

$$\lambda_{\alpha}^{\pm}(\mathbf{p}) \equiv \frac{1}{2} \left[\lambda_{\alpha}(p_1, p_2, p_3, p_4) \pm \lambda_{\alpha}(p_3, p_2, p_1, p_4) \right],$$

and

$$\mathcal{T}_{ijlm}^{(\alpha^{\pm})} \equiv \frac{1}{2} (\mathcal{T}_{ijlm}^{(\alpha)} \pm \mathcal{T}_{ljim}^{(\alpha)})$$

with the symmetry relations

$$\lambda_{\alpha}^{+}(p_1, p_2, p_3, p_4) = \lambda_{\alpha}^{+}(p_3, p_2, p_1, p_4) \\ = \lambda_{\alpha}^{+}(p_1, p_4, p_3, p_2) = \lambda_{\alpha}^{+}(p_3, p_4, p_1, p_2), \\ \lambda_{\alpha}^{-}(p_1, p_2, p_3, p_4) = -\lambda_{\alpha}^{-}(p_3, p_2, p_1, p_4) \\ = -\lambda_{\alpha}^{-}(p_1, p_4, p_3, p_2) = \lambda_{\alpha}^{-}(p_3, p_4, p_1, p_2)$$

and similar relations for the tensors.

s, t, u-channel truncation

- s, t, u -channel approximation for 4-quark vertices:

$$\lambda_{\alpha}^{\pm}(p_1, p_2, p_3, p_4) = \lambda_{\alpha}^{\pm}(s, t, u) + \Delta\lambda_{\alpha}^{\pm}(p_1, p_2, p_3, p_4) \\ \approx \lambda_{\alpha}^{\pm}(s, t, u)$$

with

$$t = (p_1 - p_2)^2 = P^2, \\ u = (p_1 - p_4)^2 = (\bar{p} - \bar{p}')^2, \\ s = (p_1 + p_3)^2 = (\bar{p} + \bar{p}')^2$$

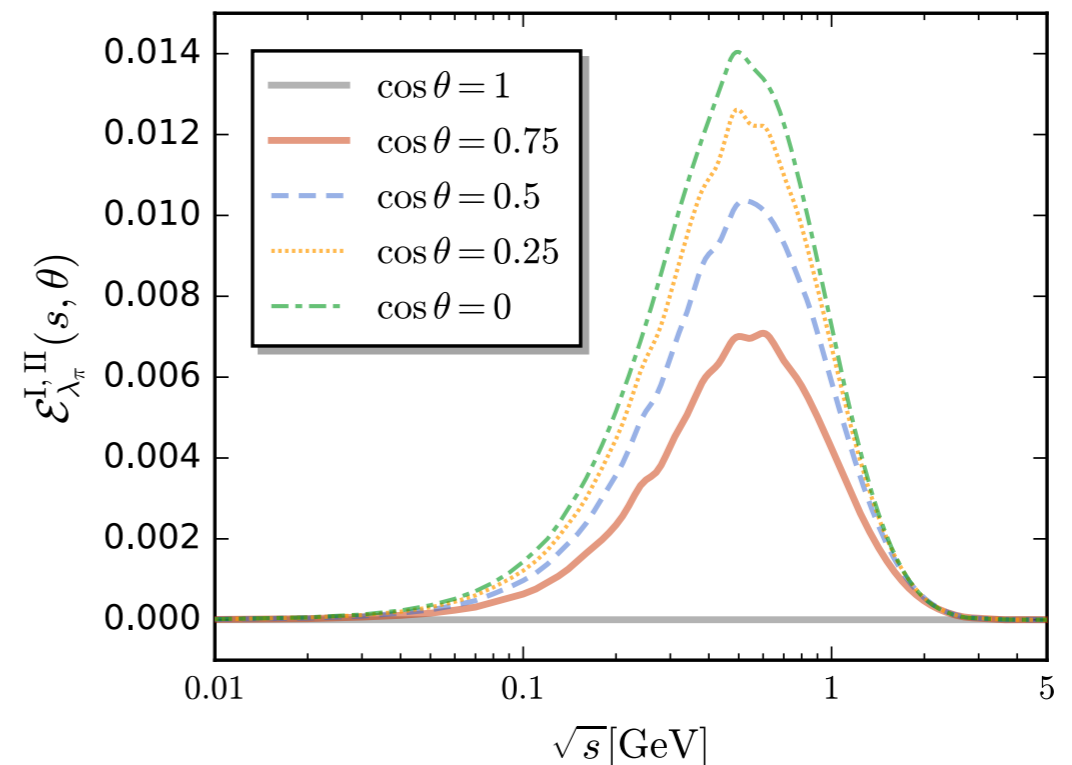
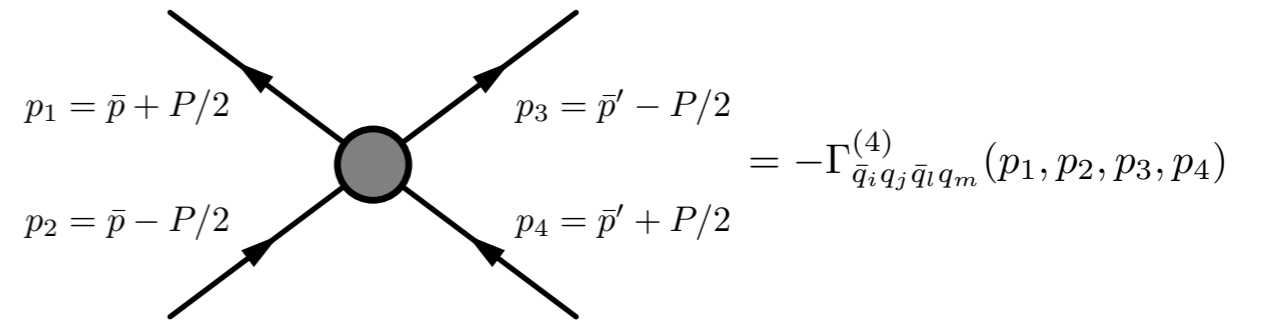
- We choose a subspace of the full momentum of 4-quark vertices as follows

$$P_{\mu} = \sqrt{P^2} (1, 0, 0, 0), \\ \bar{p}_{\mu} = \sqrt{p^2} (1, 0, 0, 0), \\ \bar{p}'_{\mu} = \sqrt{p^2} (\cos \theta, \sin \theta, 0, 0)$$

one is led to

$$t = P^2, \quad u = 2p^2(1 - \cos \theta), \quad s = 2p^2(1 + \cos \theta)$$

Here, $\{\sqrt{P^2}, \sqrt{p^2}, \cos \theta\}$ is in one-by-one correspondence with respect to $\{t, u, s\}$

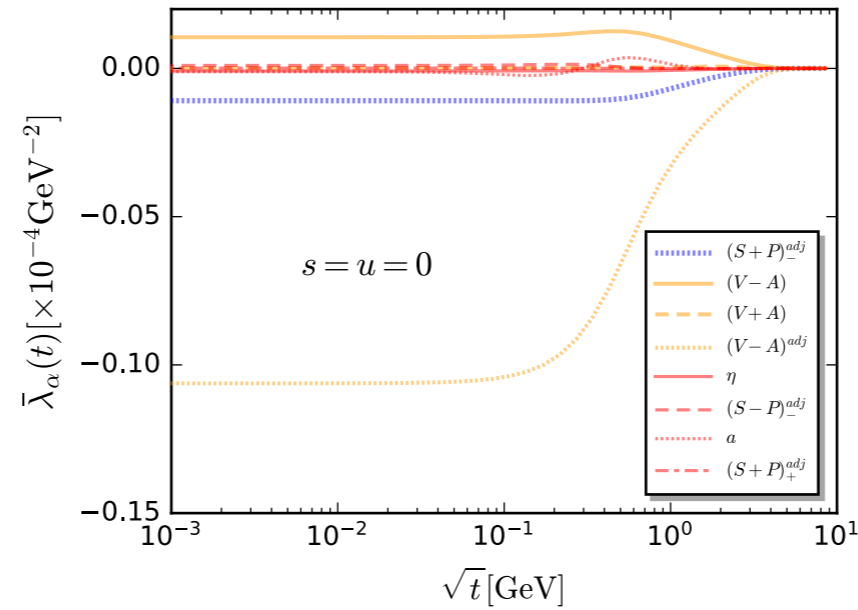
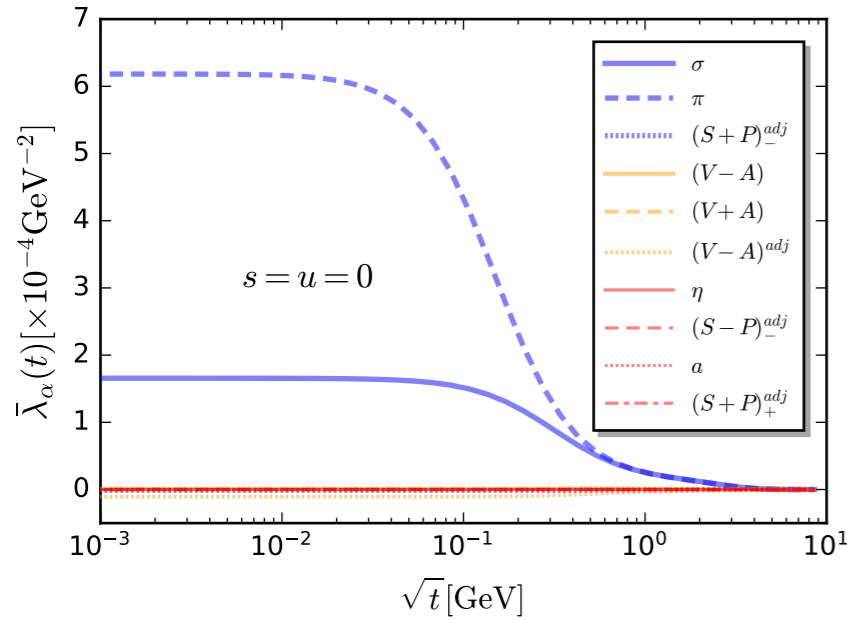


WF, Huang, Pawlowski, Tan, arXiv:2401.07638

The error for the truncation is smaller than 1.5%

Four-quark dressings

Dressings of different tensors:



Symmetry relations

$$\lambda_{\alpha}^{+}(s, t, u) = \lambda_{\alpha}^{+}(s, u, t),$$

$$\lambda_{\alpha}^{-}(s, t, u) = -\lambda_{\alpha}^{-}(s, u, t)$$

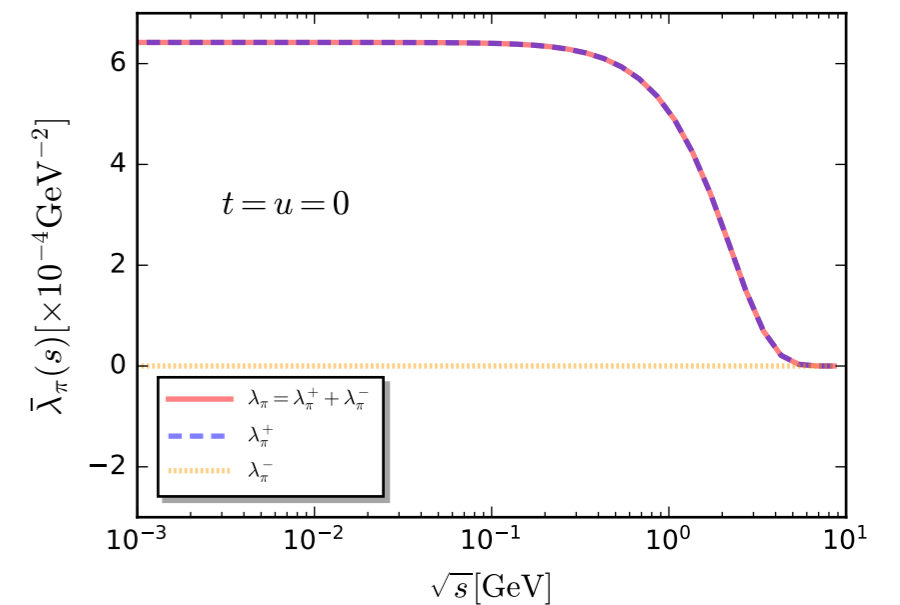
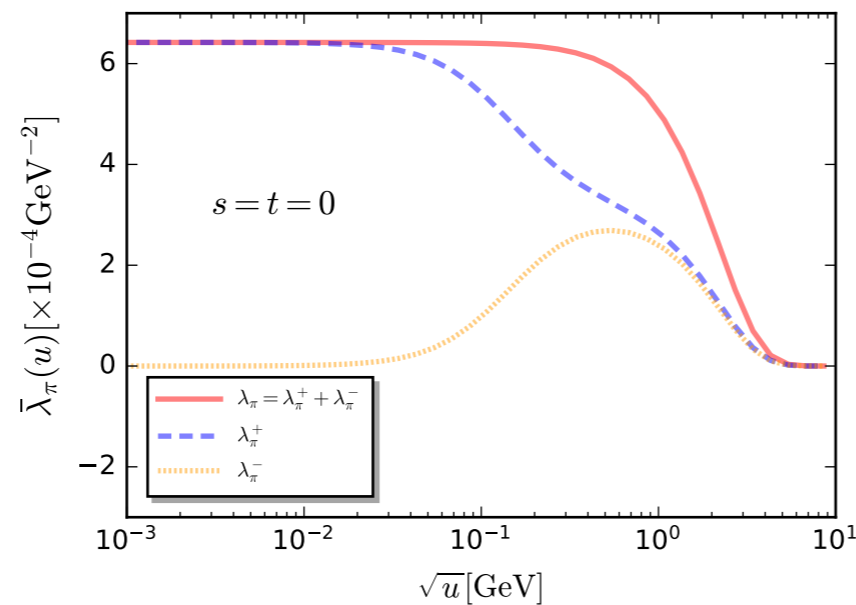
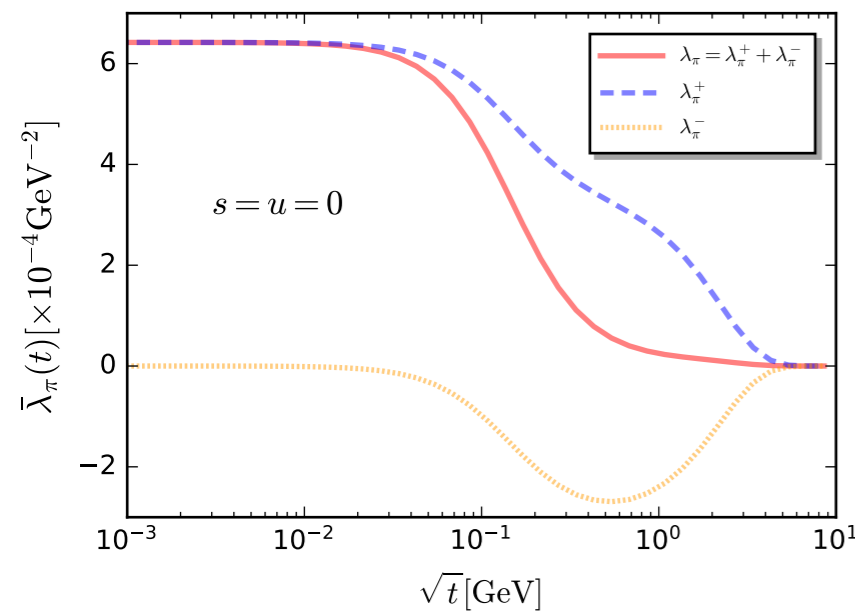
then

$$\lambda_{\alpha}^{+}(0, p^2, 0) = \lambda_{\alpha}^{+}(0, 0, p^2),$$

$$\lambda_{\alpha}^{-}(0, p^2, 0) = -\lambda_{\alpha}^{-}(0, 0, p^2)$$

Pion channel:

WF, Huang, Pawłowski, Tan, arXiv:2401.07638



Pion decay constant

The pion weak decay constant is defined as

$$\langle 0 | J_{5\mu}^a(x) | \pi^b \rangle = iP_\mu f_\pi \delta^{ab}$$

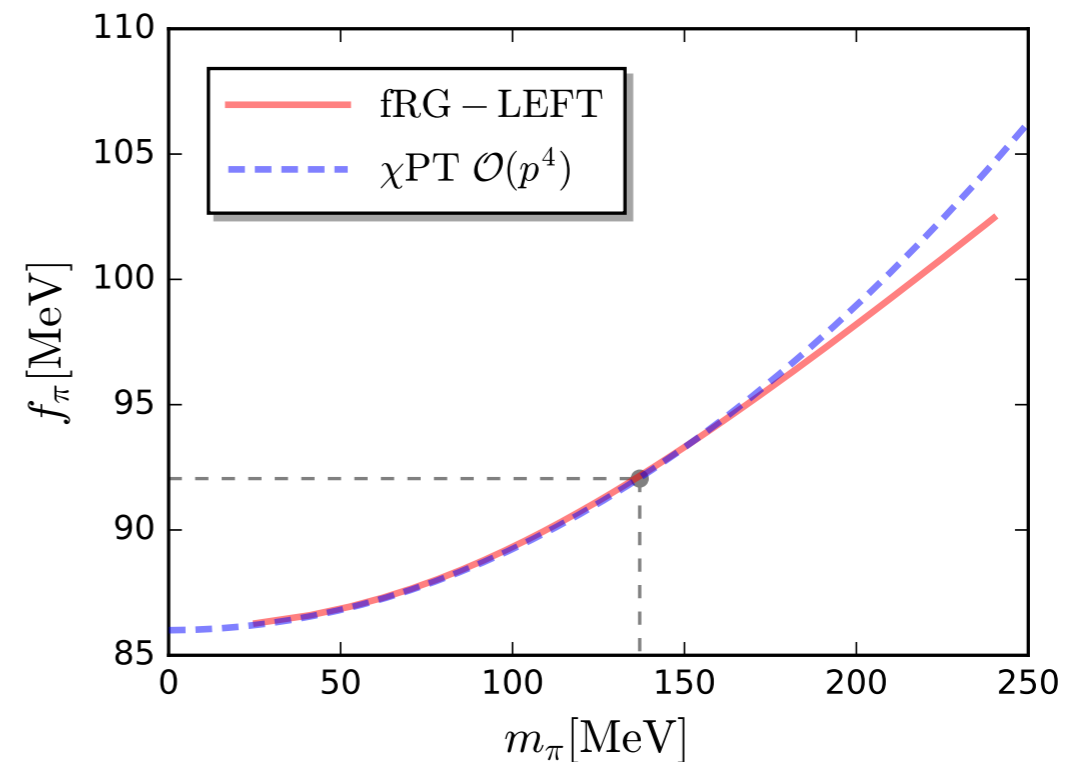
where the left hand side reads

$$\begin{aligned} & \langle 0 | J_{5\mu}^a(x) | \pi^b \rangle \\ &= \int \frac{d^4q}{(2\pi)^4} \text{Tr} \left[\gamma_\mu \gamma_5 T^a \bar{G}_q(q+P) \bar{h}_\pi(q) \gamma_5 T^b G_q(q) \right], \end{aligned}$$

then

$$f_\pi = 2N_c \int \frac{d^4q}{(2\pi)^4} \frac{\bar{h}_\pi(q) M_q(q)}{[q^2 + M_q^2(q)]^2}$$

up to leading order in powers of $P^2 = -m_\pi^2$



fRG: WF, Huang, Pawłowski, Tan, arXiv:2401.07638

chiPT: Gasser and Leutwyler, *Annals Phys.* 158 (1984) 142

Contour of k_0 integral

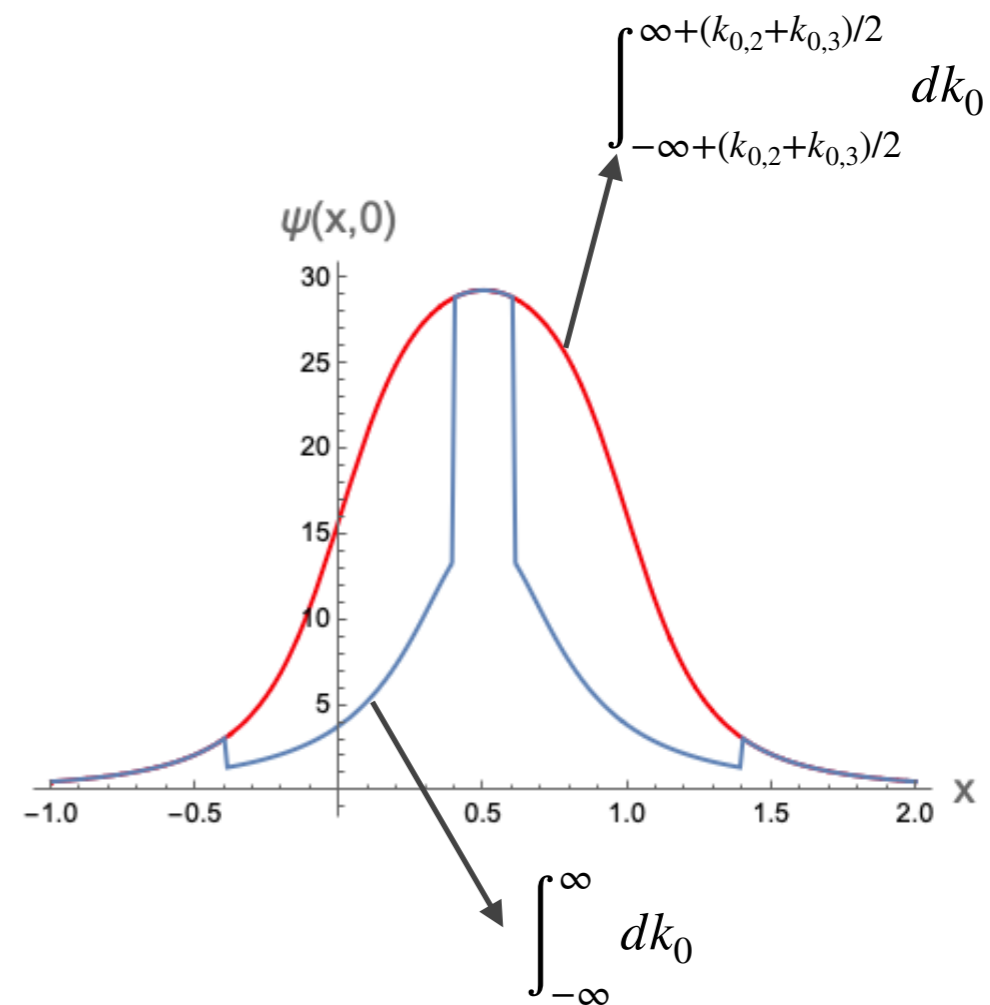
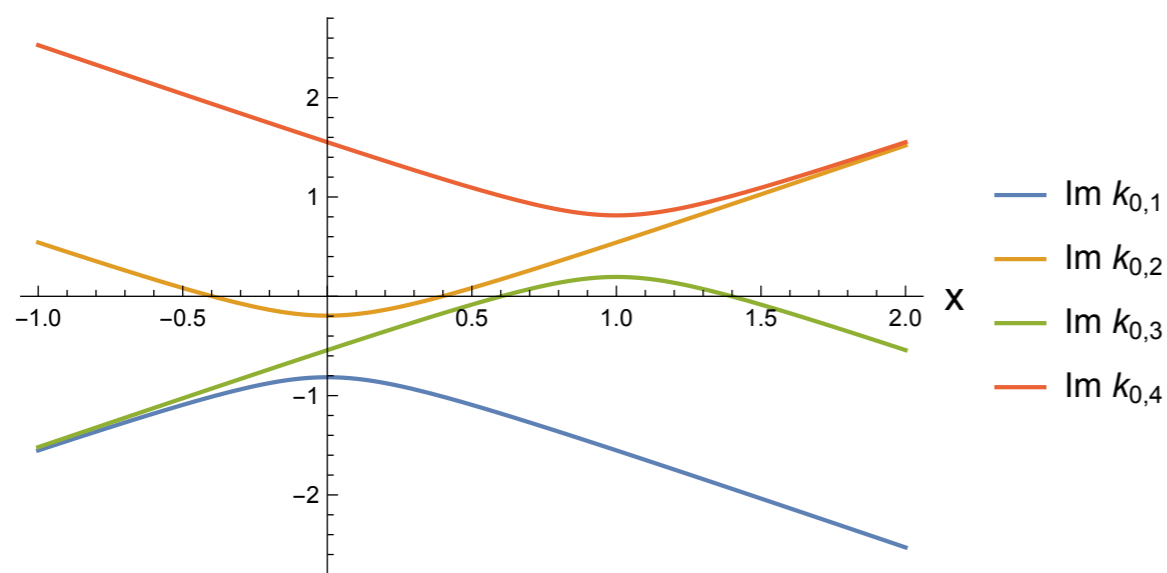
- Poles of two quark propagators:

$$k_{0,1} = i \left[-\sqrt{k_{\perp}^2 + (xP_z)^2 + M_q^2(k_+^2)} - \sqrt{P_z^2 + m_{\pi}^2/2} \right],$$

$$k_{0,2} = i \left[\sqrt{k_{\perp}^2 + (xP_z)^2 + M_q^2(k_+^2)} - \sqrt{P_z^2 + m_{\pi}^2/2} \right],$$

$$k_{0,3} = i \left[-\sqrt{k_{\perp}^2 + (x-1)^2 P_z^2 + M_q^2(k_-^2)} + \sqrt{P_z^2 + m_{\pi}^2/2} \right],$$

$$k_{0,4} = i \left[\sqrt{k_{\perp}^2 + (x-1)^2 P_z^2 + M_q^2(k_-^2)} + \sqrt{P_z^2 + m_{\pi}^2/2} \right]$$



With the increase of P_z , $k_{0,2}$ or $k_{0,3}$ cross the x axis, one has to shift the integral of k_0 towards finite imaginary part, such that one can pick up the desired pair of poles, e.g., $k_{0,1}$ and $k_{0,3}$ or $k_{0,2}$ and $k_{0,4}$

Analytic continuation

- We use Taylor expansion to continue h_π, M_q, Z_q in the complex plane of k_0 :

$$h_\pi(k^2, P^2, \cos \theta) = h_\pi(\bar{k}^2, P^2, \cos \theta) + \left. \frac{\partial}{\partial k^2} h_\pi \right|_{k^2=\bar{k}^2} k_0^2 + \dots$$

and

$$M_q(k_+^2) = M_q(\bar{k}_+^2) + \left. \frac{\partial}{\partial k_+^2} M_q \right|_{k_+^2=\bar{k}_+^2} (k_0 + iE_\pi/2)^2 + \dots$$

$$M_q(k_-^2) = M_q(\bar{k}_-^2) + \left. \frac{\partial}{\partial k_-^2} M_q \right|_{k_-^2=\bar{k}_-^2} (k_0 - iE_\pi/2)^2 + \dots$$

$$k^2 = \bar{k}^2 + k_0^2$$

$$\bar{k}^2 = k_\perp^2 + (x - 1/2)^2 P_z^2$$

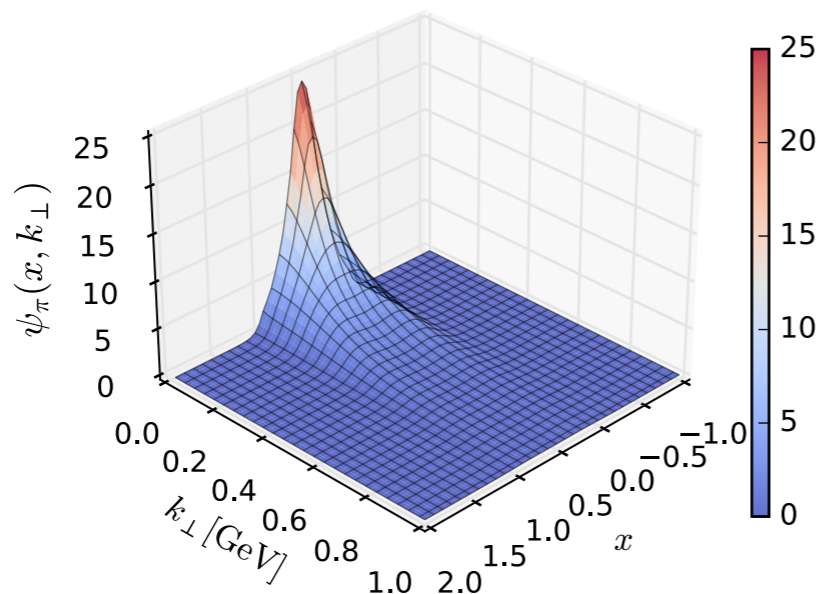
$$k_+^2 = \bar{k}_+^2 + (k_0 + iE_\pi/2)^2$$

$$\bar{k}_+^2 = k_\perp^2 + x^2 P_z^2$$

$$k_-^2 = \bar{k}_-^2 + (k_0 - iE_\pi/2)^2$$

$$\bar{k}_-^2 = k_\perp^2 + (x - 1)^2 P_z^2$$

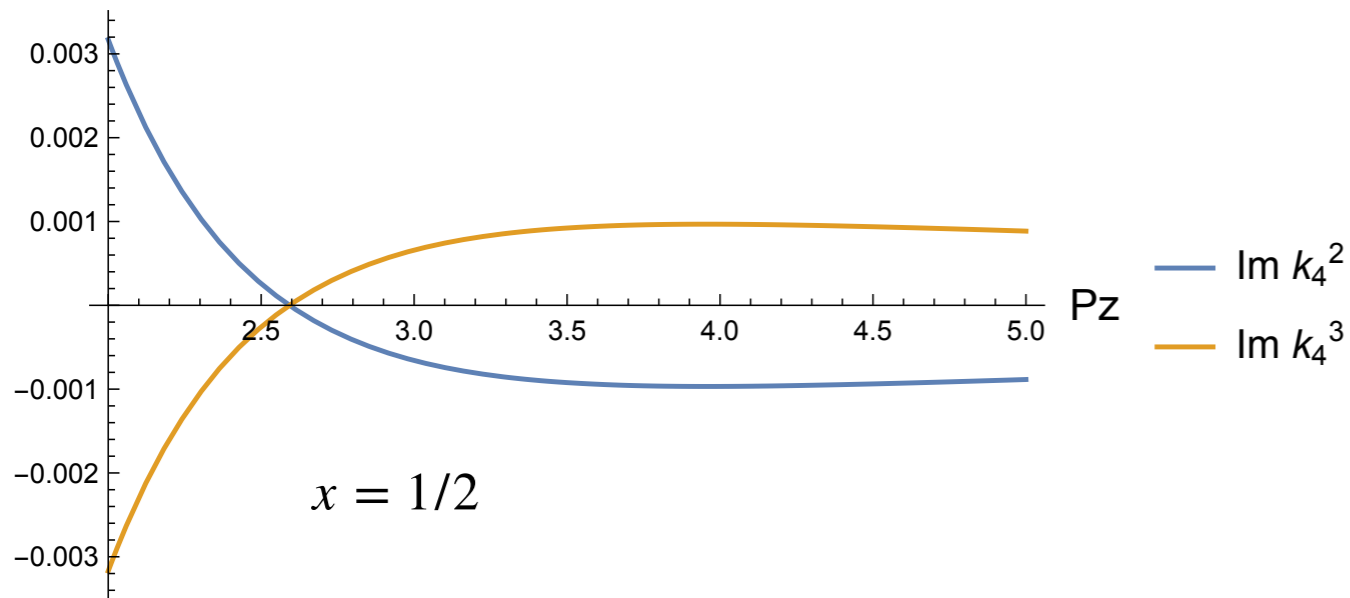
Pion wave function amplitudes:



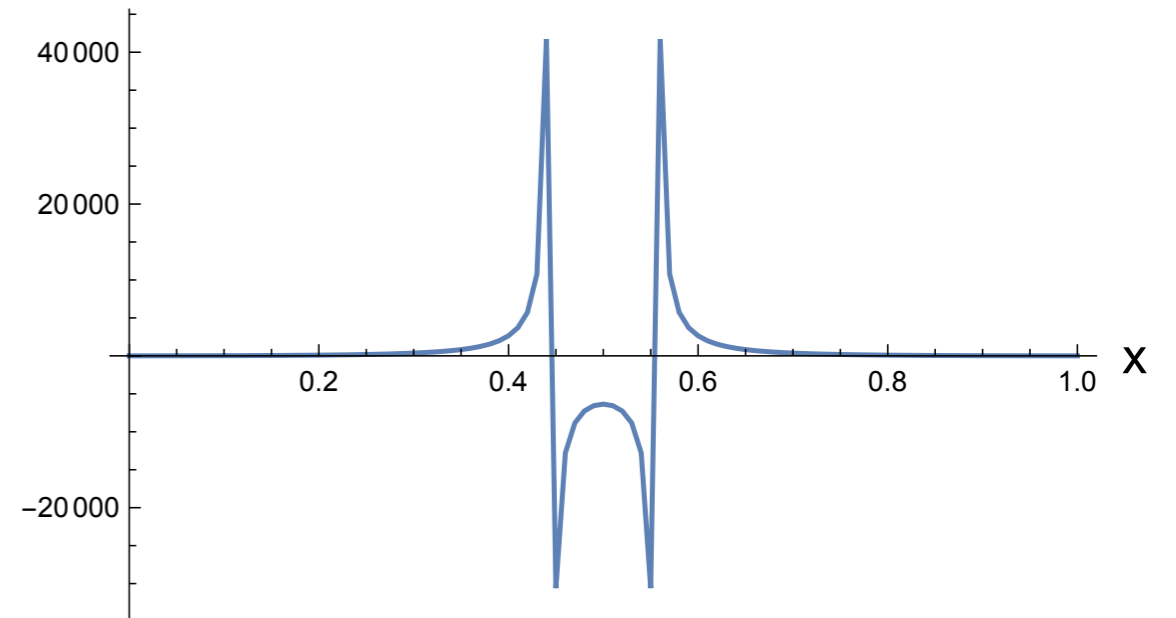
Chang, WF, Huang, Pawlowski, Zhang, in preparation

Larger P_z ?

Pole crossing:



Wave function:

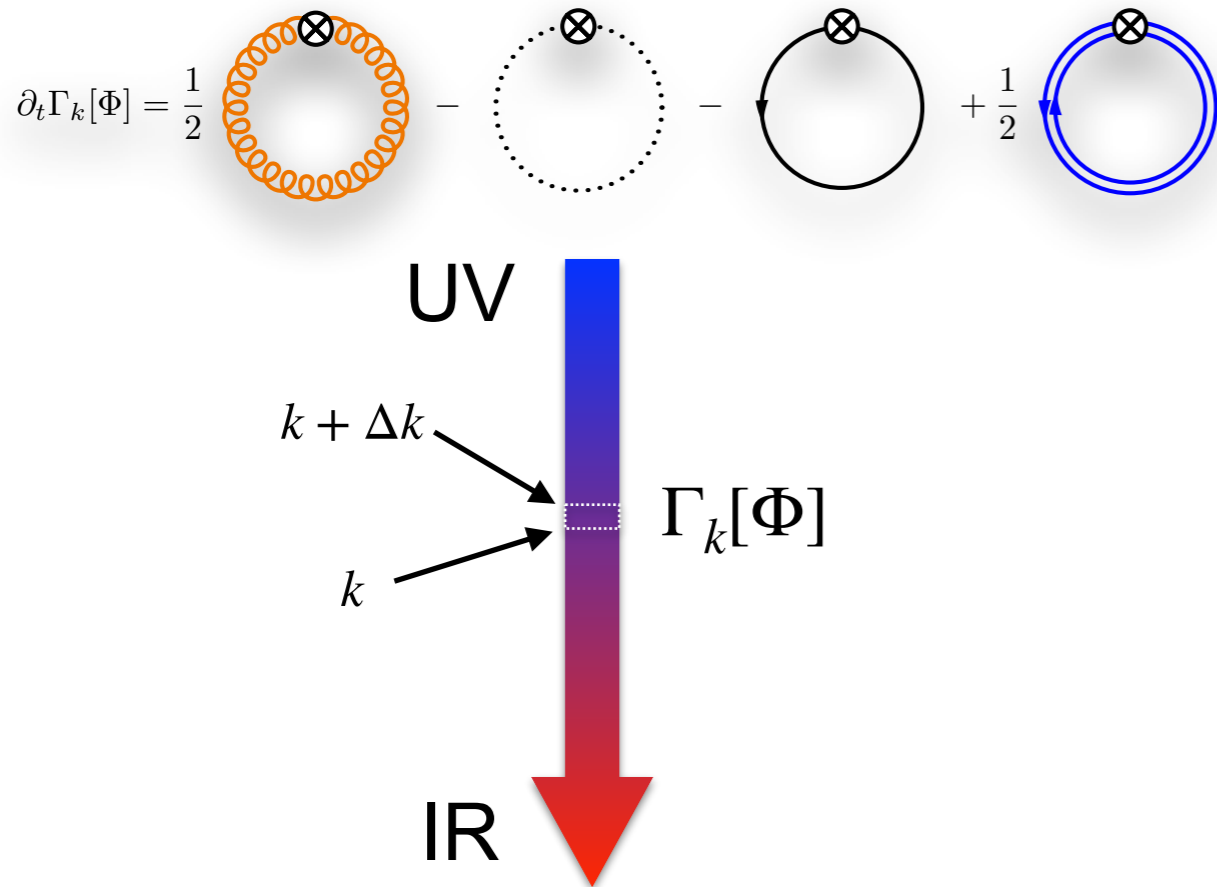


Poles of $k_{0,2}$ and $k_{0,3}$ interchange their positions, when $P_z \gtrsim 3.5$ GeV

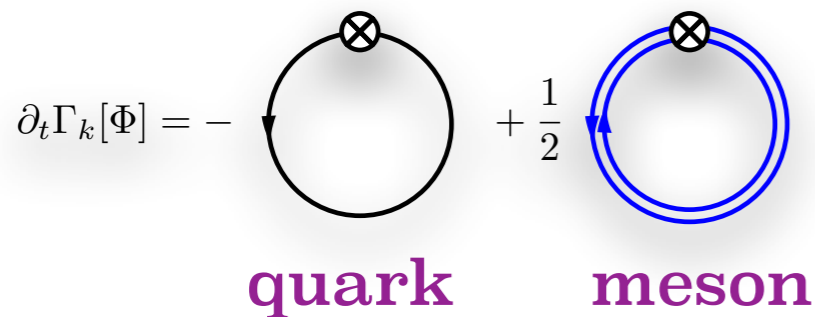
fRG: Chang, WF, Huang, Pawlowski, Zhang, in preparation

QCD-assisted LEFT

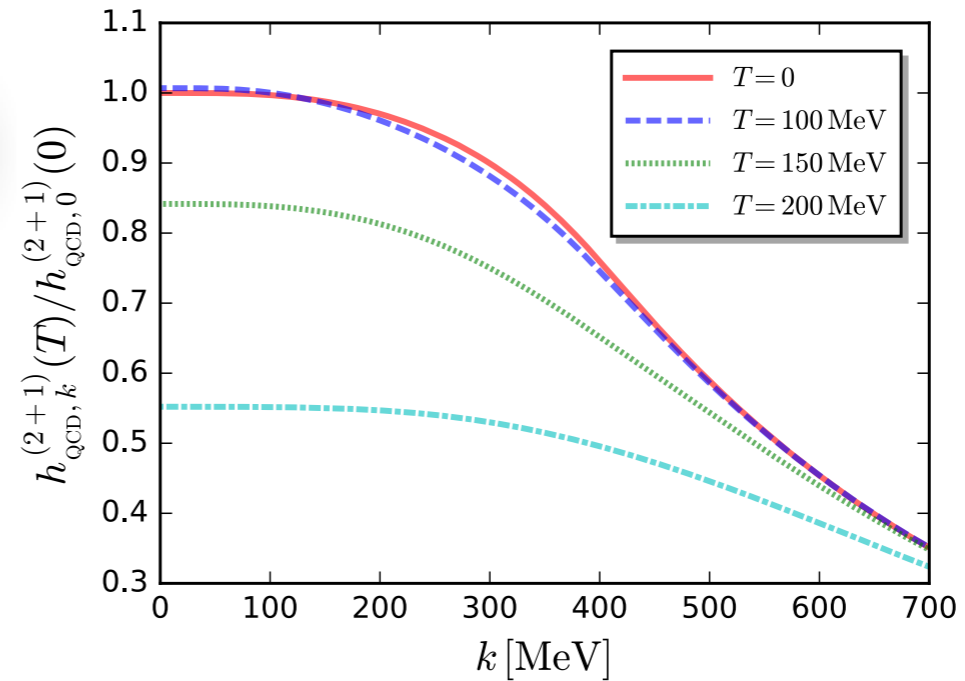
QCD flow equation:



LEFT flow equation:

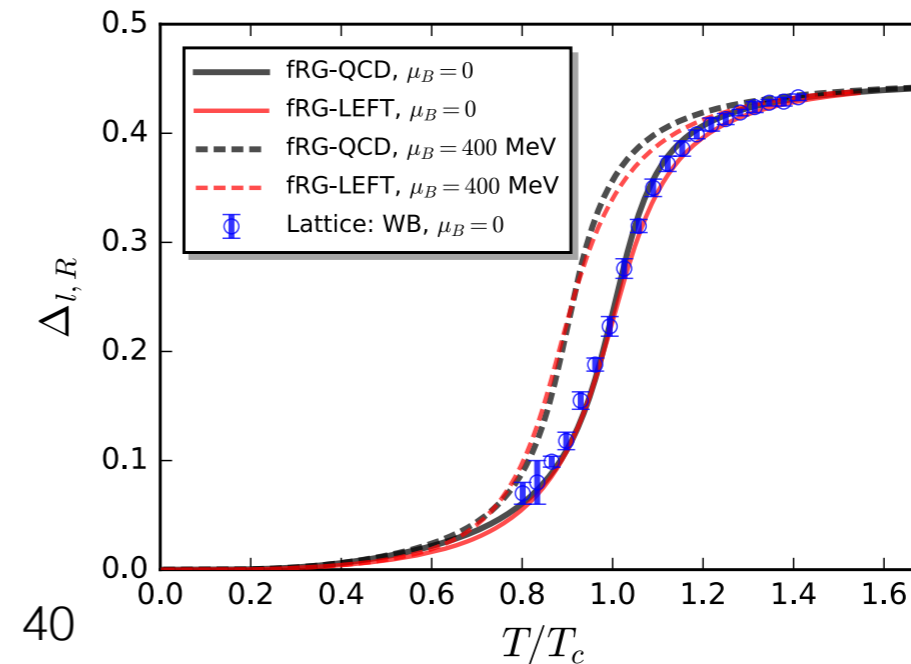


- Yukawa couplings obtained in QCD inputted in QCD-assisted LEFT



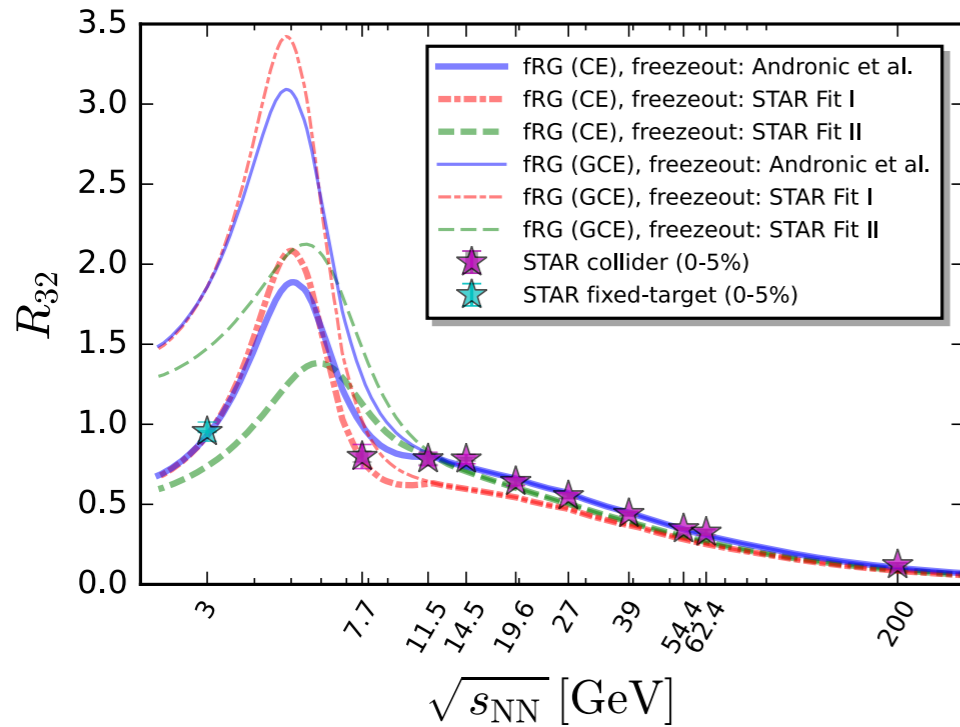
WF, Pawłowski, Rennecke, *PRD* 101 (2020) 054032

- Chiral condensates in QCD and QCD-assisted LEFT in agreement

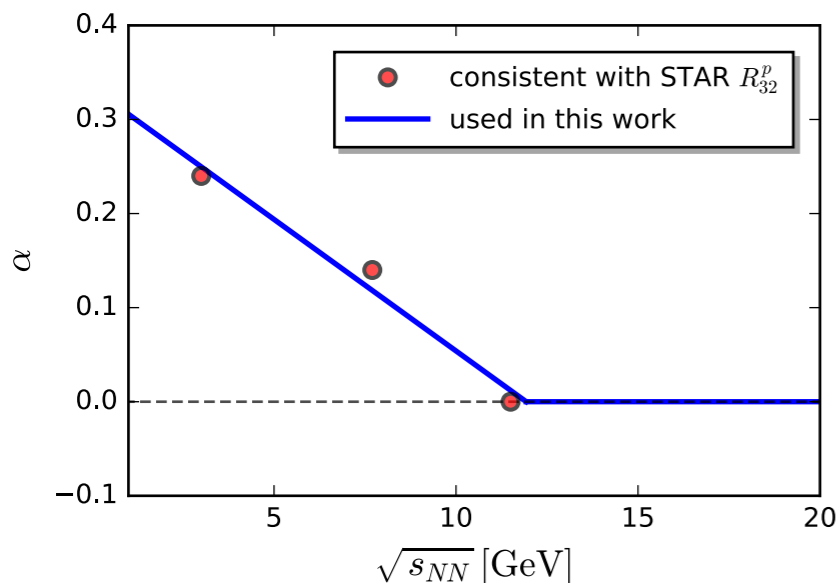


WF, Luo, Pawłowski, Rennecke, Yin, arXiv: 2308.15508

Canonical corrections with SAM



- Experimental data R_{32} is used to constrain the parameter α in the range $\sqrt{s_{NN}} \lesssim 11.5$ GeV.
- We choose the simplest linear dependence



$$\alpha(\bar{s}) = a \left(1 - \sqrt{\bar{s}}\right) \theta(1 - \bar{s})$$

$$a = 0.33, \quad \sqrt{\bar{s}} = \frac{\sqrt{s_{NN}}}{11.9 \text{ GeV}}$$

SAM:

- We adopt the subensemble acceptance method (SAM) to take into account the effects of global baryon number conservation:

$$\alpha = \frac{V_1}{V}$$

V_1 : the subensemble volume measured in the acceptance window, V : the volume of the whole system.

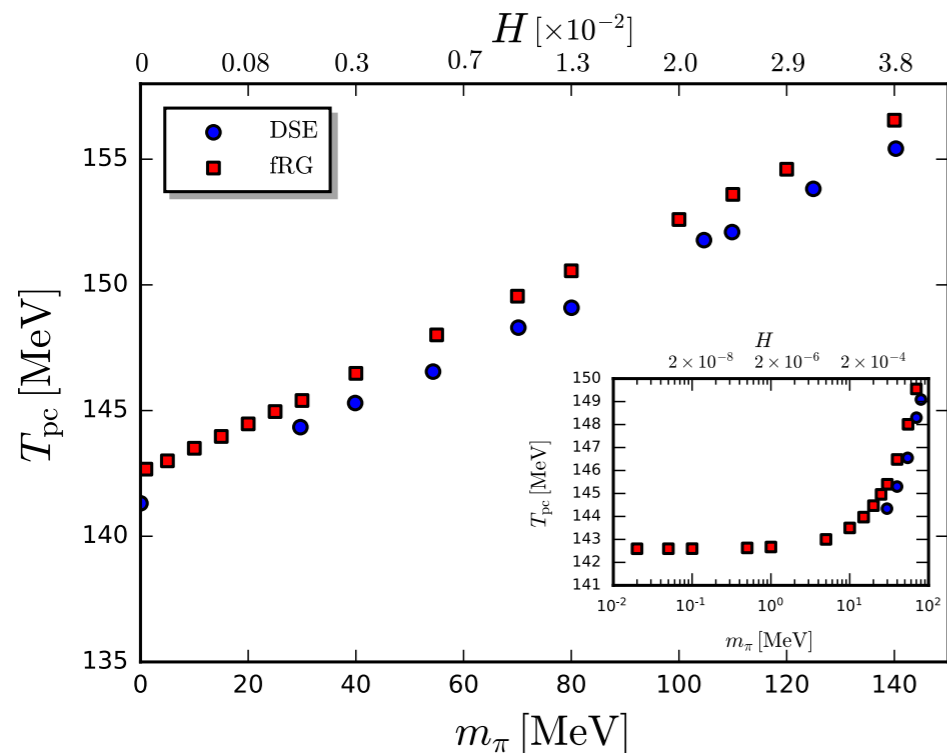
- fluctuations with canonical corrections are related to grand canonical fluctuations as follows:

$$\bar{R}_{21}^B = \beta R_{21}^B, \quad \bar{R}_{32}^B = (1 - 2\alpha)R_{32}^B,$$

$$\bar{R}_{42}^B = (1 - 3\alpha\beta)R_{42}^B - 3\alpha\beta(R_{32}^B)^2$$

SAM: Vovchenko, Savchuk, Poberezhnyuk, Gorenstein, Koch, *PLB* 811 (2020) 135868

Magnetic equation of state



$$T_{pc}(m_\pi) \approx T_c + c m_\pi^p$$

Braun, Chen, WF, Gao, Huang, Ihssen, Pawłowski, Rennecke, Sattler, Tan, Wen, and Yin, arXiv:2310.19853.

Lattice (HotQCD):

$$T_c^{\text{lattice}} = 132_{-6}^{+3} \text{ MeV},$$

Ding *et al.*, *PRL* 123 (2019) 062002.

fRG:

$$T_c^{\text{fRG}} \approx 142 \text{ MeV}, \quad p_{\text{fRG}} = 1.024$$

Braun, WF, Pawłowski, Rennecke, Rosenblüh, Yin, *PRD* 102 (2020) 056010.

DSE:

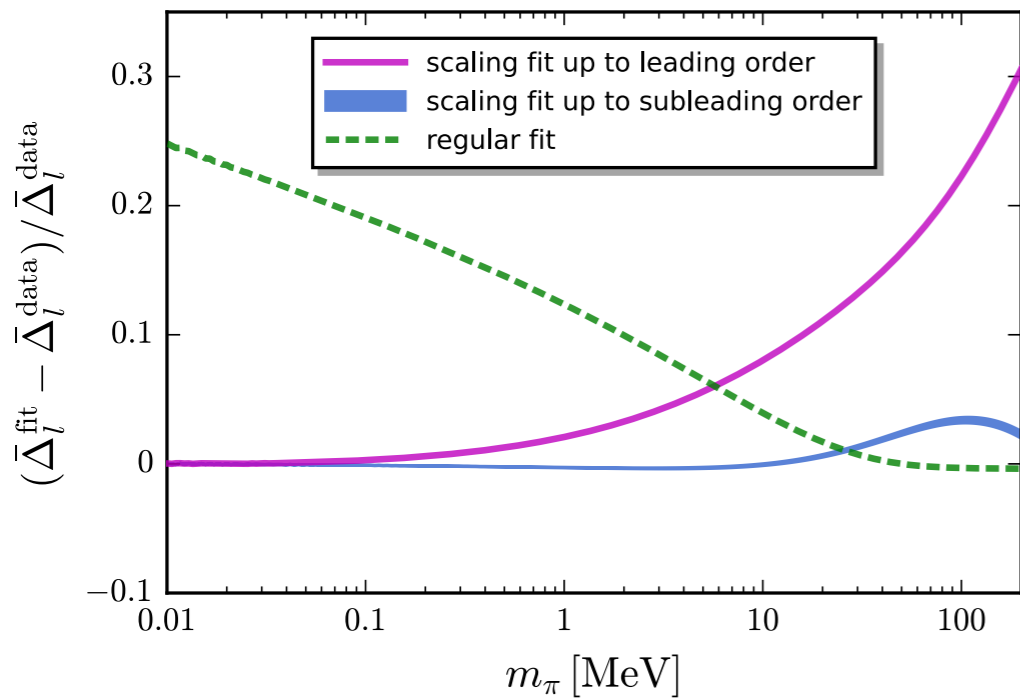
$$T_c^{\text{DSE}} \approx 141 \text{ MeV}, \quad p_{\text{DSE}} = 0.9606$$

Gao, Pawłowski, *PRD* 105 (2022) 9, 094020, arXiv: 2112.01395.

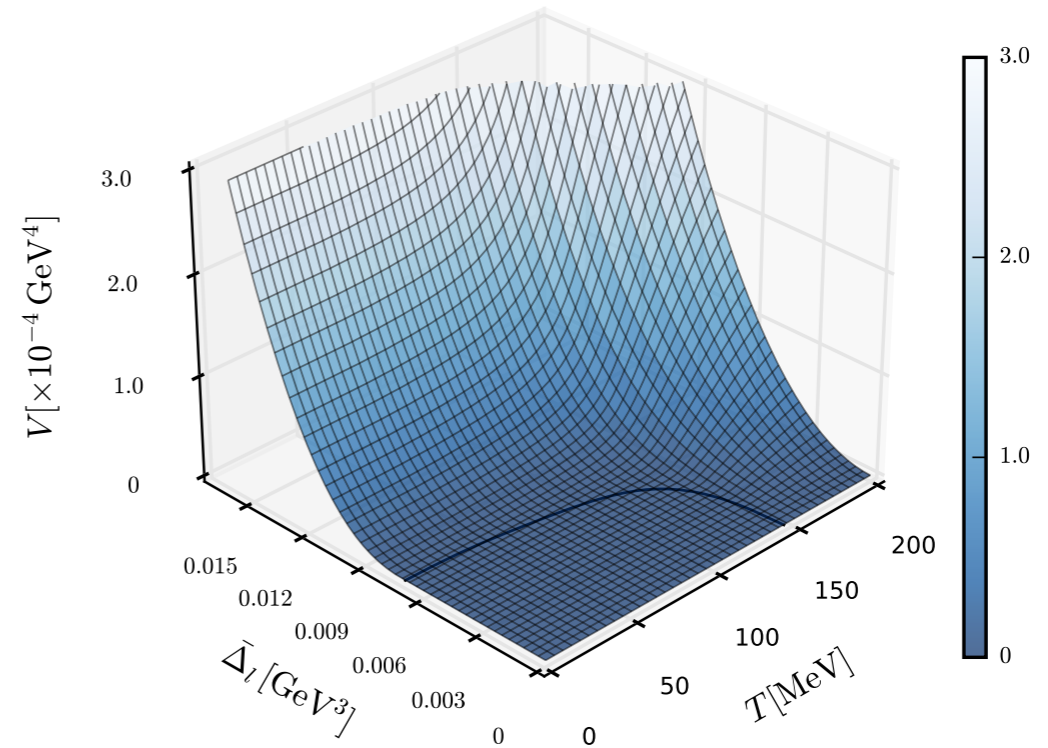
- The almost linear dependence of the pseudo-critical temperature on the pion mass has nothing to do with the criticality.
- So what is the size of the critical region in QCD?

Scaling vs regular fitting

Errors:



Potential:



$$\bar{\Delta}_l^{(\text{crit})}(m_\pi) = B_c m_\pi^{2/\delta} [1 + a_m m_\pi^{2\theta_H}]$$

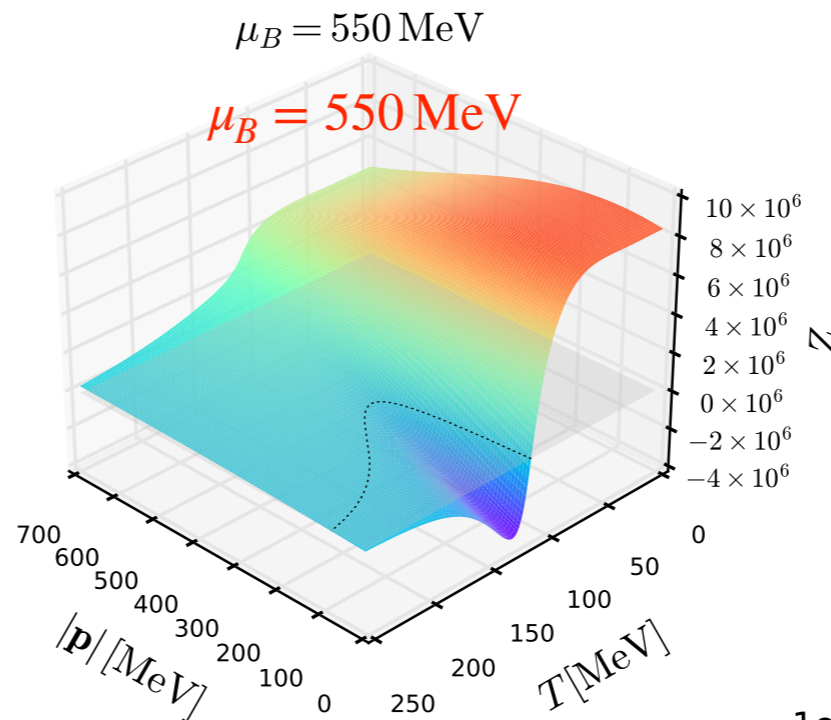
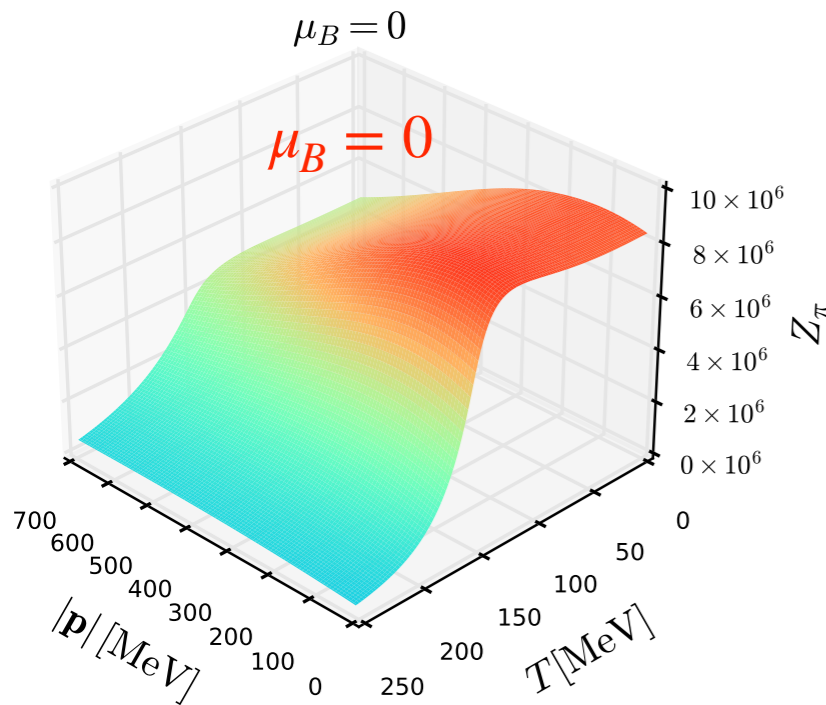
$$\Delta_l^{(\text{reg})}(m_\pi) = b_{\frac{1}{5}} m_\pi^{2/5} + b_{\frac{3}{5}} m_\pi^{6/5} + b_1 m_\pi^2$$

Braun, Chen, WF, Gao, Huang, Ihsen, Pawłowski,
Rennecke, Sattler, Tan, Wen, and Yin,
arXiv:2310.19853.

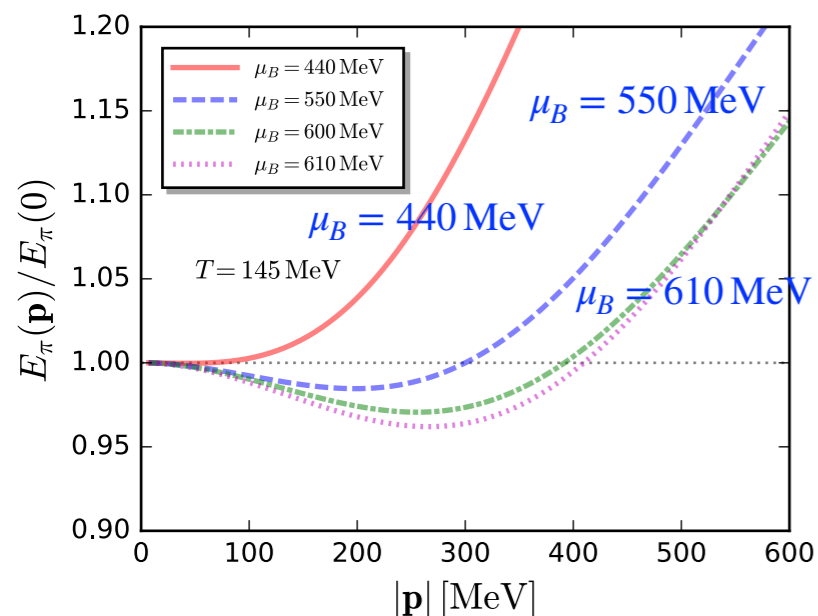
Momentum-dependent mesonic wave function

Flow equation for mesonic two-point functions:

$$\partial_t \text{---} \bullet \text{---} = \tilde{\partial}_t \left(\text{---} \bullet \text{---} \bullet \text{---} + \frac{1}{2} \text{---} \bullet \text{---} \bullet \text{---} + \frac{1}{2} \text{---} \bullet \text{---} \bullet \text{---} \right)$$



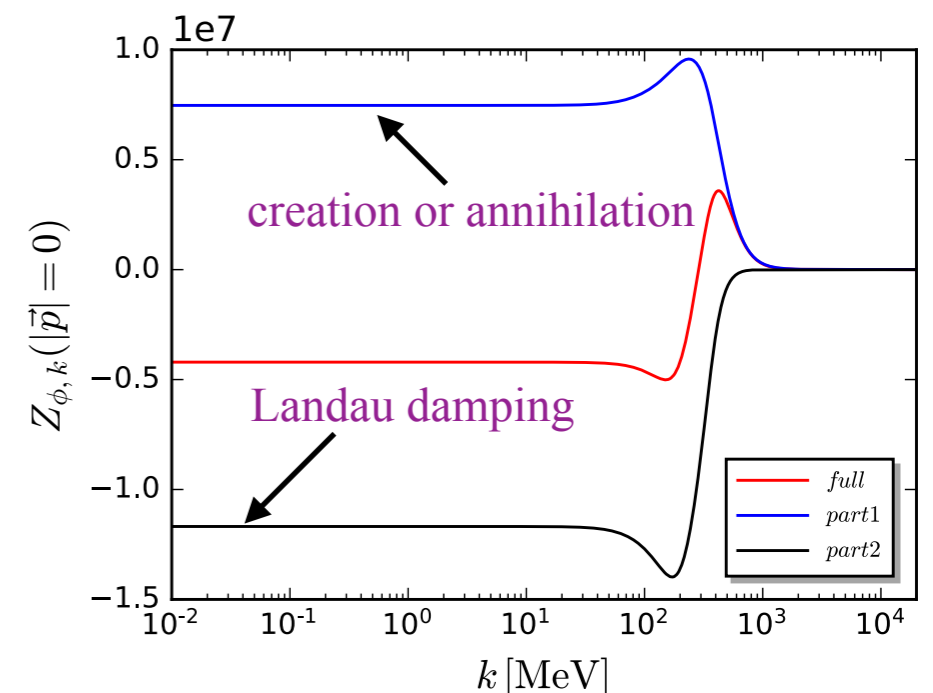
- Inhomogeneous instability is resulted from **Landau damping** of quarks in thermal bath in the regime of large baryon chemical potential.



Dispersion relation:

$$E_\phi(\mathbf{p}) = [Z_\phi^\perp(\mathbf{p}) \mathbf{p}^2 + m_\phi^2]^{1/2}$$

WF, Pawłowski, Pisarski, Rennecke, Wen, Yin, in preparation.

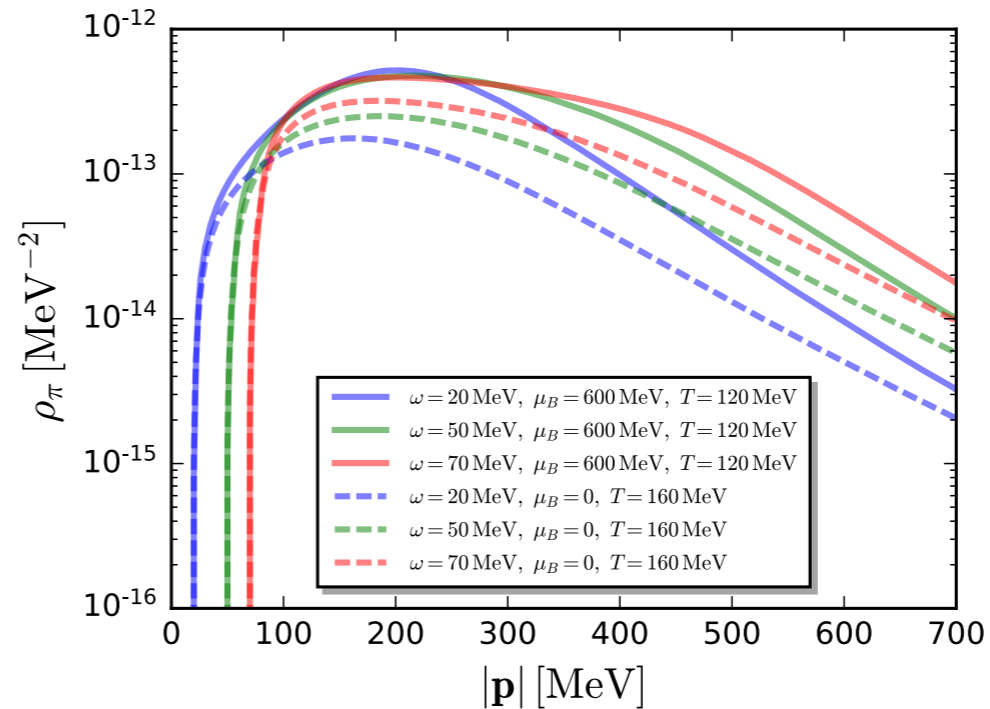


Real-time mesonic two-point functions

Analytic continuation on the flow equation:

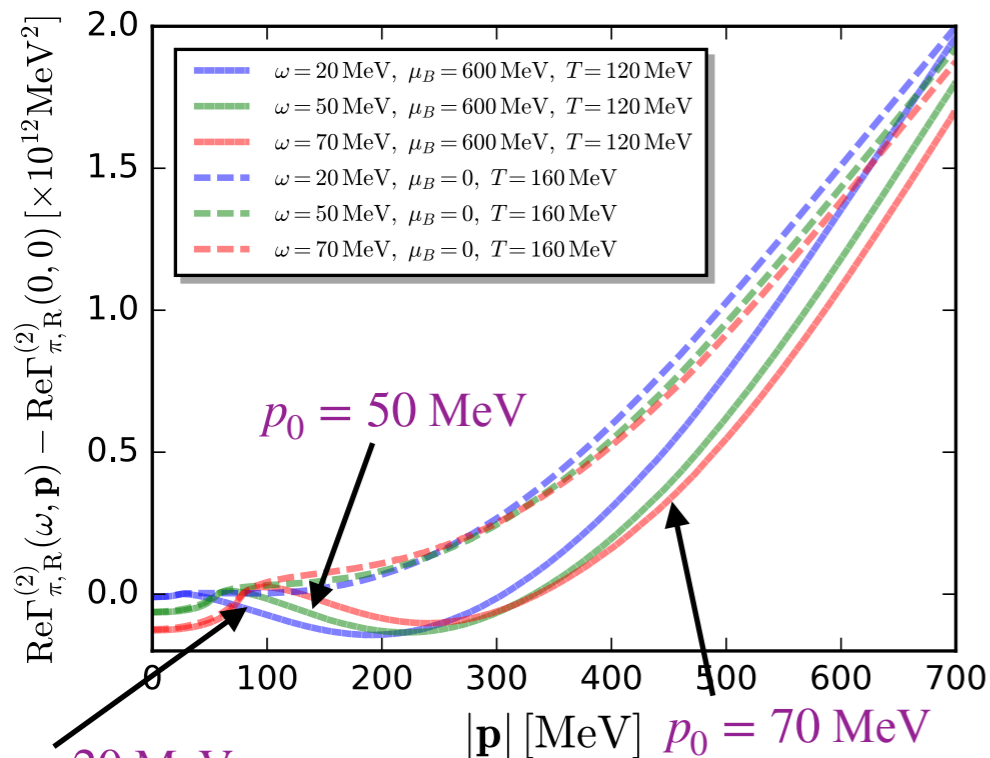
$$\Gamma_{\phi\phi,R}^{(2)}(\omega, \mathbf{p}) = \lim_{\epsilon \rightarrow 0^+} \Gamma_{\phi\phi}^{(2)}(-i(\omega + i\epsilon), \mathbf{p})$$

Note: not on data!

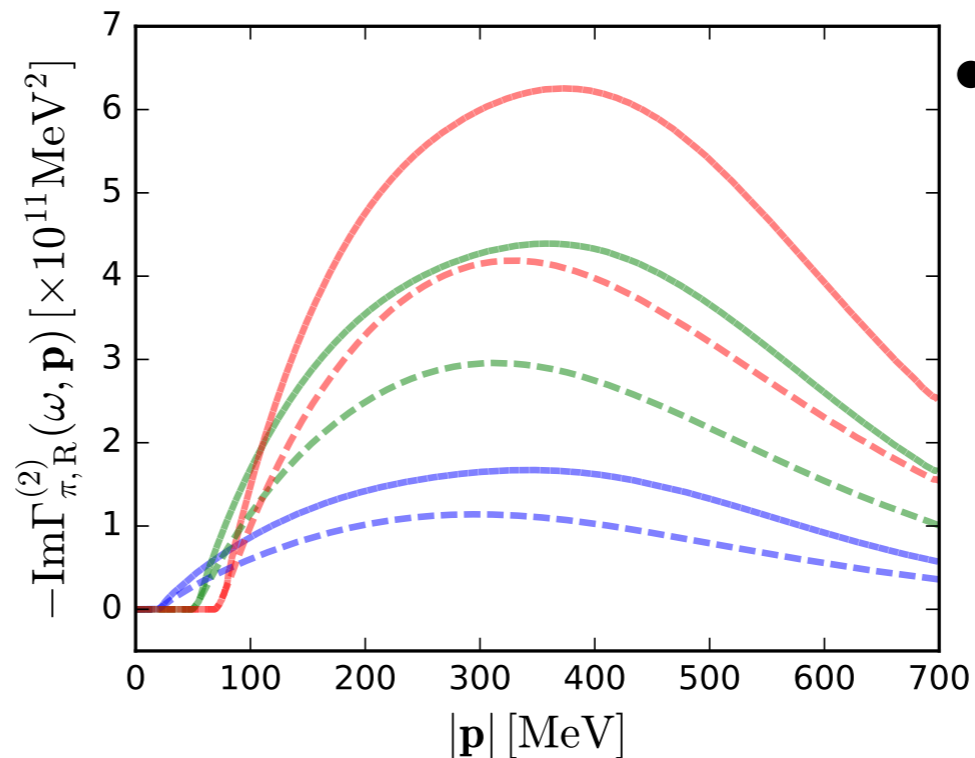


Spectral function

Real part of $\Gamma_{\phi\phi,R}^{(2)}(p_0, \mathbf{p})$:



Imaginary part of $\Gamma_{\phi\phi,R}^{(2)}(p_0, \mathbf{p})$:

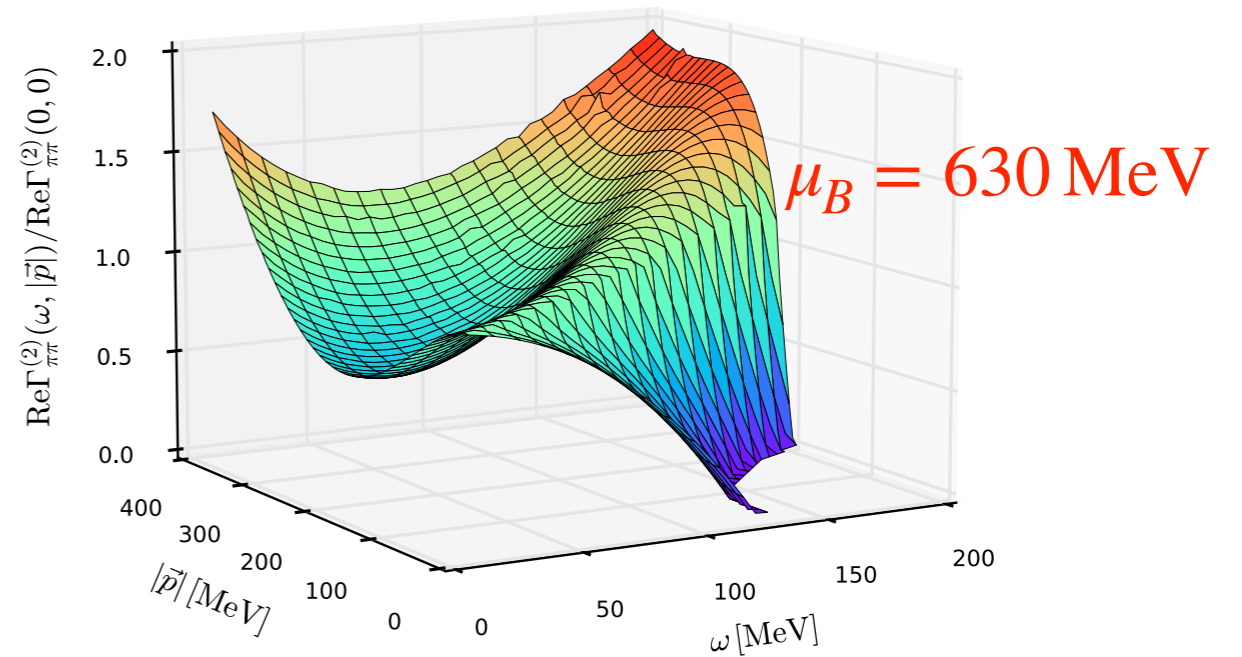
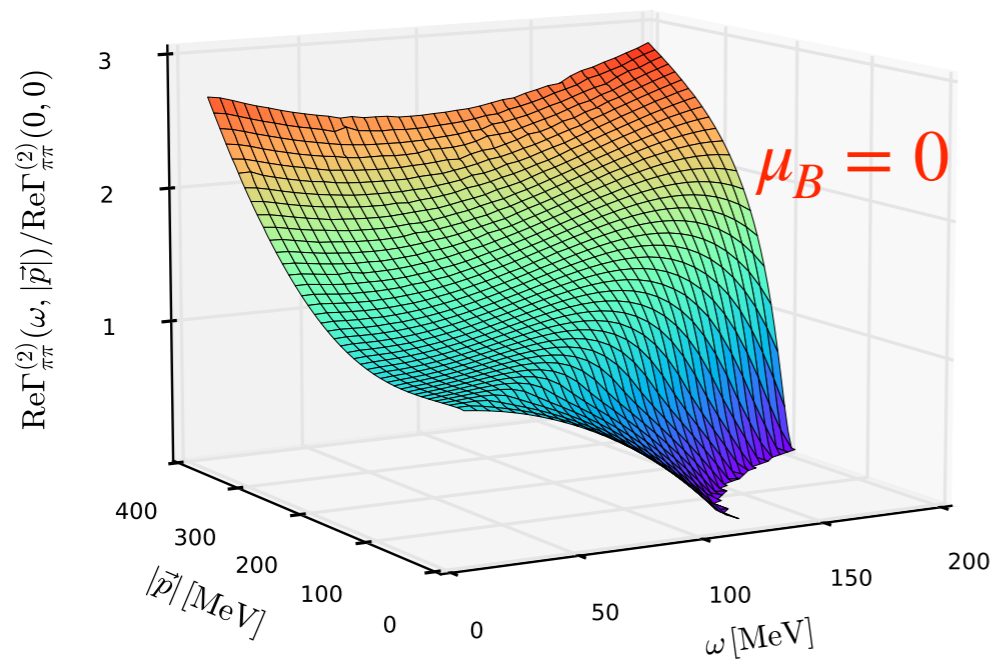


- Imaginary part of the mesonic two-point functions and spectral function are enhanced by the Landau damping effect

WF, Pawlowski, Pisarski, Rennecke, Wen, Yin, in preparation.

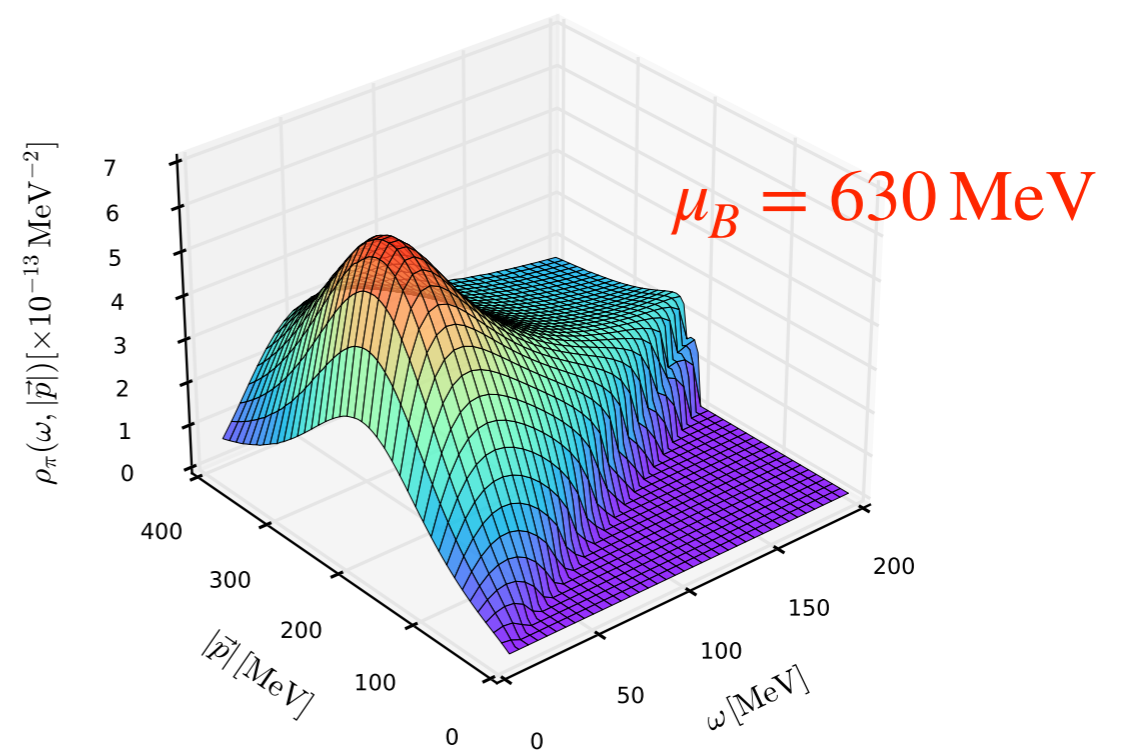
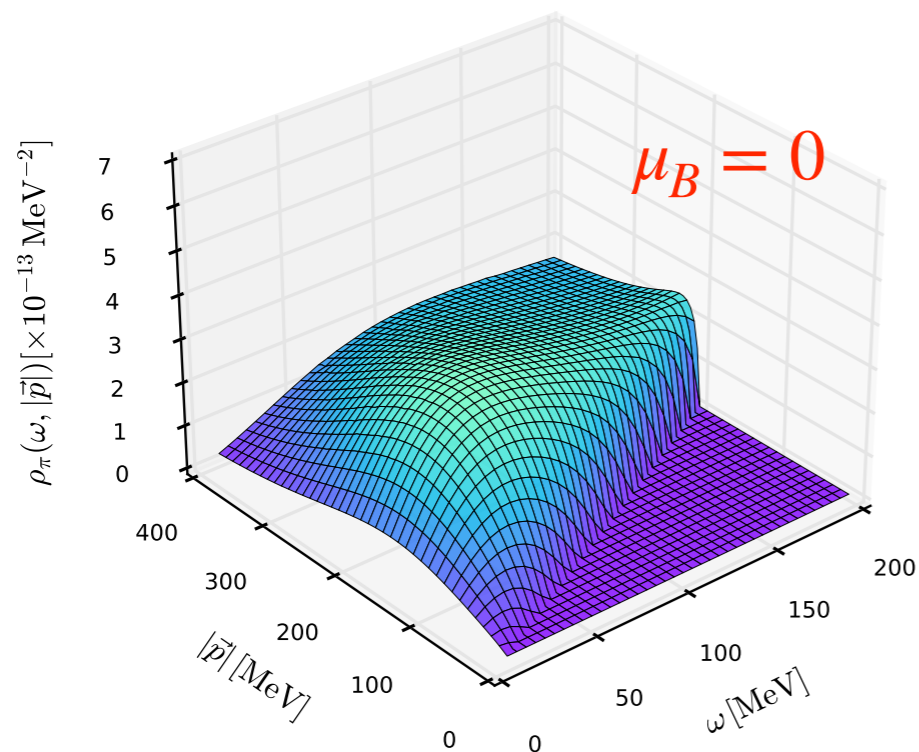
Real-time mesonic two-point functions

Real part:



Spectral function:

WF, Pawlowski, Pisarski, Rennecke,
Wen, Yin, in preparation.



Schwinger-Keldysh path integral

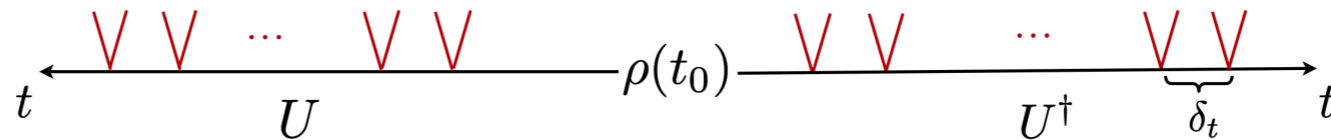
- Schrödinger equation:



$$U(t, t_0) = e^{-iH(t-t_0)}$$

$$i\partial_t |\psi(t)\rangle = H|\psi(t)\rangle \longrightarrow |\psi(t)\rangle = U(t, t_0) |\psi(t_0)\rangle,$$

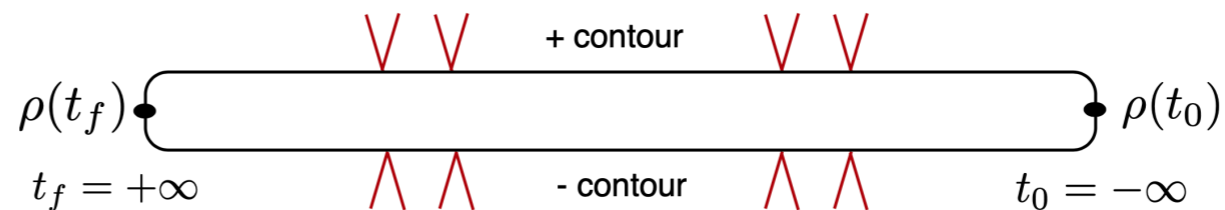
- von Neumann equation:



$$\partial_t \rho(t) = -i[H, \rho(t)] \longrightarrow \rho(t) = U(t, t_0) \rho(t_0) U^\dagger(t, t_0),$$

- Keldysh partition function:

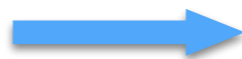
$$Z = \text{tr} \rho(t),$$



- two-point closed time-path Green's function:

$$G(x, y) \equiv -i \text{tr} \{ T_p (\phi(x) \phi^\dagger(y) \rho) \}$$

$$\equiv -i \langle T_p (\phi(x) \phi^\dagger(y)) \rangle,$$



$$G(x, y) = \begin{pmatrix} G_{++} & G_{+-} \\ G_{-+} & G_{--} \end{pmatrix}$$

$$\equiv \begin{pmatrix} G_F & G_+ \\ G_- & G_{\tilde{F}} \end{pmatrix},$$

$$G_F(x, y) \equiv -i \langle T (\phi(x) \phi^\dagger(y)) \rangle,$$

$$G_+(x, y) \equiv -i \langle \phi^\dagger(y) \phi(x) \rangle,$$

$$G_-(x, y) \equiv -i \langle \phi(x) \phi^\dagger(y) \rangle,$$

$$G_{\tilde{F}}(x, y) \equiv -i \langle \tilde{T} (\phi(x) \phi^\dagger(y)) \rangle,$$

Schwinger, J. Math. Phys. 2, 407 (1961);
 Keldysh, Zh. Eksp. Teor. Fiz. 47, 1515 (1964);
 Chou, Su, Hao, Yu, Phys. Rept. 118, 1 (1985).

FRG in Keldysh path integral

- Implement the formalism of fRG in the two time branches:

$$Z_k[J_c, J_q] = \int (\mathcal{D}\varphi_c \mathcal{D}\varphi_q) \exp \left\{ i \left(S[\varphi] + \Delta S_k[\varphi] + (J_q^i \varphi_{i,c} + J_c^i \varphi_{i,q}) \right) \right\},$$

with

$$\begin{aligned} \Delta S_k[\varphi] &= \frac{1}{2} (\varphi_{i,c}, \varphi_{i,q}) \begin{pmatrix} 0 & R_k^{ij} \\ (R_k^{ij})^* & 0 \end{pmatrix} \begin{pmatrix} \varphi_{j,c} \\ \varphi_{j,q} \end{pmatrix} \\ &= \frac{1}{2} \left(\varphi_{i,c} R_k^{ij} \varphi_{j,q} + \varphi_{i,q} (R_k^{ij})^* \varphi_{j,c} \right), \end{aligned}$$

Keldysh rotation:

$$\begin{cases} \varphi_{i,+} = \frac{1}{\sqrt{2}} (\varphi_{i,c} + \varphi_{i,q}), \\ \varphi_{i,-} = \frac{1}{\sqrt{2}} (\varphi_{i,c} - \varphi_{i,q}), \end{cases}$$

- Then we derive the flow equation in the closed time path:

$$\partial_\tau \Gamma_k[\Phi] = \frac{i}{2} \text{STr} \left[(\partial_\tau R_k^*) G_k \right], \quad R_k^{ab} \equiv \begin{pmatrix} 0 & R_k^{ij} \\ (R_k^{ij})^* & 0 \end{pmatrix},$$

$$iG(x, y) = \begin{pmatrix} iG^K(x, y) & iG^R(x, y) \\ iG^A(x, y) & 0 \end{pmatrix},$$

$$\begin{aligned} iG^R(x, y) &= \theta(x^0 - y^0) \langle [\phi(x), \phi^*(y)] \rangle, \\ iG^A(x, y) &= \theta(y^0 - x^0) \langle [\phi^*(y), \phi(x)] \rangle, \\ iG^K(x, y) &= \langle \{ \phi(x), \phi^*(y) \} \rangle, \end{aligned}$$

A relaxation critical $O(N)$ model

- The effective action on the Schwinger-Keldysh contour reads

Hohenberg and Halperin, *Rev. Mod. Phys.* 49 (1977) 435.

Model A

$$\Gamma[\phi_c, \phi_q] = \int d^4x \left(Z_a^{(t)} \phi_{a,q} \partial_t \phi_{a,c} - Z_a^{(i)} \phi_{a,q} \partial_i^2 \phi_{a,c} + V'(\rho_c) \phi_{a,q} \phi_{a,c} - 2 Z_a^{(t)} T \phi_{a,q}^2 - \sqrt{2} c \sigma_q \right)$$

$\Gamma = 1/Z_a^{(t)}$: relaxation rate

$V'(\rho_c)$: potential $\rho_c \equiv \phi_c^2/4$

Gaussian white noise with coefficient determined by fluctuation-dissipation theorem

$Z_a^{(i)}$: wave function

c : explicit breaking

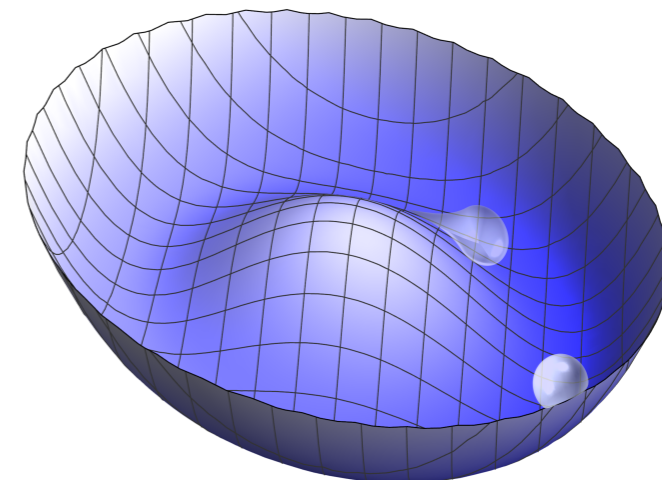
- Retarded propagator

$$G_{ab}^R = \left(\frac{\delta^2 \Gamma[\phi_c, \phi_q]}{\delta \phi_{a,q} \delta \phi_{b,c}} \right)^{-1}$$

Retarded propagator of Goldstone

$$G_{\varphi\varphi}^R(\omega, q) = \frac{1}{-iZ_\varphi^{(t)}\omega + Z_\varphi^{(i)}(q^2 + m_\varphi^2)}$$

pseudo-Goldstone:



Mass of pseudo-Goldstone

$$m_\varphi^2 = \frac{V'(\rho_0)}{Z_\varphi^{(i)}} = \frac{c}{\sigma_0 Z_\varphi^{(i)}}$$

Gell-Mann--Oakes--Renner (GMOR) relation

Universal damping or not?

From the pole of the retarded propagator of Goldstone

$$G_{\varphi\varphi}^R(\omega, q) = \frac{1}{-iZ_\varphi^{(t)}\omega + Z_\varphi^{(i)}(q^2 + m_\varphi^2)}$$

One obtains the dispersion relation of a damped mode

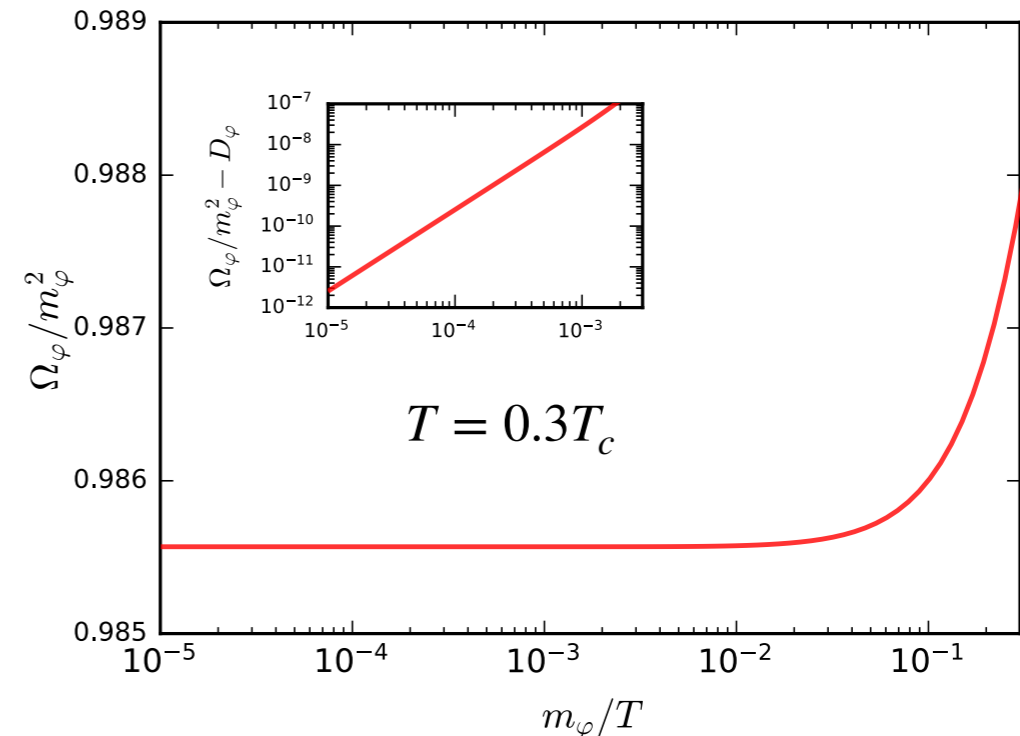
$$\omega(q) = -i \frac{Z_\varphi^{(i)}}{Z_\varphi^{(t)}} (m_\varphi^2 + q^2)$$

The relaxation rate at zero momentum reads

$$\Omega_\varphi \equiv -\text{Im} \omega(q=0) = \frac{Z_\varphi^{(i)}}{Z_\varphi^{(t)}} m_\varphi^2$$

- If $T \ll T_c$

$$\frac{\Omega_\varphi}{m_\varphi^2} \simeq D_\varphi(T) + \mathcal{O}\left(\frac{m_\varphi^2}{T^2}\right) \quad \text{with} \quad D_\varphi(T) \equiv \frac{Z_\varphi^{(i)}(T, c=0)}{Z_\varphi^{(t)}(T, c=0)}$$



Tan, Chen, WF, Li, arXiv: 2403.03503

This seemingly appears as a **universal** relation that was also observed in Holographics, Hydrodynamics, and EFT

Holographics:

Amoretti, Areán, Goutéraux, Musso, *PRL* 123 (2019) 211602;

Amoretti, Areán, Goutéraux, Musso, *JHEP* 10 (2019) 068;

Ammon *et al.*, *JHEP* 03 (2022) 015;

Cao, Baggioli, Liu, Li, *JHEP* 12 (2022) 113

Hydrodynamics:

Delacrétaz, Goutéraux, Ziogas, *PRL* 128 (2022) 141601

EFT:

Baggioli, *Phys. Rev. Res.* 2 (2020) 022022;

Baggioli, Landry, *SciPost Phys.* 9 (2020) 062

Breaking down of the universal damping in the critical region

In the critical region, the two wave function renormalizations read

$$Z_\varphi^{(i)} = t^{-\nu\eta} f^{(i)}(z), \quad Z_\varphi^{(t)} = t^{-\nu\eta_t} f^{(t)}(z)$$

Here $f^{(i)}(z), f^{(t)}(z)$: scaling functions; $z \equiv tc^{-1/(\beta\delta)}$: scaling variable; $t \equiv (T_c - T)/T_c$: reduced temperature. The static and dynamic anomalous dimensions are

$$\eta = -\frac{\partial_\tau Z_\varphi^{(i)}}{Z_\varphi^{(i)}}, \quad \eta_t = -\frac{\partial_\tau Z_\varphi^{(t)}}{Z_\varphi^{(t)}}$$

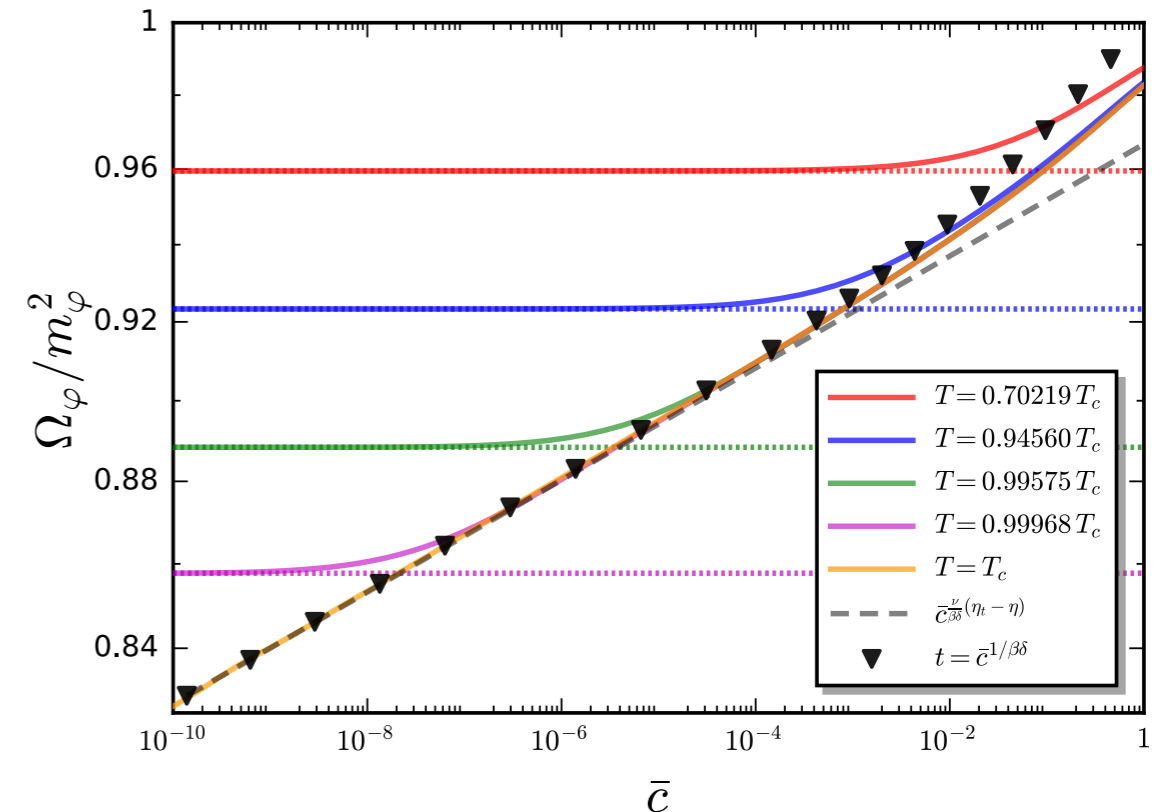
RG time $\tau = \ln(k/\Lambda)$

- In the case of $c \rightarrow 0$

$$\frac{Z_\varphi^{(i)}}{Z_\varphi^{(t)}} \propto t^{\nu(\eta_t - \eta)}$$

- In the other case of $t \rightarrow 0$

$$\frac{Z_\varphi^{(i)}}{Z_\varphi^{(t)}} \propto c^{\frac{\nu}{\beta\delta}(\eta_t - \eta)} \propto m_\varphi^{(\eta_t - \eta)} \quad \text{with} \quad m_\varphi^2 \propto c^{\frac{2\nu}{\beta\delta}}$$



Tan, Chen, WF, Li, arXiv: 2403.03503

From the fixed-point equation we determine in the O(4) symmetry

$$\eta \approx 0.0374, \quad \eta_t \approx 0.0546$$

Thus

$$\Delta_\eta \equiv \eta_t - \eta \approx 0.0172$$

Estimate of size of the dynamic critical region:

$$m_{\pi 0} \lesssim 0.1 \sim 1 \text{ MeV}$$

Large N limit

In the large N limit, the static and dynamic anomalous dimensions can be solved analytically

$$\eta = \frac{5}{N-1} \frac{(1+\eta)(1-2\eta)^2}{(5-\eta)(2-\eta)^2}$$

and

$$\eta_t = \frac{1}{9(N-1)} \frac{(1-2\eta)^2(13+15\eta-2\eta^3)}{(2-\eta)^2}$$

Tan, Chen, WF, Li, arXiv: 2403.03503

- In the limit $N \rightarrow \infty$, the breaking down of the universal damping disappears.
- One should not expect that the anomalous scaling regime can be observed in classical holographic models.

